Model Development Report: Gualala River Watershed

SUBMITTED TO:

State Water Resources Control Board
1001 I Street, 14th Floor
Sacramento, CA 95814

PREPARED BY:

Paradigm Environmental
9320 Chesapeake Drive, Suite 100
San Diego, CA 92123

JULY 25, 2025

THIS PAGE INTENTIONALLY LEFT BLANK

Contents

Figures

Tables

1 INTRODUCTION

This report provides a detailed discussion of the development and configuration of a hydrology model of the Gualala River watershed to support decision making by the California State Water Resources Control Board (Water Board) for water supply, demand, and use. In April 2021, Governor Gavin Newsom issued a state of emergency proclamation for specific watersheds across California in response to exceptionally dry conditions throughout the state. The April 2021 proclamation, as well as subsequent proclamations, directed the Board to address these emergency conditions to ensure adequate, minimal water supplies for critical purposes. To support Water Board actions to address emergency conditions, hydrologic modeling and analysis tools are being developed to contribute to a comprehensive decision support system that assesses water supply and demand, and the flow needs for watersheds throughout California.

This model development report builds on the Gualala River watershed modeling work plan (SWRCB 2024), which has additional information on the model background and over-arching model approach; the Loading Simulation Program in C++ (LSPC) was used to simulate hydrology within the watershed. The model provides an evaluation platform for (1) simulating existing instream flows that integrate current water management activities and consumptive uses, (2) evaluating the range of impacts of alternative management scenarios. Key components necessary for the development of this model are detailed in this report. Model development refers to basic building blocks for defining the surface water model domain. It includes catchments delineation, reach segments (cross-sections, hydraulic characteristics, and routing network), and Hydrologic Response Units (HRUs). Model development also includes creating and assigning representative climate forcing inputs. The final sections of this report provide details on the model calibration approach and present calibration and validation results.

- Section 2.1 describes Catchment Delineation. Catchments are the highest resolution spatial boundaries in the model. Delineated catchments were compiled from best-available topographic layers and refined as needed to align outlets with flow monitoring stations.
- Section 2.2 describes the Hydraulic Network. Hydraulic routing features include reaches, lakes/reservoirs, and other network routing elements that convey flow and pollutants from one catchment to another.
- Section 3 describes the Hydrologic Response Units. HRUs are the smallest spatial unit within the model, representing unique combinations of spatial data layers including land use/land cover, hydrologic soil group, and slope.
- Section 4 describes climate forcing inputs. Forcing inputs include precipitation and potential evapotranspiration that drive the model's rainfall-runoff response.
- Section 5 describes the surface water demand data, withdrawals, and irrigation demand.
- Section 6 describes the model calibration approach and results.
- Section 7 presents the model validation results.
- Section 8 presents a summary of the report.

2 CATCHMENT NETWORK

2.1 Catchment Delineation

The United States Geological Survey (USGS) delineates watersheds nationwide based on surface hydrological features and organizes the drainage units into a nested hierarchy using hydrologic unit codes (HUC). These HUCs have a varying number of digits to denote scale ranging from 2-digit HUCs (largest) at the regional scale to 12-digit HUCs (smallest) at the subwatershed scale. The Gualala River watershed is defined as a HUC-10 watershed that comprises 9 HUC-12 subwatersheds.

For units smaller than HUC-12 subwatersheds, the National Hydrography Dataset Plus v2 (NHDPlus) has further discretized the watershed into catchments ranging in size between 0.0017 square miles to over 7 square miles. Figure 2-1 is a map of HUC-12 subwatersheds and NHDPlus catchments within the Gualala River watershed (HUC-10). Table 2-1 presents summary statistics of NHDPlus catchment sizes by HUC-12 subwatershed.

Where necessary, catchments were either merged to eliminate braiding in the stream network or sub-delineated using the hydrologically conditioned 30-meter resolution digital elevation model (DEM), flow direction, and flow accumulation raster layers available with the NHDPlus dataset to better represent points of interest. Catchments were merged in ten cases in the Gualala River watershed to eliminate braiding on the mainstem of the Gualala River. Sub-delineations were not necessary in the Gualala River watershed. Figure 2-2 shows the final delineated catchments for the LSPC model.

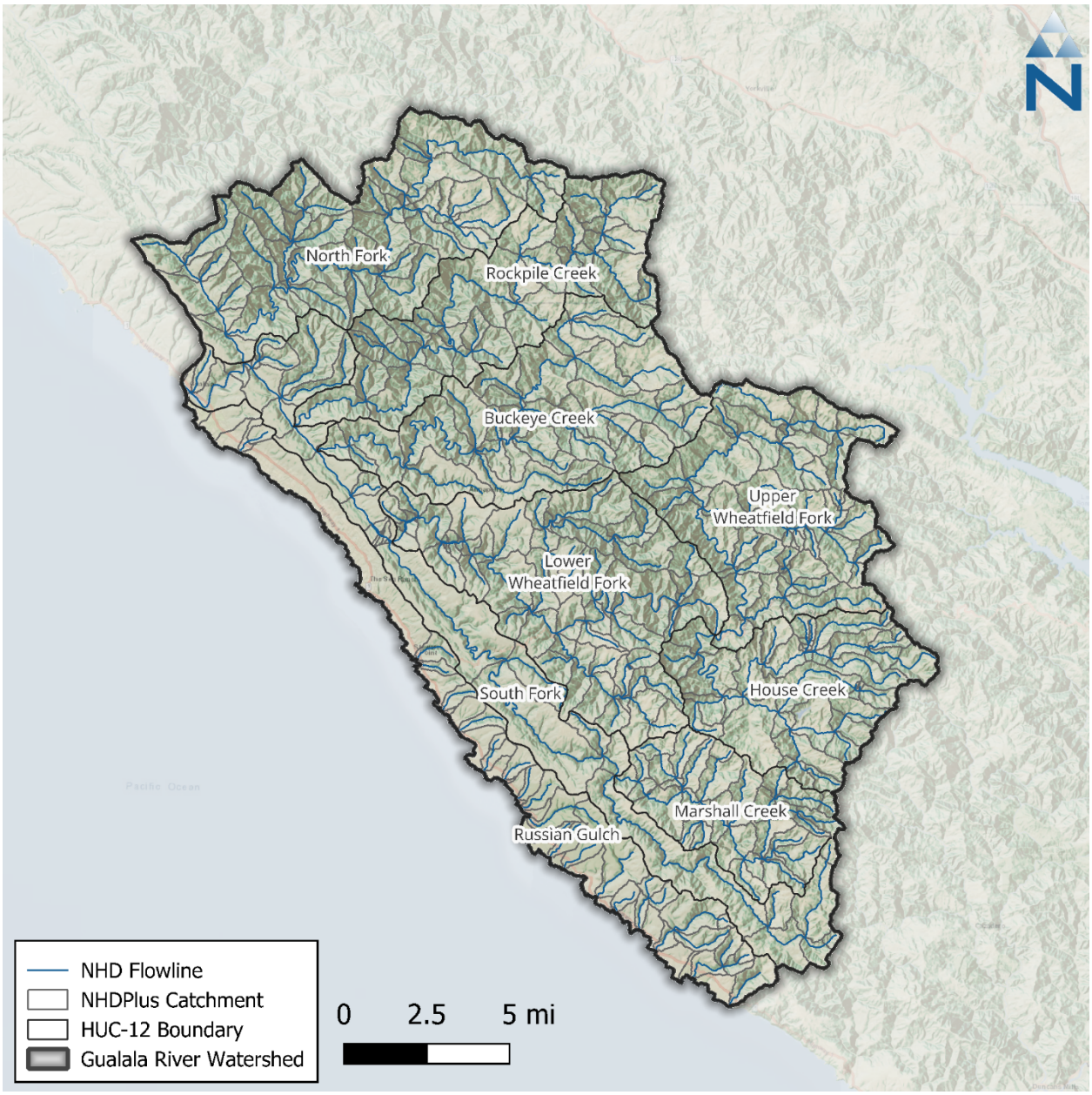

Figure 2-1. Initial NHDPlus catchment segmentation for the Gualala River watershed.

Table 2-1. Summary of finalized NHDPlus catchments within the Gualala River watershed HUC-12 subwatersheds

HUC-12	HUC-12 Name	Catchment Count	Catchment Area (acre)			
			Minimum	Average	Maximum	Total [1]
180101090101	Marshall Creek	38	4.7	333.1	969.9	12,658.8
180101090102	House Creek	40	8.9	455.9	1,802.7	18,236.7
180101090103	Upper Wheatfield Fork	53	4.9	461.6	2,150.3	24,462.8
180101090104	Lower Wheatfield Fork	64	2.4	449.0	1,995.4	28,736.2
180101090105	Buckeye Creek	35	2.9	735.3	1,959.6	25,736.9
180101090106	Rockpile Creek	31	198.8	722.8	2,744.4	22,405.7
180101090107	North Fork	46	2.4	666.0	3,159.0	30,637.0
180101090108	South Fork	36	1.1	783.3	4,571.1	28,198.7
180101090202	Russian Gulch	54	11.6	396.9	4,193.8	21,429.9
	Total	**397**	**--**	**--**	**--**	**212,503**

1. The total area of NHDPlus catchments is 35 acres larger (0.02%) than the raster-based area summaries presented later in the report because the raster layer has a coarser resolution (i.e., 30-m grid) than the vector catchment layer.

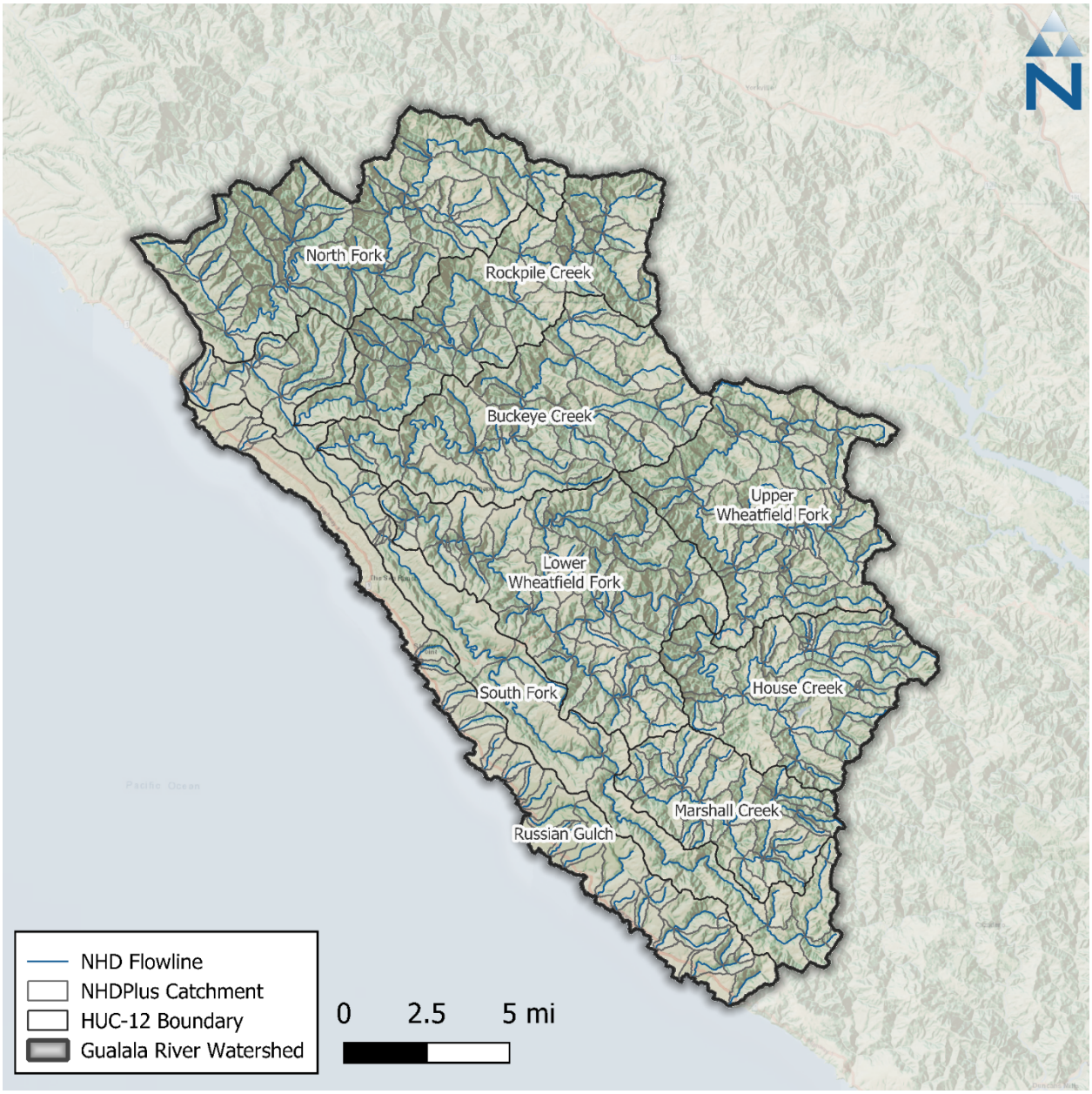

Figure 2-2. Final NHDPlus catchment segmentation for the Gualala River watershed.

2.2 Routing & Connectivity

Once catchments have been delineated, the connectivity of flow within and between each catchment needs to be specified so that water can be routed from upstream to downstream areas. Within the Gualala River watershed model, surface flow is conveyed through a reach network with one representative reach segment for each catchment. Within a catchment, water from all other upstream physical conveyances is routed directly to the top of and through the representative stream segment.

The reach network for the Gualala River watershed is based on the NHD flowlines available with the NHDPlus dataset. Those flowlines were edited as described in Section 2.1 to eliminate braiding and are shown in Figure 2-2. Within the NHDPlus schema, catchments can be related to flowlines through the catchment *FEATUREID* and flowline *COMID*. The flowline *COMID* was joined to the

PlusFlowlineVAA (value-added attributes) table available with the NHDPlus dataset to determine flow routing.

2.3 Stream Characteristics

The discharge for each stream segment is calculated in LSPC using the Manning equation, presented below as Equation 1:

$$Q = VA = (1.49/n)\, AR^{2/3}\sqrt{S}]$$

Where (A) is the cross-sectional area in square feet, (R) is the hydraulic radius in feet, (V) is the velocity in feet per second, (S) is the longitudinal slope in feet/feet, and (n) is the channel roughness coefficient.

Length and slope are derived from the NHDPlus VAA table, which includes precalculated reach characteristics based on local conditions. For reaches that were merged, split, or edited, the slope was recalculated as the length-weighted average slope (derived from DEM described in Section 3.4) based on the new reach length. The default cross-section representation in LSPC is a symmetrical trapezoidal channel defined using the terms shown in Figure 2-3. Stream segments are represented in the model as having the same cross-section for the entire reach length. Numerous studies have developed empirical relationships between stream channel geometry and upstream contributing area (Bent and Waite, 2013; McCandless, 2003a, 2003b; McCandless and Everett, 2002); these were used to derive channel geometry for each stream segment in LSPC. An initial estimate of n = 0.04 representing natural streams with vegetation was used for all reach segments and may be updated as needed during model calibration (Arcement and Schneider, 1989).

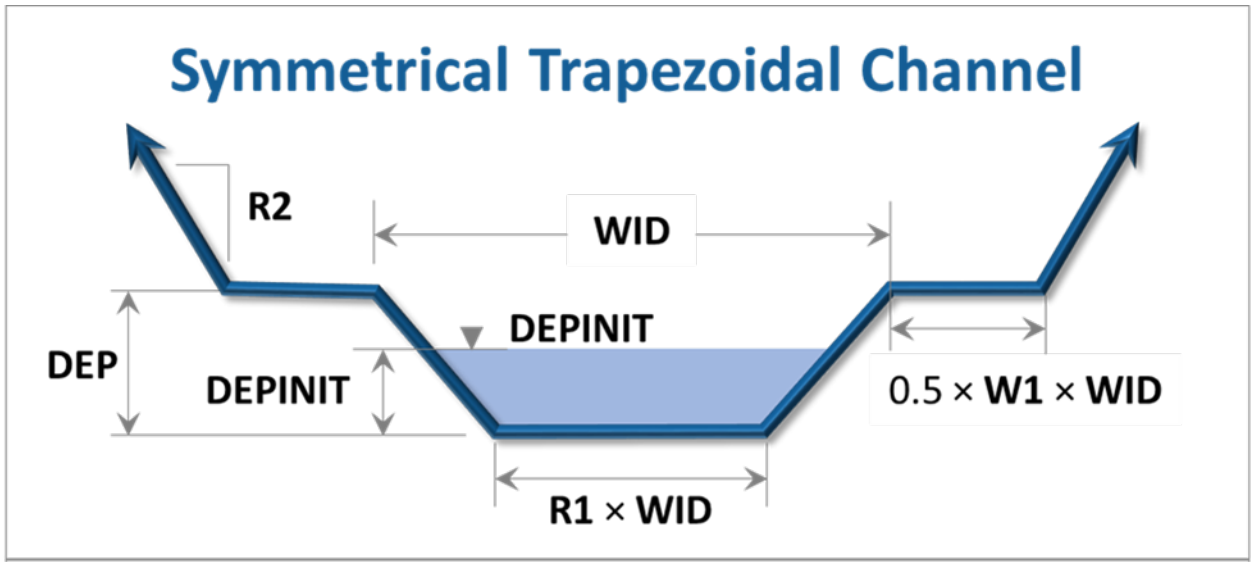

WID	Estimated Bankfull-Width	**R1**	Ratio of channel bottom width to **WID**
DEP	Estimated Bankfull-Depth	**R2**	Side slope for floodplain
DEPINIT	Initial water depth	**W1**	Floodplain width parameter

Figure 2-3. Example cross-section representations in LSPC.

3 HYDROLOGIC RESPONSE UNITS

Within LSPC, the land is categorized into HRUs, which are the core hydrologic modeling land units in the watershed model. Each HRU represents areas of similar physical characteristics attributable to certain processes. The HRU development process uses data types that are typically closely associated with hydrology (and water quality, when applicable) in the watershed. For the Gualala River watershed, this includes data such as land cover, cropland, soil type, and slope. The HRUs are developed by overlaying these datasets in raster format and identifying the unique combinations over catchments. Ultimately, some consolidation of HRUs was implemented to balance the model computational efficiency and optimal spatial resolution, resulting in a set of meaningful HRUs for model configuration. Percent tree canopy was also summarized as a secondary attribute by HRU and used to estimate initial values for the interception storage and lower-zone evapotranspiration rate for model configuration.

Table 3-1 lists the spatial data used in the HRU analysis along with the corresponding data sources. The following subsections summarize the data that were used to develop each of these spatial layers and the processes for consolidating them as HRUs.

Table 3-1. Summary of input datasets detailing data source and type

GIS Layer	Data Source	Site	Description	Date Downloaded
Digital Elevation Model	USGS 3D Elevation Program (3DEP)	Science Base	2020 – 27.79m resolution grid	August 1, 2024
Land Cover	MRLC (NLCD)	MRLC	2021 – 30m resolution grid	June 30, 2023
Cropland	USDA (CDL)	USDA	2022 – 30m resolution grid	January 2, 2023
Percent Imperviousness	MRLC (NLCD)	MRLC	2021 – 30m resolution grid	June 30, 2023
Percent Tree Canopy	MRLC	MRLC	2021 – 30m resolution grid	October 5, 2023
Soil Survey Geographic Database (SSURGO)	USDA (NRCS)	USDA	2022 – polygon layer	October 5, 2023

3.1 Land Cover

The land cover data were obtained from the 2021 National Land Cover Database (NLCD) maintained by the Multi-Resolution Land Consortium (MRLC), a joint effort between multiple federal agencies. The primary objective of the MRLC NLCD is to provide a current data product in the public domain with a consistent characterization of land cover across the United States. The 2021 NLCD provides a 16-class scheme at a 30-meter grid resolution.

Table 3-2 summarizes the NLCD 2021 land cover distribution for the Gualala River watershed; Figure 3-1 shows the land cover for the Gualala River watershed. Evergreen forest is the dominant land cover classification covering approximately 67% of the watershed area. When combined, evergreen forest plus the undeveloped categories of deciduous forest, mixed forest, shrub/scrub, and grassland/herbaceous, account for about 96% of the total watershed area. Developed land cover makes up less than 5% of the total watershed area and is classified mostly as "Developed, Open Space", which suggests that much of the developed area is dispersed. None of the watershed areas are categorized as cultivated cropland. For HRU development, similar NLCD classes (i.e., forest and grassland) were grouped.

Table 3-2. Distribution of 2021 NLCD land cover classes within the Gualala River watershed

NLCD Class	Description	Model Group [1]	Area	
			Acres	%
22	Developed, Low Intensity	Developed_Impervious	735.9	0.35%
23	Developed, Medium Intensity	Developed_Impervious	215.7	0.10%
24	Developed, High Intensity	Developed_Impervious	102.7	0.05%
21	Developed, Open Space	Developed_Pervious	6,170.5	2.90%
31	Barren Land (Rock/Sand/Clay)	Barren	15.3	0.01%
41	Deciduous Forest	Forest	655.6	0.31%
42	Evergreen Forest	Forest	141,564.4	66.63%
43	Mixed Forest	Forest	15,141.9	7.13%
52	Shrub/Scrub	Scrub	38,968.3	18.34%
71	Grassland/Herbaceous	Grassland	7,491.8	3.53%
81	Pasture/Hay	Pasture	2.2	0.00%
82	Cultivated Crops	Agriculture	0.0	0.00%
90	Woody Wetlands	Forest	705.7	0.33%
95	Emergent Herbaceous Wetlands	Grassland	316.7	0.15%
11	Open Water	Water	381.2	0.18%
		Total	**212,468**	**100%**

1. Developed land cover was refined and redistributed into effective Developed_Impervious and Developed_Pervious areas as described in Section 3.6.1. All other model groups categories are mapped for consolidation as shown.

Color Gradient: Lowest | Low | Med | High | Highest

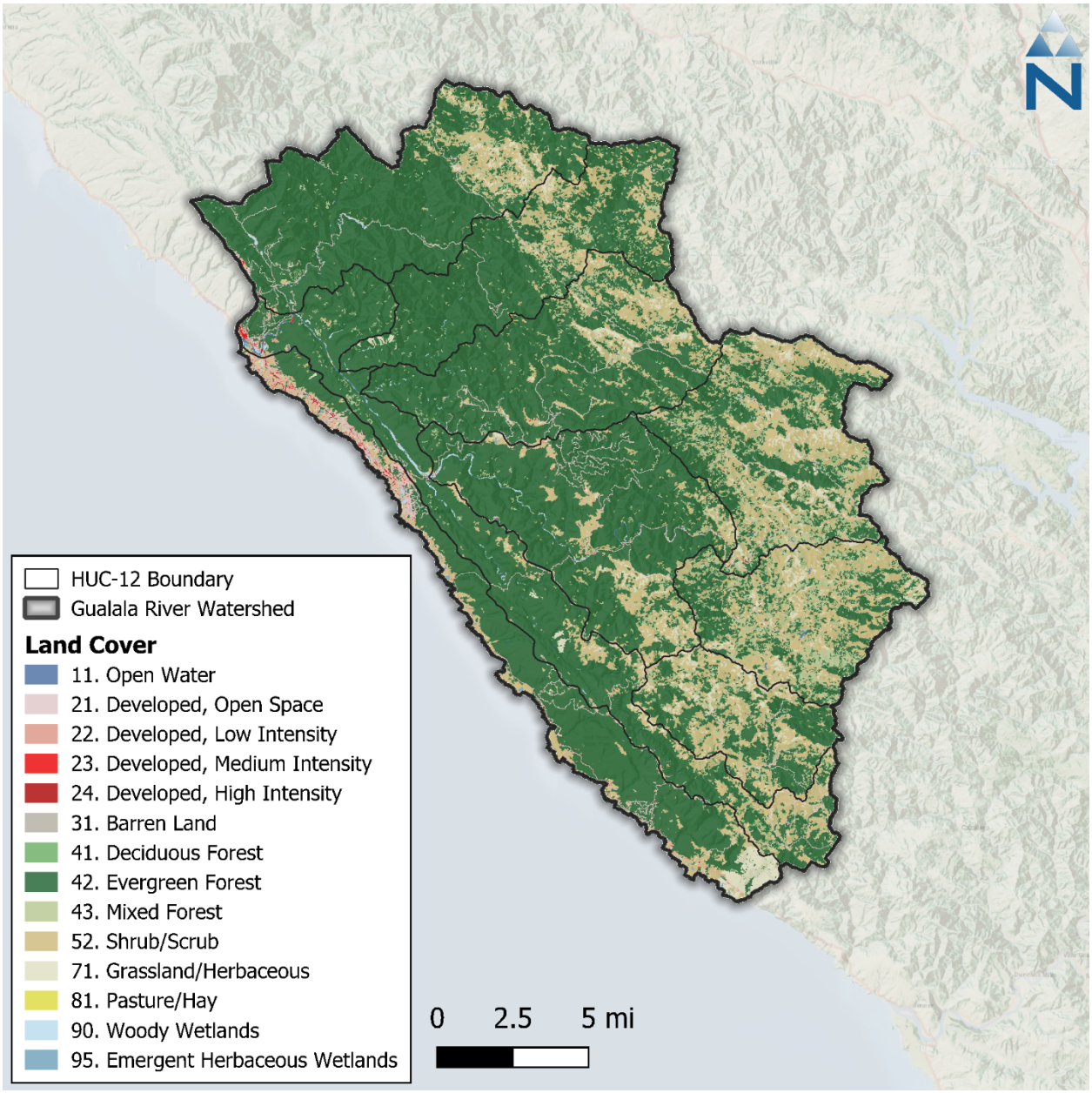

Figure 3-1. NLCD 2021 land cover within the Gualala River watershed.

3.2 Agriculture & Crops

Land cover data for the Gualala River Watershed (see Section 3.1) was analyzed to identify predominant cropland vegetation classes. This analysis revealed that less than 0.01% of the Gualala River watershed area is classified as Pasture/Hay (class 81) and 22% of the watershed was classified as either Shrub/Scrub (class 52) or Grassland/Herbaceous (class 71); of these areas, a portion may include areas of cultivated crops that were not automatically recognized through processing of the remote sensing data or include cultivated crops on a rotating schedule. To reflect these situations, supplemental information published by the United States Department of Agriculture (USDA) was used.

The USDA Cropland Data Layer (CDL) (USDA 2024) is an annual updated raster dataset that geo-references crop-specific land use. The dataset comes as a 30-meter resolution raster with a linked lookup table of 85 standard crop types that can be used to classify agricultural land. Figure 3-2 shows the spatial distribution of these classes through the study area, and Table 3-3 summarizes their areal coverage. The CDL Land use layer was intersected with the NLCD Land Cover layer, and CDL Agriculture and Pasture land use classifications overwrote the original NLCD classifications. The combined Land Use/Land Cover (LULC) increased "Cropland" to 788 acres (0.37%), which was classified as "Agriculture" in the final HRU layer— "Pasture" area was also updated to match CDL land use. The LULC intersection redistributes HRU area between originally classified Grassland, Pasture, and Agriculture categories from NLCD.

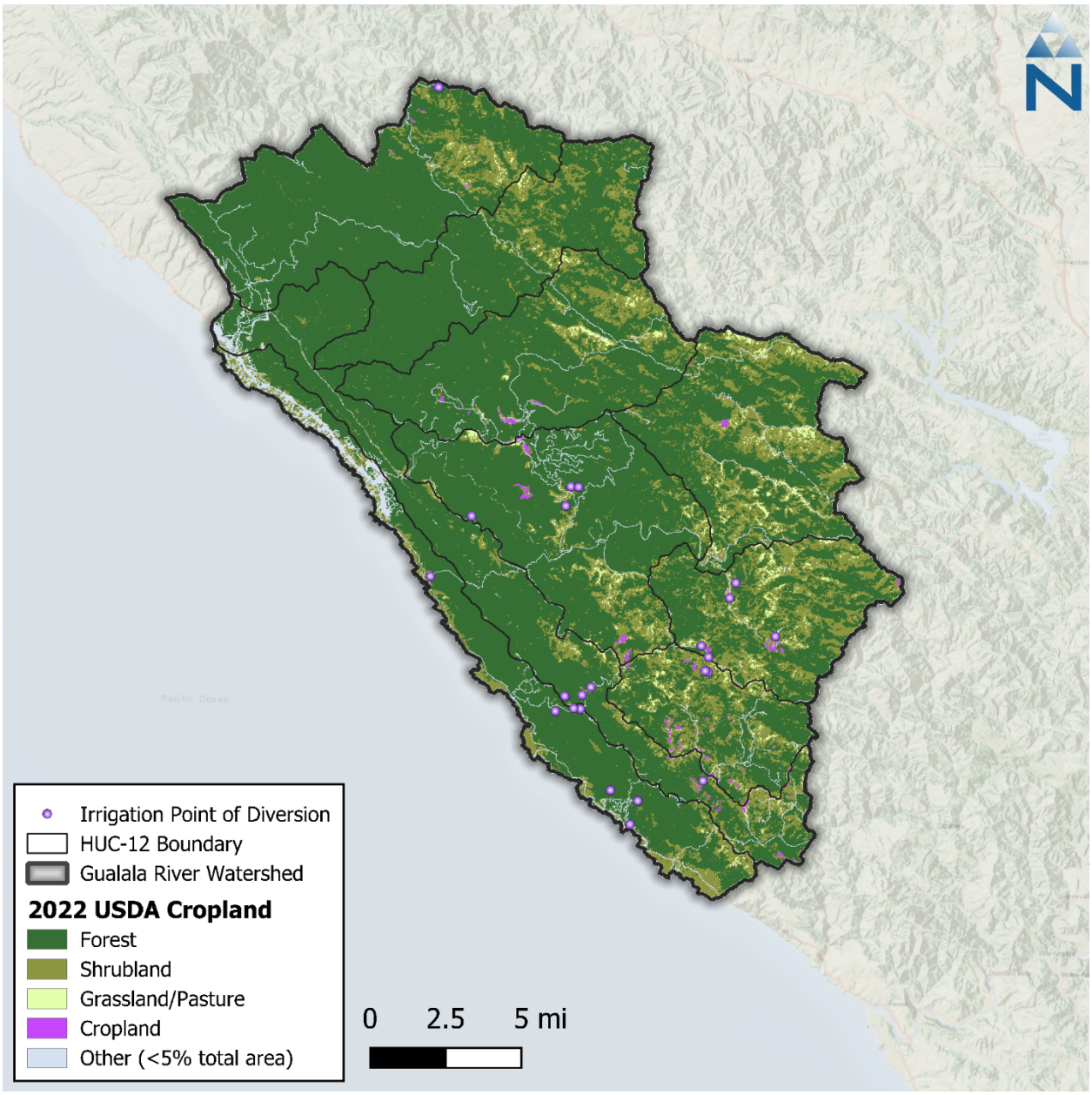

Figure 3-2 USDA 2022 Cropland Data within the Gualala River watershed.

Table 3-3 USDA 2022 Cropland Data summary within the Gualala River watershed

Crop Type	Area (ac)	Area (%)
Forest	157,200.1	73.99%
Shrubland	42,347.8	19.93%
Grassland/Pasture	4,016.9	1.89%
Cropland	788.4	0.37%
Other (<5% Total Area)	8,114.9	3.82%
Total	**212,468.1**	**100.00%**

Color Gradient: Lowest | Low | Medium | High | Highest

Table 3-4 shows the impact that intersecting NLCD with CDL has on mapped cropland and pasture areas. It also shows which NLCD categories were reclassified into Cropland and Pasture, and which were unchanged.

Table 3-4 Intersection of NLCD and USDA 2022 Cropland Data Layer for the Gualala River watershed

NLCD Class	Description	NLCD (acres)		Crop Data Layer (acres)		
		Original	Changed[1]	No Change	Cropland	Pasture
22	Developed, Low Intensity	735.9	0.00%	734.1	1.8	0.0
23	Developed, Medium Intensity	215.7	0.00%	215.7	0.0	0.0
24	Developed, High Intensity	102.7	0.00%	102.7	0.0	0.0
21	Developed, Open Space	6,170.5	0.00%	6,166.3	1.1	3.1
31	Barren Land (Rock/Sand/Clay)	15.3	0.00%	12.9	1.1	1.3
41	Deciduous Forest	655.6	0.00%	652.7	0.0	2.9
42	Evergreen Forest	141,564.4	0.05%	141,465.5	33.1	65.8
43	Mixed Forest	15,141.9	0.02%	15,098.1	5.6	38.3
52	Shrub/Scrub	38,968.3	0.80%	37,261.4	681.2	1,025.7
71	Grassland/Herbaceous	7,491.8	1.38%	4,565.3	60.3	2,866.2
81	Pasture/Hay	2.2	0.00%	2.2	0.0	0.0
82	Cultivated Crops	0.0	--	0.0	0.0	0.0
90	Woody Wetlands	705.7	0.00%	701.7	0.9	3.1
95	Emergent Herbaceous Wetlands	316.7	0.01%	305.6	1.8	9.3
11	Open Water	381.2	0.00%	378.5	1.6	1.1
	Total:	**212,467.9**	**2.26%**	**207,662.8**	**788.4**	**4,016.9**

1. Expressed as a percentage of the entire Gualala River Watershed

3.3 Soils

Soil data for the Gualala River watershed were obtained from the Soil Survey Geographic Database (SSURGO) published by the Natural Resource Conservation Service (NRCS). Four primary hydrologic soil groups (HSG) are used to characterize soil runoff potential. Group A generally has the lowest runoff potential, whereas Group D has the highest runoff potential. The SSURGO soils database is composed of a GIS polygon layer of map units and a linked tabular database with multiple layers of soil properties.

Table 3-5 and Figure 3-3 present summaries of the SSURGO hydrologic soil groups for the Gualala River watershed. The dominant soil group in the watershed is Group B (57%), containing moderately well to well-drained silt loams and loams. Group C (32%) is the next most common soil group in the watershed, containing sandy clay loam that typically has low infiltration rates. Group D, with the lowest infiltration rates, makes up approximately 9% of the watershed. Less than 1% of the watershed areas have mixed soil. For modeling purposes, mixed soils were grouped with the nearest primary group as follows: A/D → B, B/D → C, and C/D → D. Less than 1% of the watershed HSG area is classified as unknown in the SSURGO database. Since most of the soil in the watershed is Group B, the "Unclassified" soil areas are also considered to be Group B in the analysis.

Table 3-5. NRCS Hydrologic soil groups in the Gualala River watershed

Soil Group	Model Group	Area (acre)	Area (%)
A	A	2,687	1.3%
B	B	121,239	57.1%
C	C	67,796	31.9%
C/D	D	301	0.1%
D	D	18,615	8.8%
Unclassified	B	1,829	0.9%
	Total	**212,468**	**100%**

Color Gradient: Lowest | Low | Medium | High | Highest

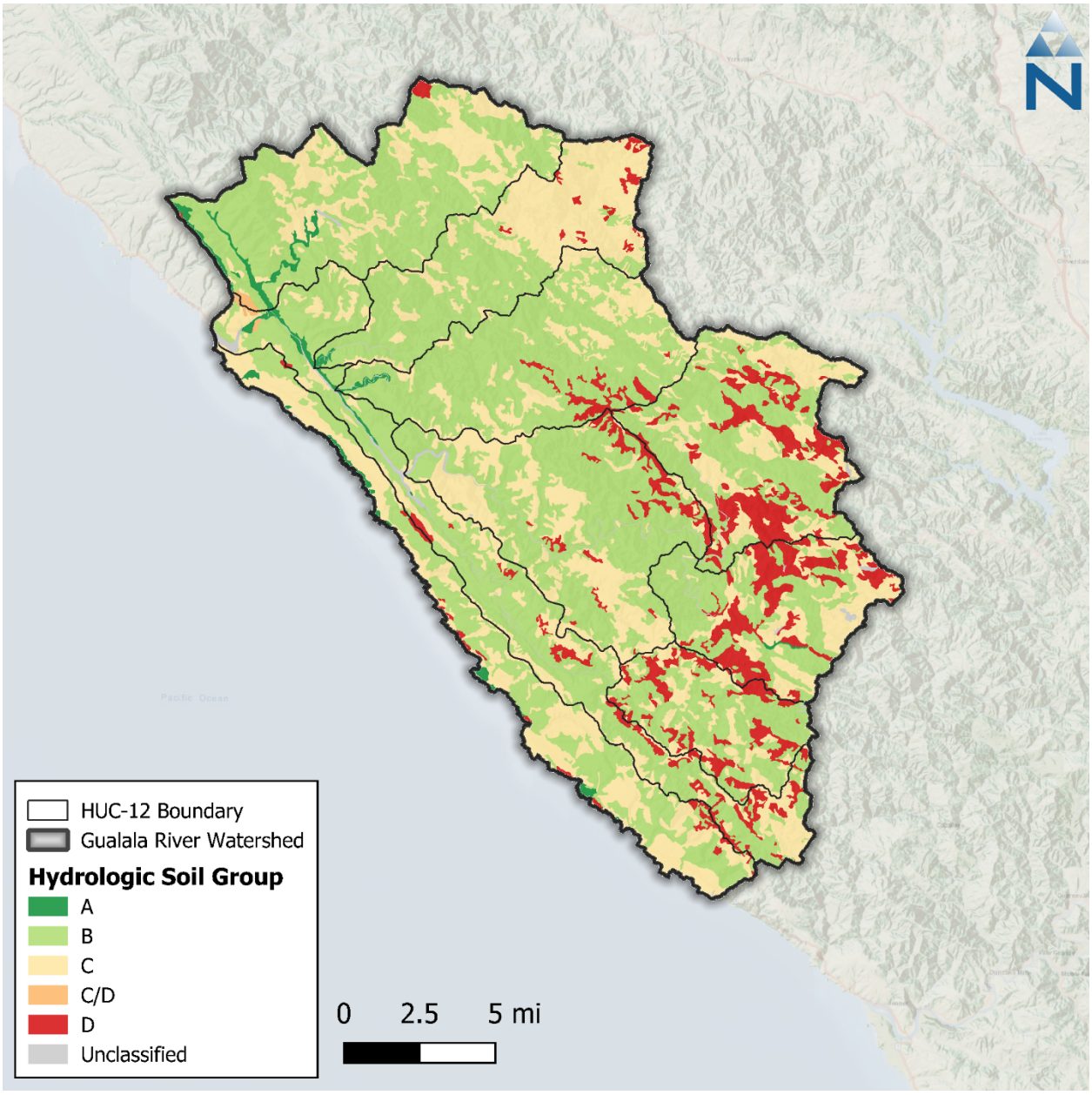

Figure 3-3. SSURGO hydrologic soil groups within the Gualala River watershed.

3.4 Elevation and Slope

The United States Geological Survey (USGS) 3D Elevation Program (3DEP) publishes DEMs expressing landscape elevation through a raster grid data product with a 1 arc-second (approximately 30-meter) horizontal resolution. The 1 arc-second data covering the Gualala watershed had a resolution of 27.79 meters and thus was resampled to 30 meters for consistency with the rest of the datasets for the HRU analysis. The Gualala watershed ranges in elevation from near sea level along the coastline to over 800 meters at several of the highest elevation peaks in the eastern portion of the watershed.

The 30-meter DEM was used to generate a slope (percent rise) raster for the watershed. Figure 3-4 illustrates the cumulative distribution function (CDF) of the slope raster values across the model domain as a percentage of the total watershed land area (i.e., excluding major water bodies). The CDF was used to identify appropriate bins for HRU slope categories during the HRU definition process. Slopes were categorized as low (< 5%), medium (5 to 15%), and high (>15%) according to their distribution and overlap with the land cover layer. Table 3-6 and Figure 3-5 present the distribution of slope categories within the watershed.

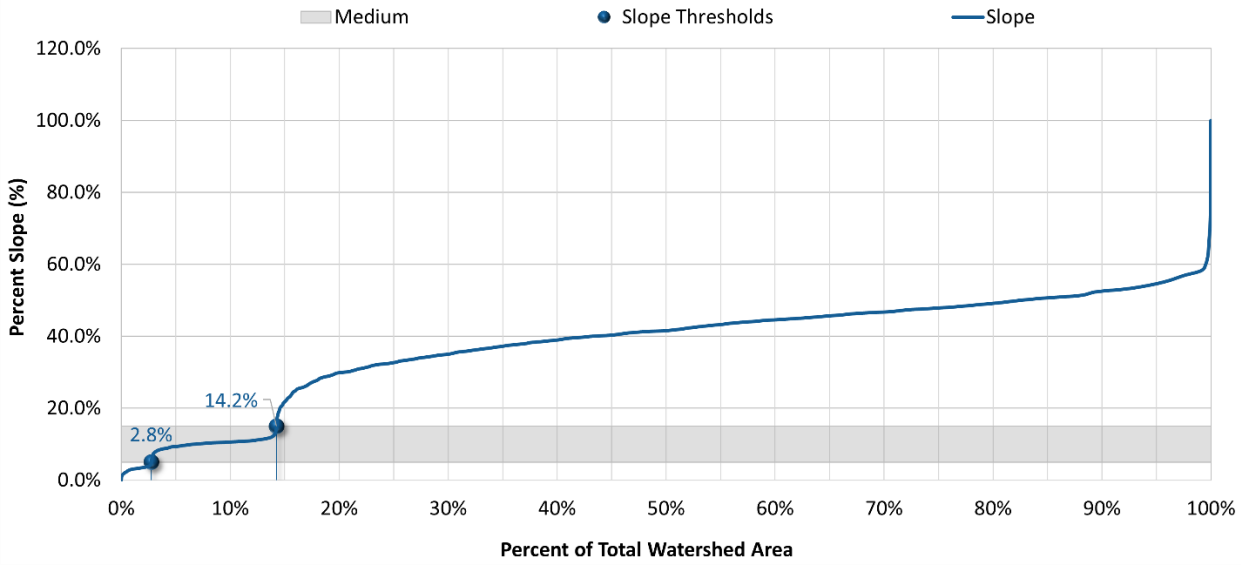

Figure 3-4. Cumulative distribution of slope categories within the Gualala River watershed.

Table 3-6. Distribution of slope categories within the Gualala River watershed

Slope (%)	Slope Category	HRU Group	Area (ac)	Area (%)
0-5	Low	Low	5,860.1	2.8%
5-15	Medium	Med	24,395.7	11.5%
>15	High	High	182,212.3	85.8%
		Total	**212,468**	**100%**

Color Gradient: Lowest | Low | Medium | High | Highest

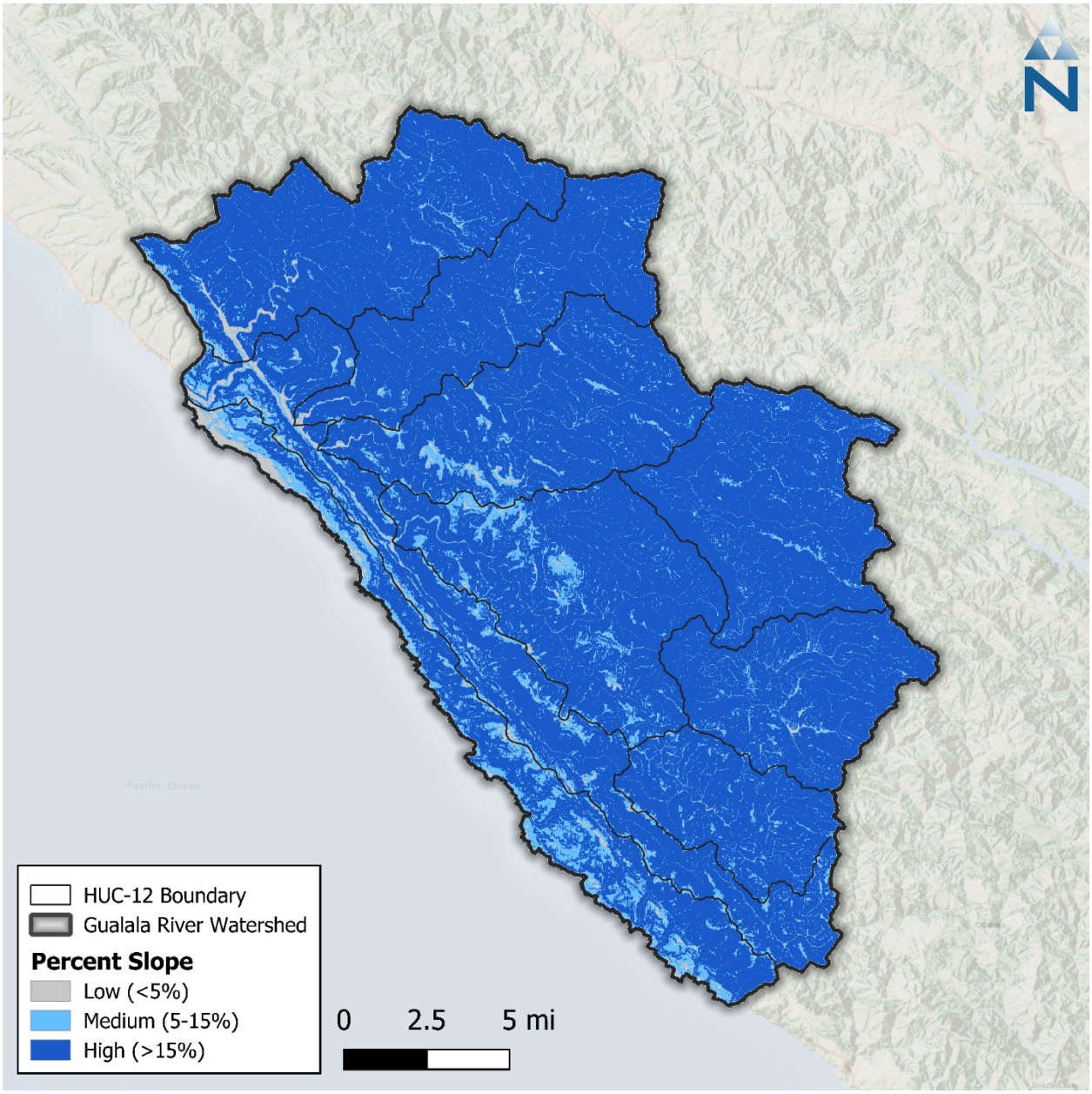

Figure 3-5. Percent Slope derived from the DEM within the Gualala River watershed.

3.4.1 Length and Slope of Overland Flow

Overland flow lengths on high slopes are generally shorter and more direct and have faster travel times on high slopes, but generally longer and less direct with slower travel times on lower slopes. It was found during the Navarro River modeling effort that using an empirical relationship shown in Figure 3-6, derived by inversely scaling length of overland flow (LSUR) with slope of overland flow (SLSUR), improved model prediction of peak flow timing. Figure 3-7 is the resulting cumulative distribution of LSUR and SLSUR in the Gualala River watershed. Longer flow lengths on shallow sloped areas increase the opportunity for attenuation, surface storage, and infiltration. On the other hand, shorter flow lengths on steeper slopes retain the flashiness where applicable. Similar modeling efforts have historically used discrete/fixed values and ranges for SLSUR and LSUR to better manage

the degrees of freedom among model variables. However, because SLSUR can be measured by HRU from remotely-sensed data, applying a relationship to also estimate LSUR as a function of SLSUR preserves some natural variability throughout the watershed that (1) can provide some improvement relative to initial hydrology prediction using constant values and (2) helps to reduce the chance of adjusting other parameters during calibration that are better explained by the influence of LSUR and SLSUR.

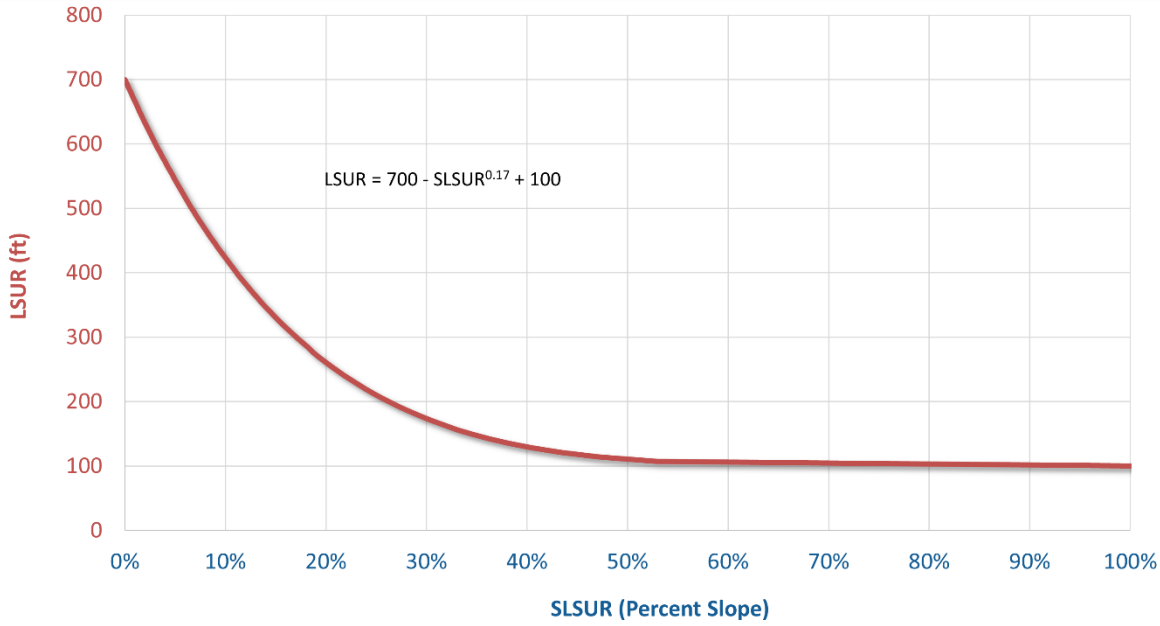

Figure 3-6. Empirical relationship of LSUR vs. SLSUR.

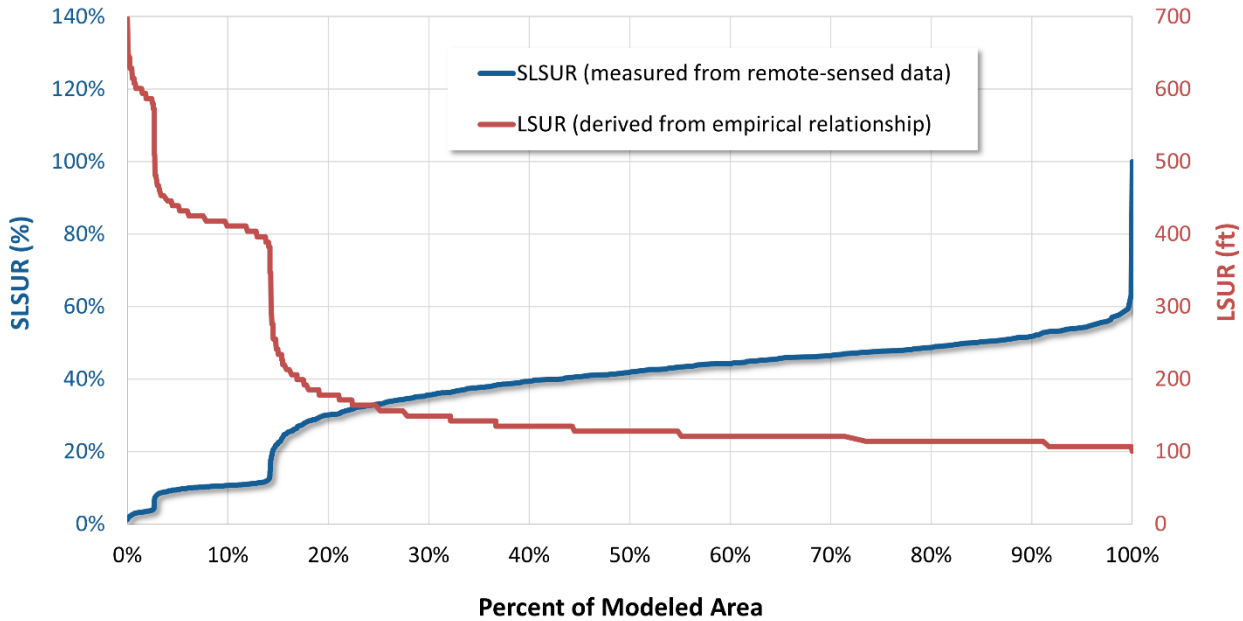

Figure 3-7. Cumulative distribution of LSUR and SLSUR in the Gualala River watershed derived from the generalized empirical relationship.

3.5 Secondary Attributes

Secondary attributes can be included in the HRU development process to provide additional information not directly mapped in the HRU categories. Secondary attributes used for the Gualala River watershed include impervious and tree canopy cover percentages. The impervious cover percentage is used for the translation of mapped impervious cover to effective impervious cover, while percent canopy estimates can inform certain hydrologic parameters but won't be represented in the HRUs as a category.

3.5.1 Impervious Cover

MRLC publishes a developed impervious cover dataset as a companion to the NLCD land cover. This dataset is also provided as a raster with a 30-meter grid resolution. Impervious cover is expressed in each raster pixel as a percentage of the total area ranging from 0 to 100 percent. Figure 3-8 shows the NLCD impervious 2021 cover dataset for the Gualala River watershed. Because this dataset provides impervious cover estimates for areas classified as developed, non-zero values closely align with developed areas (NLCD classification codes 21 through 24).

The percentage impervious cover was used in HRU development to further group developed land cover classes into pervious or impervious and to distinguish between mapped impervious area (MIA) and effective impervious area (EIA), as discussed in Section 3.6.1.

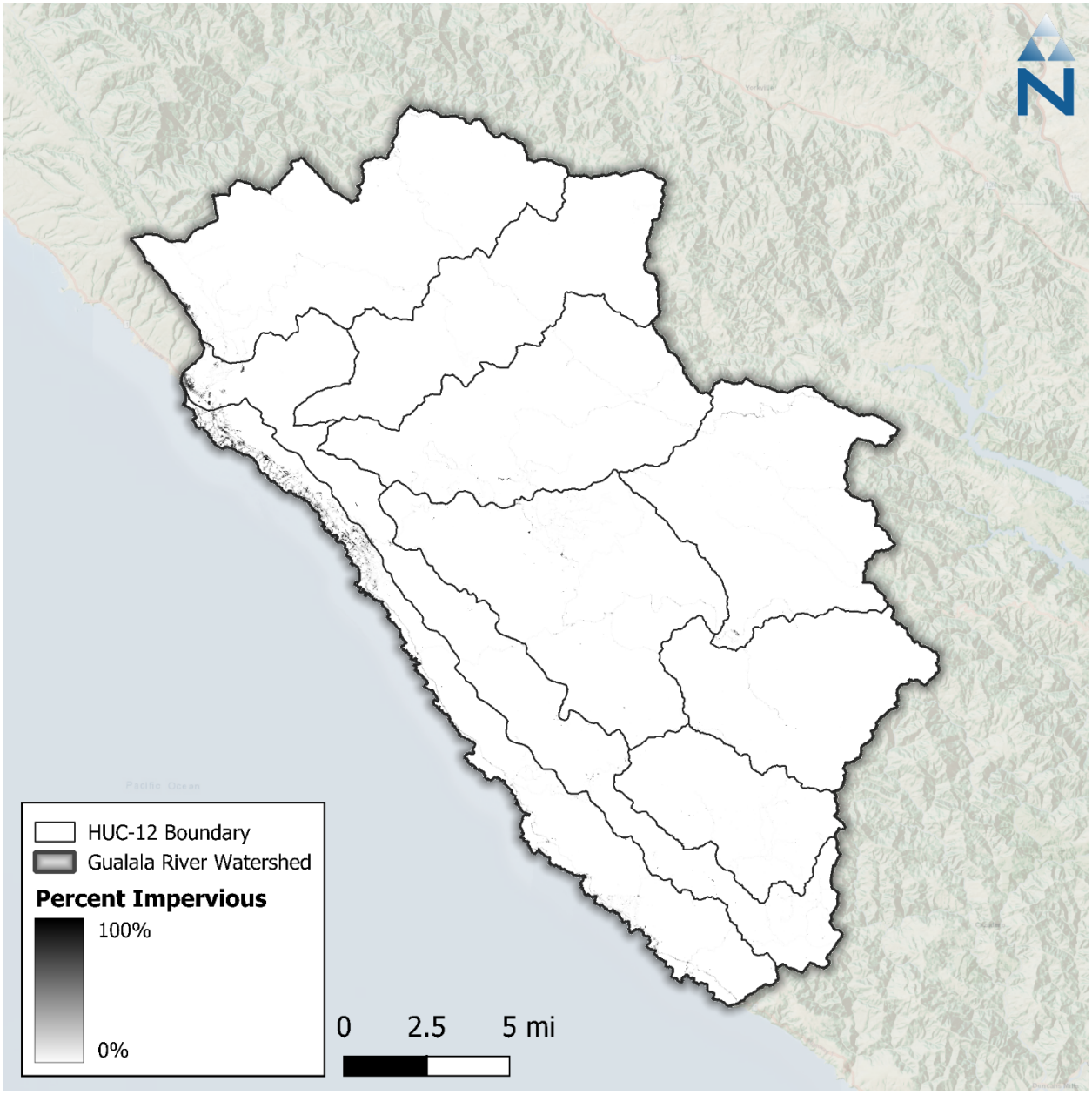

Figure 3-8. NLCD 2021 percent impervious cover in the Gualala River watershed.

3.5.2 Tree Canopy

MRLC publishes a tree canopy dataset as a companion to the NLCD land cover dataset that estimates the percentage of tree canopy cover spatially. The United States Forest Service (USFS) developed the underlying data model, which is available through its partnership with the MRLC. This dataset is also provided as a raster with a 30-meter grid resolution. Like the impervious cover dataset, each raster grid cell expresses the percentage of grid cell area covered by tree canopy with values ranging from 0 to 100 percent. The Gualala watershed has the highest canopy coverage of 91% toward the northwest (Figure 3-9). Tree canopy cover data was used to estimate model parameters such as interception storage and lower-zone evapotranspiration rates.

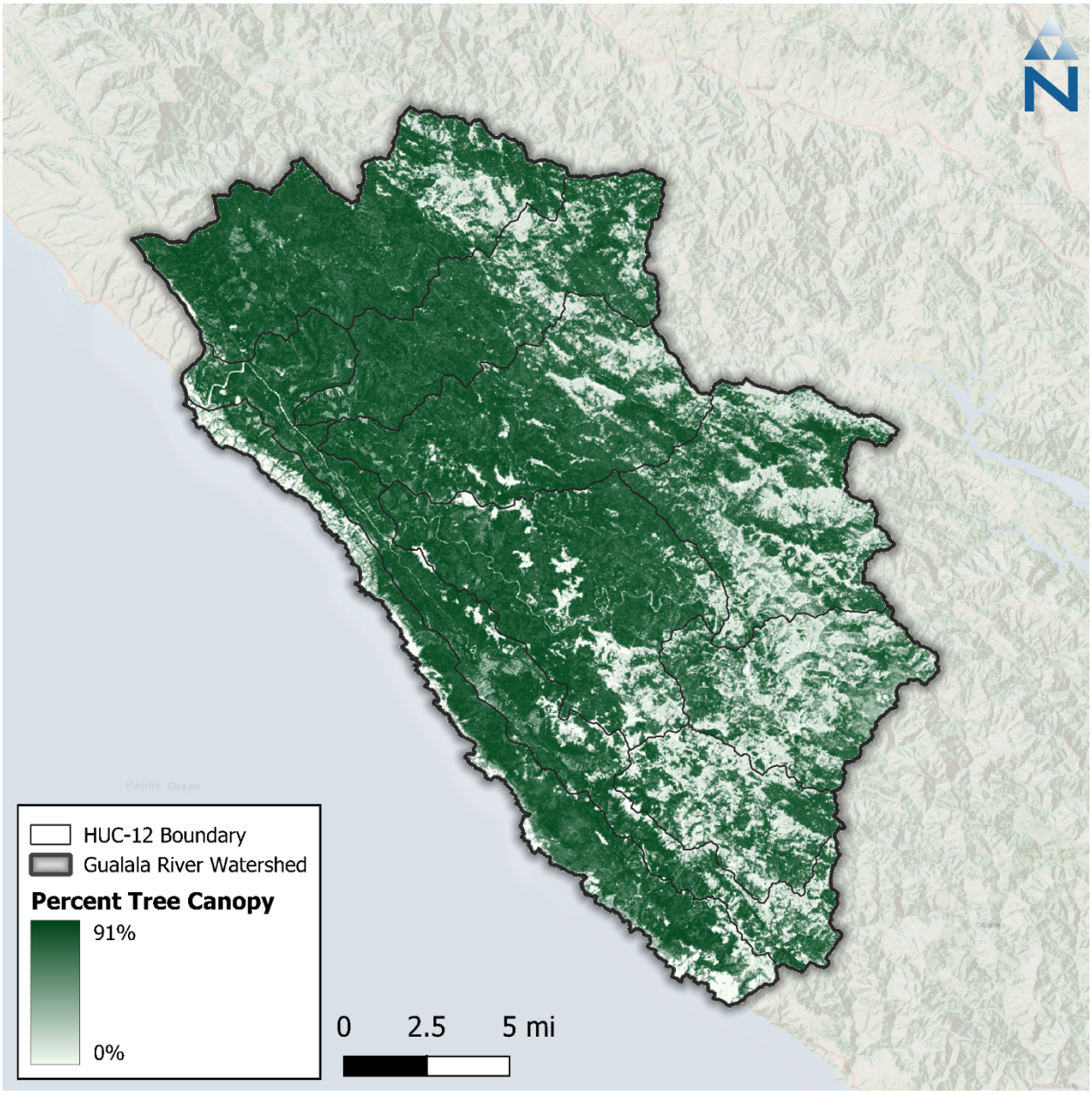

Figure 3-9. NLCD 2021 percent tree canopy cover in the Gualala River Watershed.

3.6 HRU Consolidation

The five spatial datasets described above (land cover, cropland, impervious cover, soils, and slope) were spatially overlayed in GIS to derive a composite raster where each grid cell shows the combination of the values from the overlayed datasets. A zonal statistics operation is then performed in GIS to generate a summary table identifying unique grid cell values (i.e., HRUs) from the composite raster and corresponding areas across catchments. The combination of these datasets resulted in 132 potential HRUs. To balance model computational efficiency, the impervious HRUs were consolidated for soil and slope combinations to reduce the overall number of unique HRUs. This step was necessary to develop a model with a reasonable run time while maintaining the optimal model resolution to characterize hydrologic conditions adequately. The HRU refinement process involves analyzing the

percentage of the model area attributed to each unique HRU combination as shown in Table 3-7. The spatial distribution of mapped HRUs across the watershed is shown in Figure 3-10. Additionally, the impervious percentage is used to adjust and group developed land cover classes (Section 3.6.1) and agriculture areas located in the catchments of point of diversions were assigned as irrigation HRUs (Section 5.2.2). The final 98 modeled HRU categories are described in Section 3.6.2.

Table 3-7. Percent land cover distribution by mapped HRU category for the Gualala River watershed

Land Use / Land Cover (LULC)	Total Area (%)	Soil Group (% LULC Area)				Slope (% LULC Area)		
		A	B	C	D	0-5	5-15	>15
Developed_Low_Intensity	0.3%	15.5%	16.6%	62.0%	6.0%	29.9%	44.0%	26.1%
Developed_Medium_Intensity	0.1%	15.7%	29.8%	51.6%	2.9%	34.6%	44.8%	20.5%
Developed_High_Intensity	0.0%	15.8%	21.2%	62.1%	0.9%	38.5%	48.3%	13.2%
Developed_Open_Space	2.9%	5.3%	44.0%	42.6%	8.1%	10.1%	30.8%	59.1%
Barren	0.0%	3.4%	72.4%	22.4%	1.7%	15.5%	37.9%	46.6%
Forest	74.3%	1.1%	68.7%	25.8%	4.5%	2.0%	9.4%	88.6%
Scrub	17.5%	1.1%	25.7%	49.6%	23.6%	3.3%	13.7%	83.0%
Grassland	2.3%	1.0%	25.4%	54.6%	18.9%	4.4%	17.1%	78.5%
Pasture	1.9%	0.4%	11.6%	54.6%	33.3%	3.5%	18.1%	78.4%
Agriculture	0.4%	3.5%	24.5%	57.9%	14.2%	11.2%	41.9%	47.0%
Water	0.2%	8.8%	68.3%	17.7%	5.2%	27.4%	35.5%	37.1%
Total	**100.0%**	**1.3%**	**57.9%**	**31.9%**	**8.9%**	**2.8%**	**11.5%**	**85.8%**

Color gradients indicate more Watershed Area and an increasing percentage of Soil and Slope, respectively.

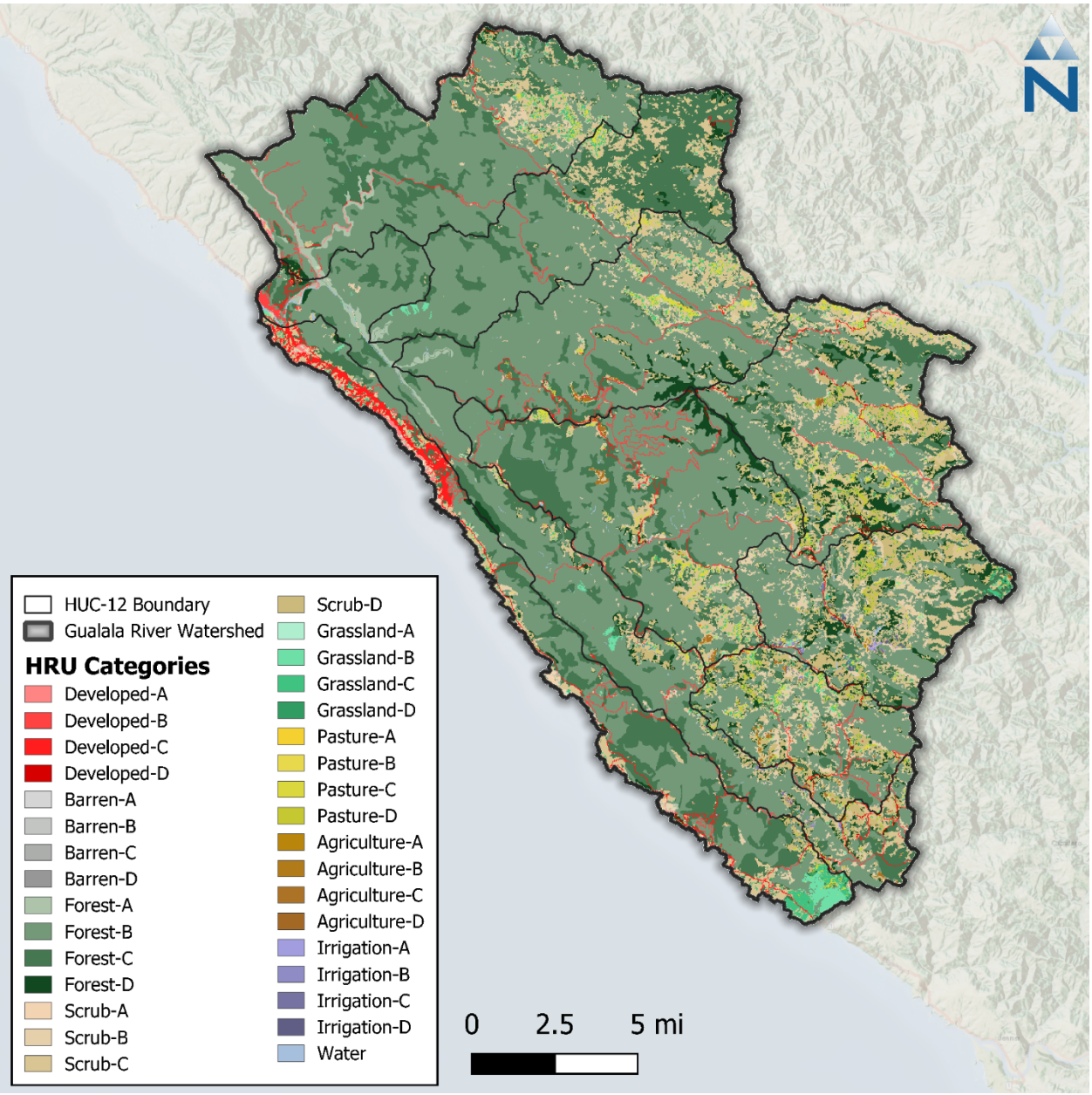

Figure 3-10. Mapped HRU categories within the Gualala River watershed. Note that developed area and slope categories are consolidated for visual clarity.

3.6.1 Directly Connected Impervious Area

The HRU approach not only highlights the predominant composition of an area within the catchment but also provides additional texture and physical basis for parameterizing and representing natural processes. Within a given modeled catchment, HRU segments are modeled as being parallel to one another. Each HRU segment flows directly to the routing stream segment without any interaction with neighboring HRU segments. However, in the physical environment, the lines between impervious and pervious land are not as clearly distinguished—impervious land may flow downhill over pervious land on route to a storm drain or watercourse.

For modeling purposes, Effective Impervious Area (EIA) represents the portion of the total, or Mapped Impervious Area (MIA), that routes directly to the stream segments. It is derived as a function of the percent Directly Connected Impervious Area (DCIA), with other adjustments as needed to account for other structural and non-structural management practices in the flow network. Figure 3-11 illustrates the transitional sequence from MIA to DCIA. Impervious areas that are not connected to the drainage network can flow onto pervious surfaces, infiltrate, and become part of the pervious subsurface and overland flow. Because segments are modeled as being parallel to one another in LSPC, this process can be approximated using a conversion of a portion of impervious land to pervious land. On the open landscape, runoff from disconnected impervious surfaces can overwhelm the infiltration capacity of adjacent pervious surfaces during large rainfall/runoff events creating sheet flow over the landscape—therefore, the MIA→EIA translation is not actually a direct linear conversion. Finding the right balance between MIA and EIA can be an important part of the hydrology calibration effort.

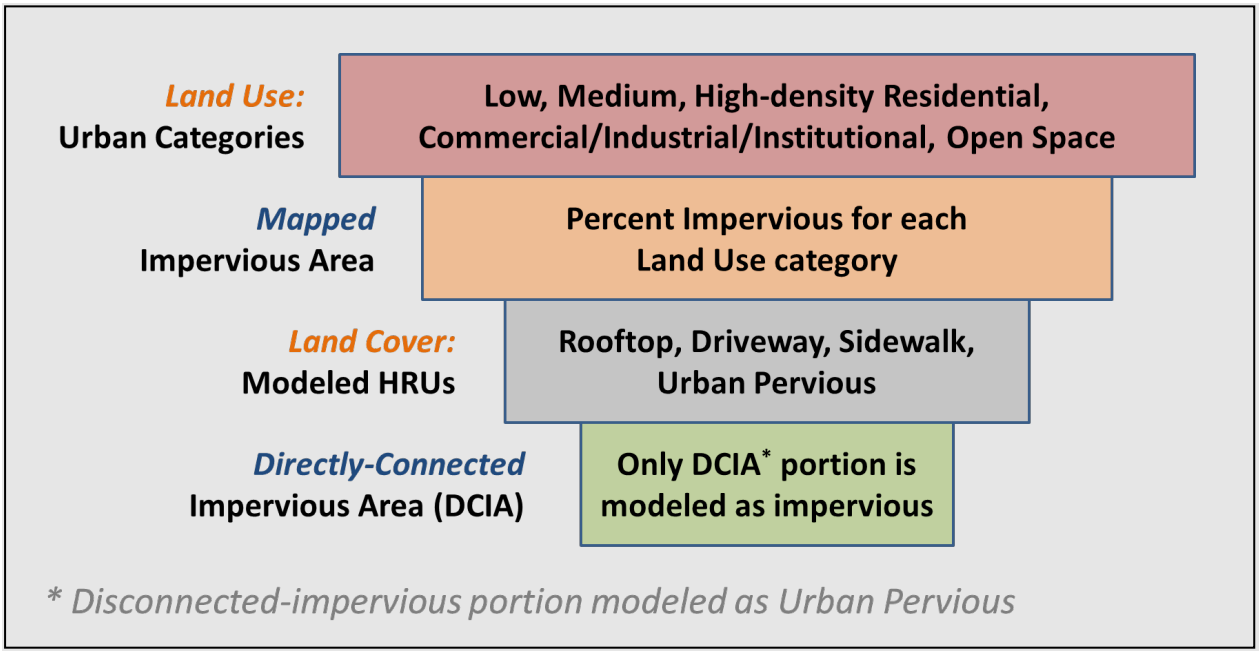

Figure 3-11. Generalized translation sequence from MIA to DCIA.

Empirical relationships like the Sutherland Equations (Sutherland, 2000) presented in Figure 3-12 show a strong correlation between the *density* of developed areas and DCIA. The curve for high-density developed land trends closer to the line of equal value than the curve for less developed areas. Similarly, as the density of the mapped impervious area approaches 100%, the translation to DCIA also approaches 100%. An initial estimate of EIA is equal to MIA × DCIA. This empirical approximation can be further refined during model calibration to account for other flow disconnections resulting from structural or non-structural BMP practices or other inline hydraulic routing features.

For the Gualala River watershed, each developed land cover category was assigned a DCIA curve as shown in Table 3-8. The MIA, which is the impervious portion of each grid, was converted to EIA areas using these equations. Sutherland (2000) notes that areas with less than 1% MIA effectively behave like 100% pervious areas; therefore, EIA adjustments were only applicable to "Developed" areas. Table 3-9 is a summary of resampled MIA and calculated EIA by the land cover groups.

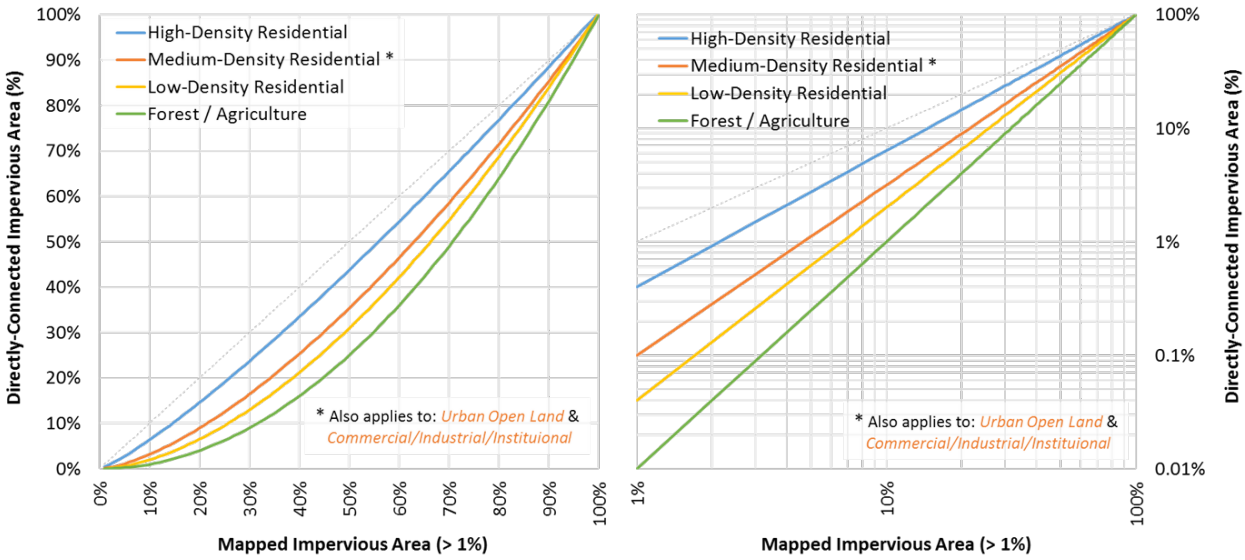

Figure 3-12. Mapped and directly connected impervious area relationships (Sutherland, 2000).

Table 3-8. Assignment of DCIA curves by land cover category

Land Cover	MIA *	EIA	EIA:MIA	Equation
High Density Developed	85.05%	82.74%	97%	$DCIA=0.4(MIA)^{1.2}$
Medium Density Developed	62.45%	49.39%	79%	$DCIA=0.1(MIA)^{1.5}$
Low Density Developed	30.59%	13.48%	44%	$DCIA=0.04(MIA)^{1.7}$
Open Space	3.65%	0.17%	5%	$DCIA=0.01(MIA)^{2.0}$
Undeveloped	0.00%	0.00%	0%	DCIA=0

* Areas with MIA < 1% are assumed be 100% disconnected (EIA = 0)

Color Gradient:	Lowest	Low	Medium	High	Highest

Table 3-9. Distribution of impervious area by grouped NLCD land cover class

Model Group	Total Area		Impervious (acre)		Impervious (%)	
	Acre	%	MIA	EIA	MIA	EIA
Developed_Low_Intensity	734.1	0.35%	224.58	98.98	30.6%	13.5%
Developed_Medium_Intensity	215.7	0.10%	134.71	106.55	62.4%	49.4%
Developed_High_Intensity	102.7	0.05%	87.39	85.01	85.1%	82.7%
Developed_Open_Space	6,166.3	2.90%	224.97	10.41	3.6%	0.2%
Barren	12.9	0.01%	0.00	0.00	0.0%	0.0%
Forest (Deciduous)	652.7	0.31%	0.00	0.00	0.0%	0.0%
Forest (Evergreen)	141,465.5	66.58%	0.00	0.00	0.0%	0.0%
Forest (Mixed)	15,098.1	7.11%	0.00	0.00	0.0%	0.0%
Scrub	37,261.4	17.54%	0.00	0.00	0.0%	0.0%
Grassland (Herbaceous)	4,565.3	2.15%	0.00	0.00	0.0%	0.0%
Pasture	4,019.1	1.89%	0.03	0.00	0.0%	0.0%
Agriculture	788.4	0.37%	0.66	0.00	0.1%	0.0%
Forest (Woody Wetlands)	701.7	0.33%	0.00	0.00	0.0%	0.0%
Grassland (Herbaceous Wetland)	305.6	0.14%	0.00	0.00	0.0%	0.0%
Water	378.5	0.18%	0.00	0.00	0.0%	0.0%
Total	**212,468**	**100%**	**672.3**	**300.9**	**--**	**--**

Color gradients indicate model groups with more Watershed Area and Imperviousness, respectively.

3.6.2 Modeled HRU Categories

The combinations of LULC, HSG, and slope represent the physical characteristics that influence hydrology. After accounting for DCIA, the four developed land cover classes were rolled up as either "Developed Impervious" or "Developed Pervious" stratified by HSG and slope. Agriculture HRUs (i.e., 4 HSGs × 3 slopes = 12 combinations) were further divided into irrigated and non-irrigated counterparts for a total of 24 HRUs. Altogether, a total of 98 HRU categories comprised the basic building blocks used in LSPC to represent hydrologic responses in the watershed. The "Agriculture" and "Pasture" HRU areas within catchments where streamflow was withdrawn for agricultural use were re-assigned to their "Irrigation" HRU counterparts. Irrigation was simulated for those HRUs as described in Section 5.2. The final HRU distribution in the watershed is shown in Table 3-10.

Table 3-10. Modeled HRU distribution within the Gualala River watershed

HRU ID	Land Use - Land Cover	HSG	Slope	Area	
				Acre	%
1000	Developed_Impervious	All	All	300.96	0.1%
2110	Developed_Pervious	A	Low	150.52	0.1%
2120	Developed_Pervious	A	Med	187.98	0.1%
2130	Developed_Pervious	A	High	107.27	0.1%
2210	Developed_Pervious	B	Low	126.15	0.1%

HRU ID	Land Use - Land Cover	HSG	Slope	Area	
				Acre	%
2220	Developed_Pervious	B	Med	549.05	0.3%
2230	Developed_Pervious	B	High	2,175.45	1.0%
2310	Developed_Pervious	C	Low	535.40	0.3%
2320	Developed_Pervious	C	Med	1,343.81	0.6%
2330	Developed_Pervious	C	High	1,201.46	0.6%
2410	Developed_Pervious	D	Low	41.64	0.0%
2420	Developed_Pervious	D	Med	150.36	0.1%
2430	Developed_Pervious	D	High	348.86	0.2%
3110	Barren	A	Low	0.22	0.0%
3120	Barren	A	Med	0.00	0.0%
3130	Barren	A	High	0.22	0.0%
3210	Barren	B	Low	1.56	0.0%
3220	Barren	B	Med	3.78	0.0%
3230	Barren	B	High	4.00	0.0%
3310	Barren	C	Low	0.22	0.0%
3320	Barren	C	Med	1.11	0.0%
3330	Barren	C	High	1.56	0.0%
3410	Barren	D	Low	0.00	0.0%
3420	Barren	D	Med	0.00	0.0%
3430	Barren	D	High	0.22	0.0%
4110	Forest	A	Low	672.96	0.3%
4120	Forest	A	Med	467.03	0.2%
4130	Forest	A	High	529.74	0.2%
4210	Forest	B	Low	1,302.12	0.6%
4220	Forest	B	Med	8,133.17	3.8%
4230	Forest	B	High	98,979.99	46.6%
4310	Forest	C	Low	996.10	0.5%
4320	Forest	C	Med	5,715.30	2.7%
4330	Forest	C	High	33,954.44	16.0%
4410	Forest	D	Low	157.01	0.1%
4420	Forest	D	Med	587.79	0.3%
4430	Forest	D	High	6,422.29	3.0%
5110	Scrub	A	Low	99.85	0.0%
5120	Scrub	A	Med	185.48	0.1%
5130	Scrub	A	High	112.09	0.1%
5210	Scrub	B	Low	196.60	0.1%
5220	Scrub	B	Med	945.40	0.4%
5230	Scrub	B	High	8,421.61	4.0%
5310	Scrub	C	Low	794.84	0.4%

HRU ID	Land Use - Land Cover	HSG	Slope	Area	
				Acre	%
5320	Scrub	C	Med	3,110.85	1.5%
5330	Scrub	C	High	14,589.04	6.9%
5410	Scrub	D	Low	138.11	0.1%
5420	Scrub	D	Med	859.78	0.4%
5430	Scrub	D	High	7,807.81	3.7%
6110	Grassland	A	Low	11.34	0.0%
6120	Grassland	A	Med	17.57	0.0%
6130	Grassland	A	High	19.79	0.0%
6210	Grassland	B	Low	45.81	0.0%
6220	Grassland	B	Med	147.45	0.1%
6230	Grassland	B	High	1,046.14	0.5%
6310	Grassland	C	Low	130.55	0.1%
6320	Grassland	C	Med	523.96	0.2%
6330	Grassland	C	High	2,006.88	0.9%
6410	Grassland	D	Low	25.58	0.0%
6420	Grassland	D	Med	144.11	0.1%
6430	Grassland	D	High	751.69	0.4%
7110	Pasture	A	Low	3.11	0.0%
7120	Pasture	A	Med	6.45	0.0%
7130	Pasture	A	High	1.33	0.0%
7210	Pasture	B	Low	17.79	0.0%
7220	Pasture	B	Med	81.84	0.0%
7230	Pasture	B	High	331.37	0.2%
7310	Pasture	C	Low	78.51	0.0%
7320	Pasture	C	Med	412.99	0.2%
7330	Pasture	C	High	1,572.77	0.7%
7410	Pasture	D	Low	20.46	0.0%
7420	Pasture	D	Med	135.66	0.1%
7430	Pasture	D	High	1,007.89	0.5%
8110	Agriculture	A	Low	5.34	0.0%
8120	Agriculture	A	Med	2.67	0.0%
8130	Agriculture	A	High	1.11	0.0%
8210	Agriculture	B	Low	13.57	0.0%
8220	Agriculture	B	Med	56.93	0.0%
8230	Agriculture	B	High	71.83	0.0%
8310	Agriculture	C	Low	42.48	0.0%
8320	Agriculture	C	Med	192.82	0.1%
8330	Agriculture	C	High	168.35	0.1%
8410	Agriculture	D	Low	2.67	0.0%

HRU ID	Land Use - Land Cover	HSG	Slope	Area	
				Acre	%
8420	Agriculture	D	Med	22.24	0.0%
8430	Agriculture	D	High	52.93	0.0%
9000	Water	All	All	378.51	0.2%
10110	Irrigation	A	Low	12.90	0.0%
10120	Irrigation	A	Med	8.01	0.0%
10130	Irrigation	A	High	4.67	0.0%
10210	Irrigation	B	Low	4.67	0.0%
10220	Irrigation	B	Med	21.13	0.0%
10230	Irrigation	B	High	61.60	0.0%
10310	Irrigation	C	Low	15.35	0.0%
10320	Irrigation	C	Med	70.94	0.0%
10330	Irrigation	C	High	95.63	0.0%
10410	Irrigation	D	Low	10.90	0.0%
10420	Irrigation	D	Med	46.48	0.0%
10430	Irrigation	D	High	152.12	0.1%
			Total	**212,468**	**100%**

4 CLIMATE FORCING INPUTS

The Gualala River watershed LSPC model uses hourly climate data forcing inputs to drive the hydrology module. In general, hydrologic models are highly dependent on the quantity and quality of meteorological input data (Quirmbach and Schultz, 2002). Conventionally, meteorological boundary conditions for stormwater modeling rely on ground-based stations across an area; however, challenges arise when trying to associate point-sampled weather station data over complex and/or large terrain (Henn et al., 2018). Model representation of precipitation in regions with low station density is susceptible to distortion when using linearized downscaling methods (e.g., Thiessen polygons).

The approach described here is a hybrid that supplements spatial and temporal gaps in observed meteorological data with gridded meteorological products from the Parameter-elevation Regressions on Independent Slopes Model (PRISM) and North American Land Data Assimilation System-2 (NLDAS). NLDAS and PRISM are Land Surface Model (LSM) datasets with 1/8th degree and 4-km spatial resolution, respectively, which are ideal for supplementing spatial gaps in the observed station network as well as patching missing or erroneous temporal gaps in the observed time series data. The use of a hybrid approach that blends ground-based stations with remotely sensed precipitation products, i.e., increasing the rainfall gauge density over the watershed, has been shown to improve the representation of rainfall and increase forecast accuracy more than using ground-based stations alone (Kim et al., 2018; Looper and Vieux, 2012; Xia et al., 2012a, 2012b). This approach has been applied for large watershed-scale modeling applications in Los Angeles County (LACFCD, 2020).

Potential evapotranspiration (PEVT) is another critical forcing input for hydrology simulation. Section 4.2 describes how PEVT was derived for this modeling effort.

4.1 Precipitation

Figure 4-1 presents a summary of the hybrid approach to blend observed precipitation with gridded meteorological products. Observed data and gridded products were processed in parallel (1) to identify the highest quality gauge data and (2) to merge gridded products to produce continuous hourly time series. Gridded products were used to fill spatial and temporal gaps in the observed precipitation coverage. The final coverage shown in Figure 4-2 comprises the highest quality observed time series, supplemented by gridded products only where spatial and temporal gaps occurred in the observed coverage. The parallel processing of observed and gridded precipitation is presented in Section 4.1.1. Section 4.1.2 describes how those outputs were synthesized into the model's final set of precipitation time series.

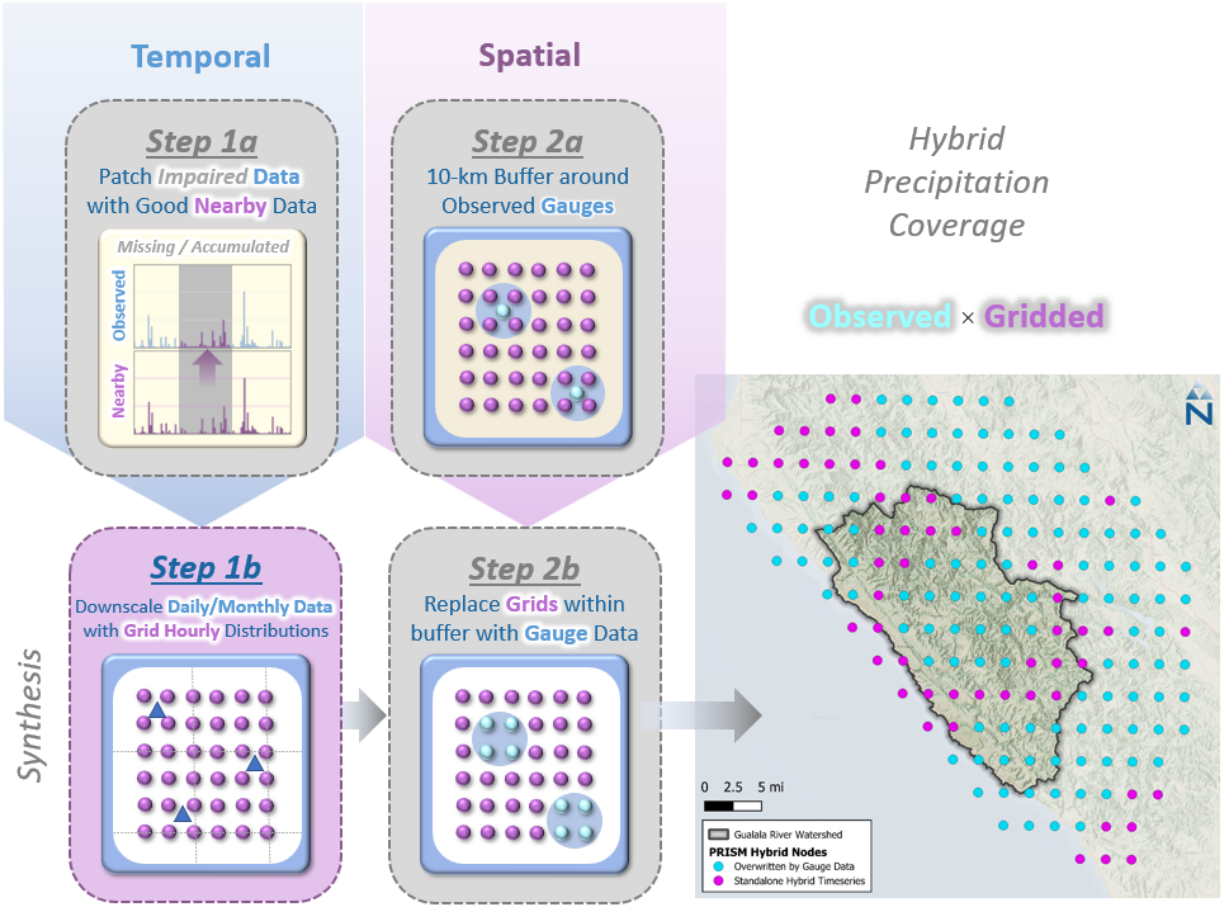

Figure 4-1. Hybrid approach to blend observed precipitation with gridded meteorological products.

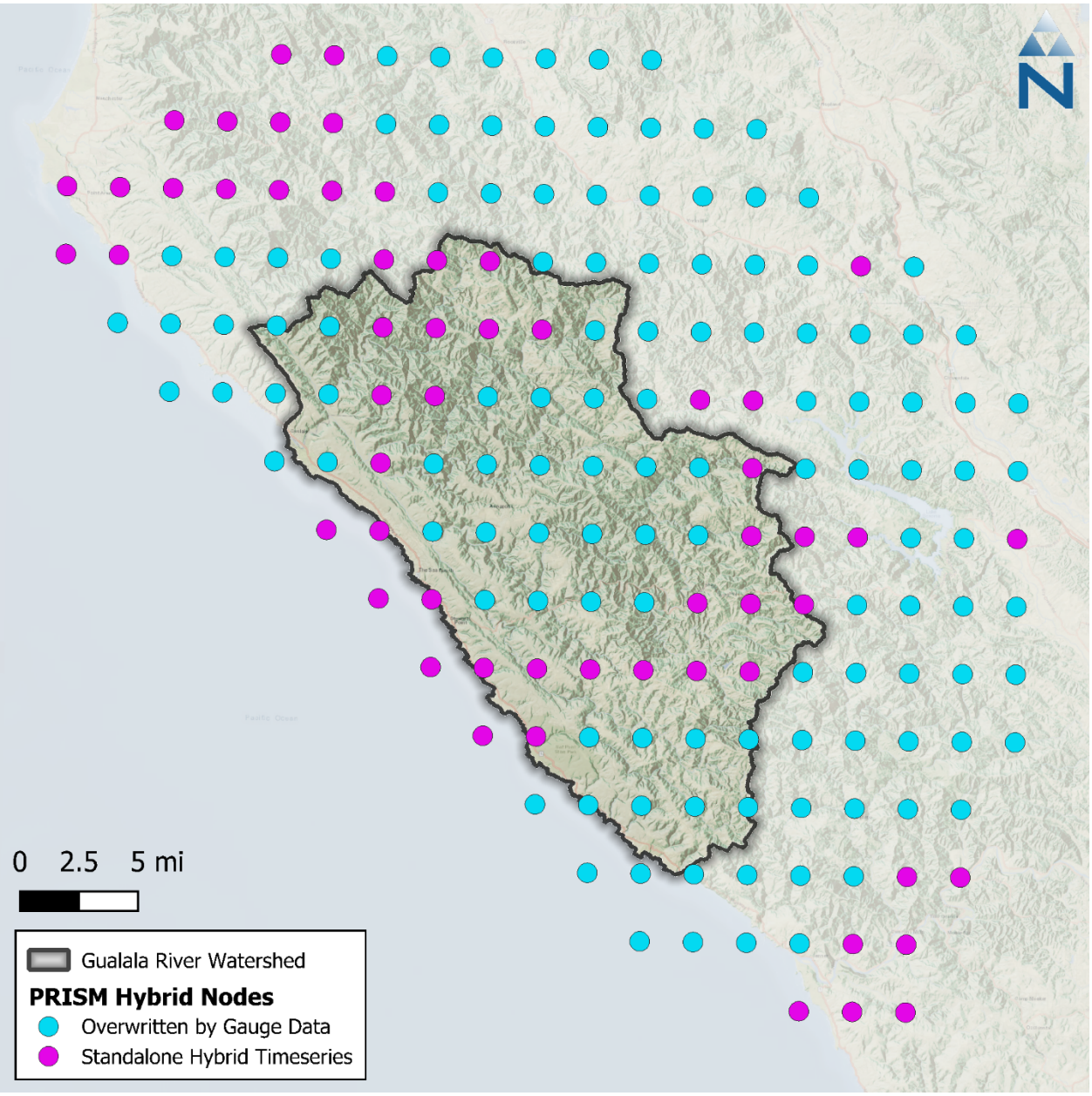

Figure 4-2. Spatial coverage of PRISM nodes by hybrid data source.

4.1.1 Parallel Processing of Observed Data and Gridded Products

Data from 5 observed precipitation gauges, summarized in Table 4-1, were processed for use in the hybrid precipitation time series. These stations report daily precipitation totals, which were disaggregated to hourly based on the distribution of the nearest NLDAS grid cell, while maintaining observed daily totals. Three of the gauges are from the Global Historical Climatology Network Daily (GHCND) database which is operated by The National Ocean and Atmospheric Association (NOAA). Additional stations from the Remote Automated Weather Stations (RAWS) and the California Data Exchange Center (CDEC) were also used. The relationship between annual average total precipitation and elevation, data quality control impacts, and temporal distribution of average annual precipitation for these stations are summarized in the Figure 4-3 violin plot. The Gualala River

work plan had additional precipitation gauges listed; however, those stations were dropped from further use because they were either duplicates or were outside of the 10km buffer used to create hybrid time series.

Table 4-1. Precipitation stations used to develop hybrid precipitation time series

Agency	Station ID[1]	Name	Start Date	End Date	Lat.	Long.	Elevation (meters)	Data Coverage (%)[2]
NOAA	GHCND:US1CASN0098	CAZADERO 5.6 W, CA US	10/6/2012	8/2/2024	38.53	-123.19	369.1	94%
	GHCND:USC00043191	FORT ROSS, CA US	9/30/1895	7/30/2024	38.52	-123.25	34.1	93%
	GHCND:US1CAMD0050	GUALALA 3.7 NW, CA US	4/9/2022	8/1/2024	38.81	-123.58	144.8	100%
CDEC	YOR	YORKVILLE	1/31/1984	Present	38.91	-123.23	335.3	100%
RAWS	OAAC1	OAK RIDGE	7/18/2016	Present	38.74	-123.31	576.1	100%

1. Stations presented have at least 90% data coverage.
2. NOAA data coverage as reported; RAWS estimated based on data flagging and count of time steps.

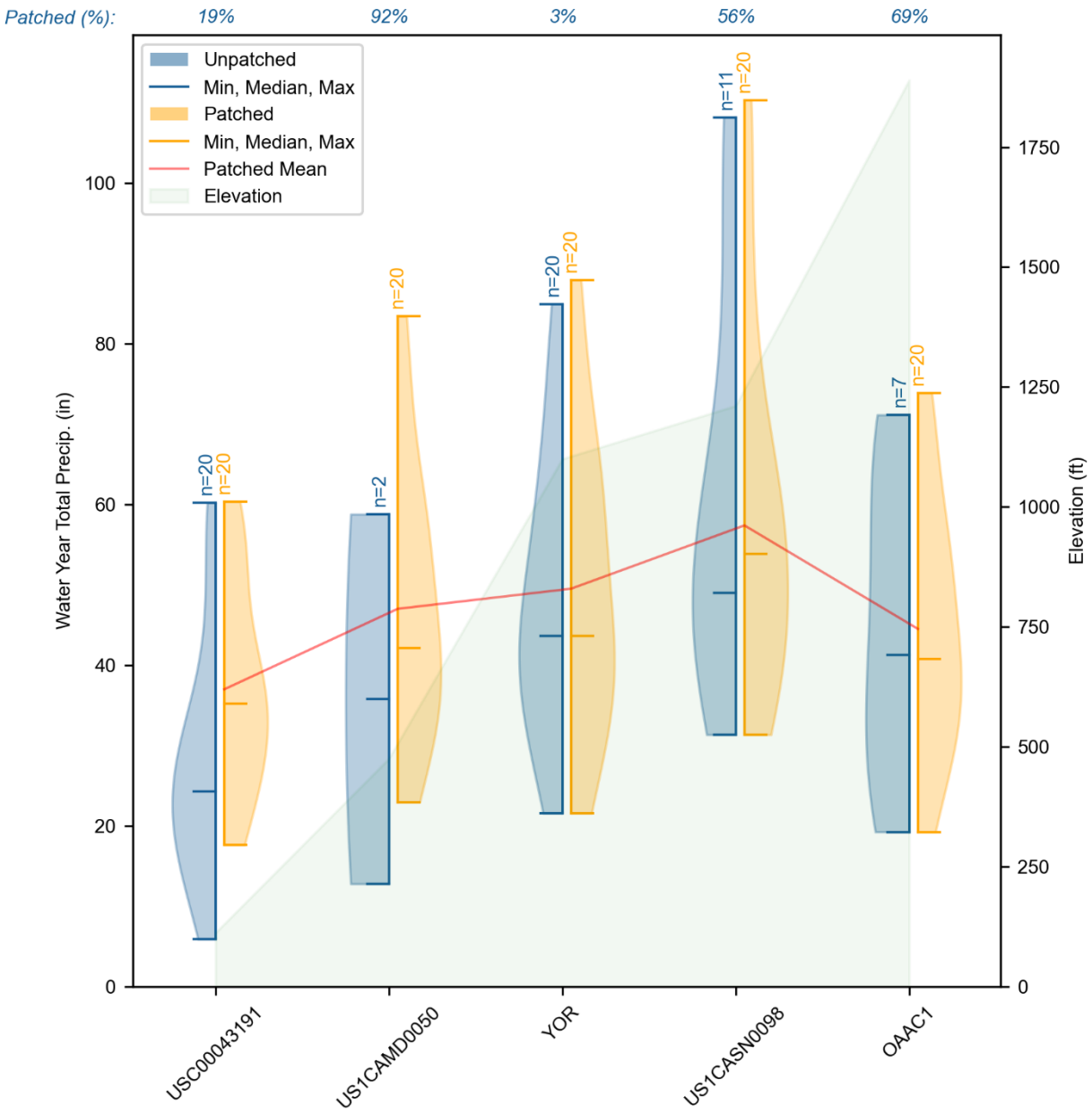

Figure 4-3. Annual average precipitation totals and elevation of selected precipitation gauges.

The gridded meteorological products were processed in parallel with the observed data and used to patch spatial and temporal gaps in the observed data record. PRISM monthly precipitation time series data are available at a 4-km spatial resolution across the conterminous United States (Daly et al., 1997, 1994; Gibson et al., 2002). PRISM combines point data and spatial datasets (primarily DEMs) via statistical methods to generate estimates of annual, monthly, and event-based precipitation in a gridded format from as early as 1961 (Daly et al., 2000). PRISM has undergone several iterations of refinement, extensive peer review, and performance validation through case study applications.

NLDAS is a quality-controlled meteorological dataset designed specifically to support continuous simulation modeling activities (Cosgrove et al., 2003; Mitchell et al., 2004). NLDAS provides hourly predictions of meteorological data at a 1/8th degree spatial resolution for North America (approximately 8.6-mile intervals), with retrospective simulations beginning in January 1979. For this

model, hourly NLDAS precipitation distributions were mapped to the nearest PRISM grid cell and used to disaggregate the monthly PRISM totals to hourly—the resulting set of gridded precipitation time series reflects monthly PRISM totals that have hourly distributions from the nearest NLDAS grid. Using monthly PRISM totals with hourly NLDAS, as opposed to daily PRISM totals, eliminates the need to estimate distributions for occasional but rare instances where an hourly distribution does not coincide with a daily total.

4.1.2 Synthesis of Observed Data and Gridded Products

Where data of adequate quantity and quality were available, observed precipitation data were preferentially selected over gridded data. Impaired intervals are gaps in the observed record flagged as missing, deleted, or accumulated rainfall. Gridded time series are used to patch impaired intervals as follows. First, a 10-km buffer was created around each of the observed gauges that were prescreened for quality. Next, the 10-km gauge buffer was intersected with the PRISM grid layer. The time series at any grid falling within the buffer is overridden by the associated observed gauge time series, except for impaired intervals, where the gridded data are retained to patch those temporal impairments. Consequently, most of the observed data at a PRISM grid location will be identical to a neighboring grid within a 10-km buffer of the gauge but will have slightly different PRISM time series for impaired intervals.

After the creation of the hybrid precipitation time series, each catchment is assigned a time series based on the Thiessen polygon its centroid falls within. Figure 4-4 illustrates the final assignment of gauge-based or LSM-based hybrid time series by catchment. Figure 4-5 shows the distribution of monthly total precipitation across all hybrid time series within the watershed and Figure 4-6 illustrates the spatial distribution of annual average precipitation from the hybrid time series by catchment.

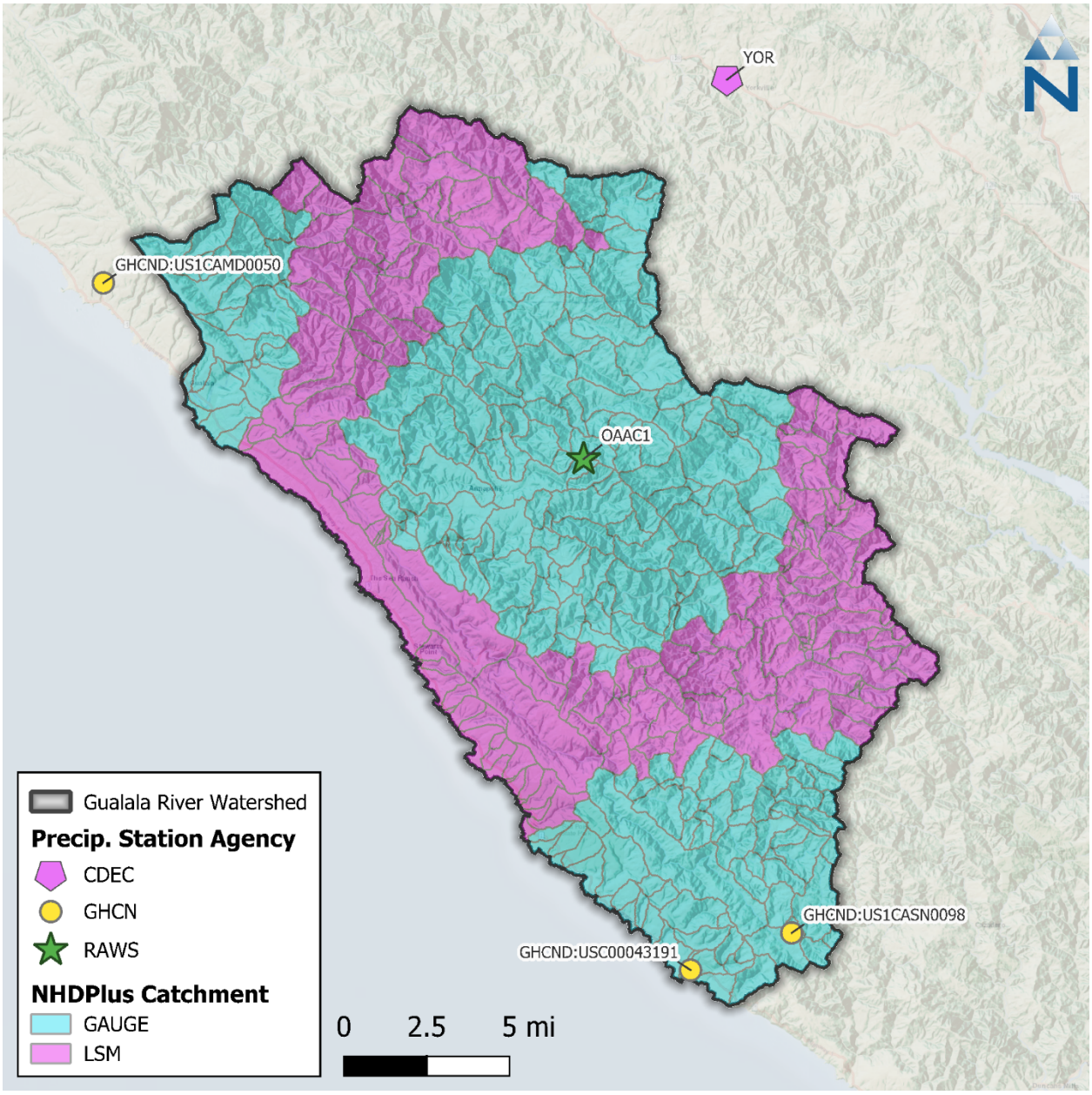

Figure 4-4. Final spatial coverage of precipitation time series by catchment.

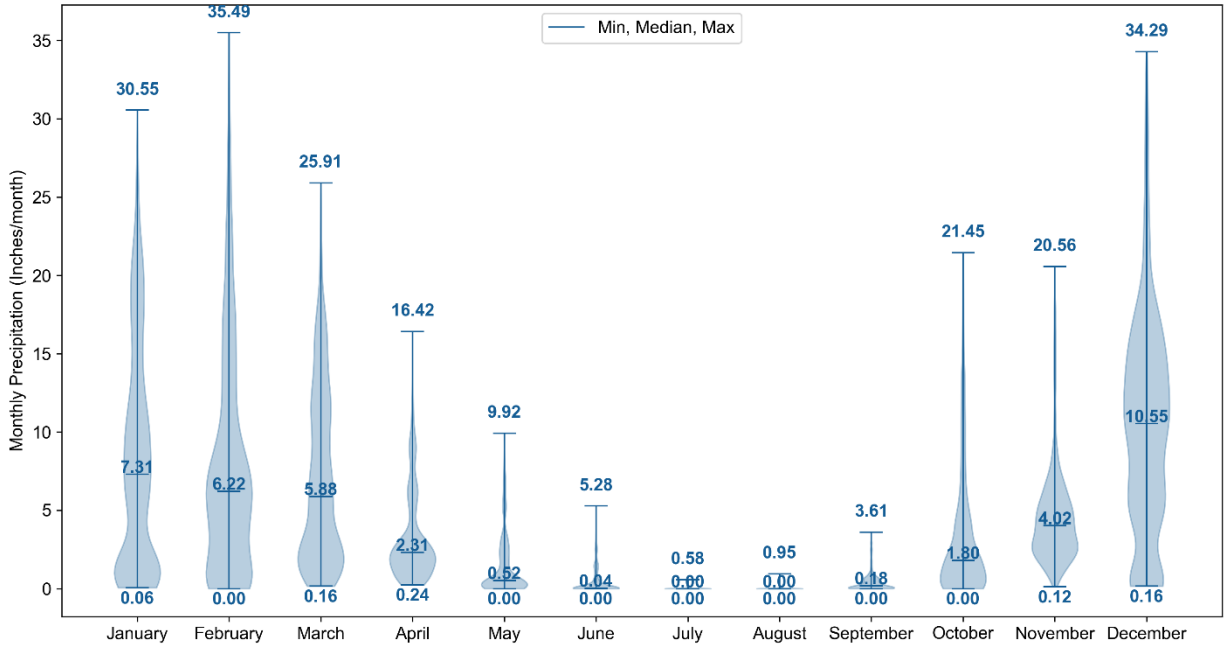

Figure 4-5. Distribution of monthly precipitation across all hybrid time series within the Gualala River watershed for Water Years 2004 to 2023.

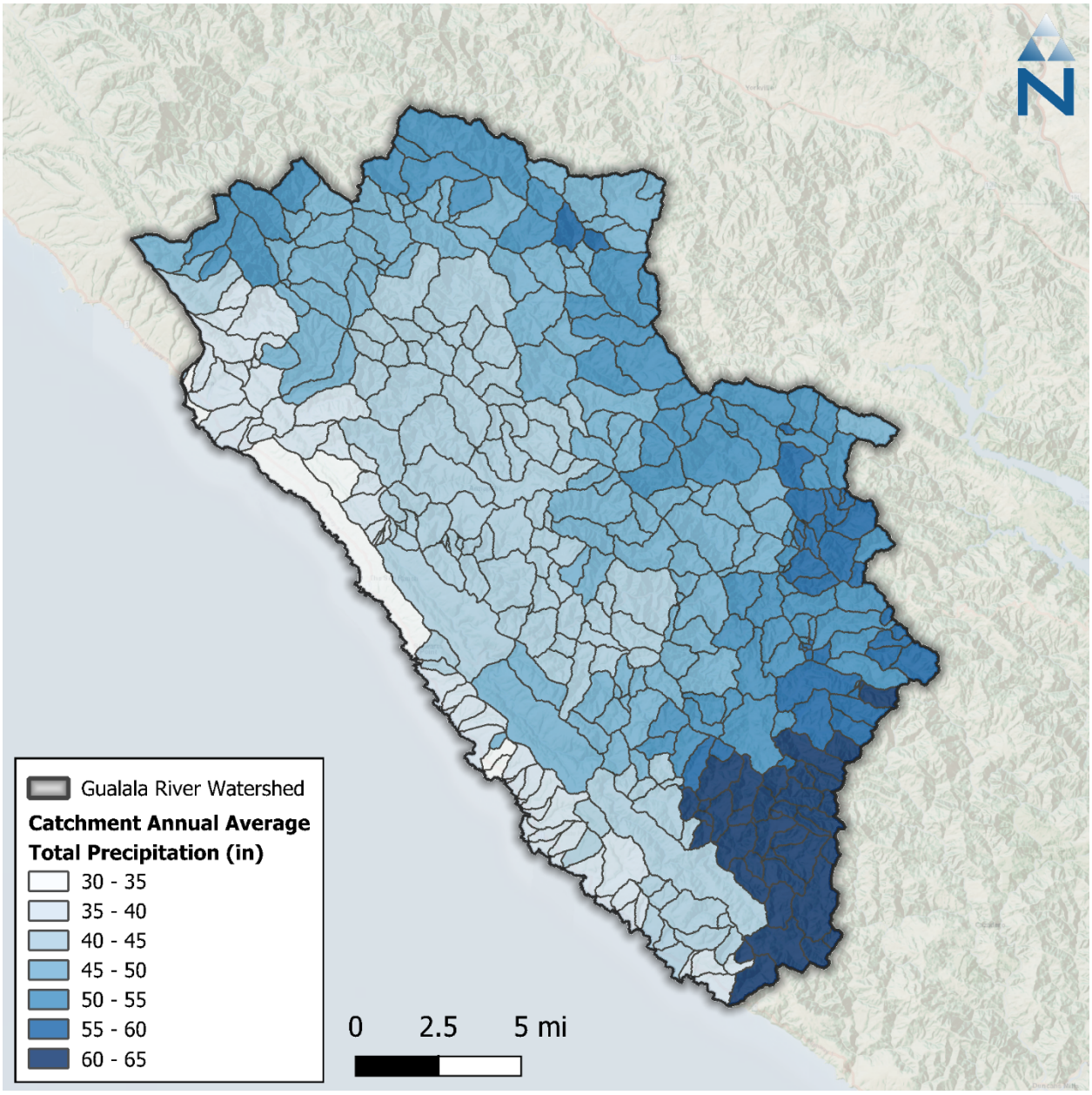

Figure 4-6. Annual average hybrid precipitation totals by catchment from Water Years 2004-2023.

4.2 Potential Evapotranspiration

In addition to precipitation, potential evapotranspiration forcing input time series were created and assigned to each catchment. Daily total reference evapotranspiration (ET_o) from the California Irrigation Management Information System (CIMIS) Spatial dataset was disaggregated to hourly using the NLDAS hourly solar radiation. CIMIS Spatial expresses daily ET_o estimates calculated at a statewide 2-km spatial resolution using the American Society of Civil Engineers version of the Penman-Monteith equation (ASCE-PM). This product provides a consistent spatial estimate of ET_o that is California-specific, implicitly captures macro-scale spatial variability and orographic influences, is available from 2004 through the Present, and is routinely updated. Within each catchment, actual ET is calculated for each Hydrologic Response Unit (HRU) during the model simulation as a function

of parameters representing differences in vegetation (type, height, and density) and soil conditions. Figure 4-7 shows the distribution of monthly total ET_o across all grid points within the watershed. Figure 4-8 shows the spatial distribution of CIMIS annual average total ET_o across the watershed. Despite the color gradient variation, it should be noted that annual average potential evaporation rainfall varies between 38 and 44 inches per year. There is a slight increase in annual potential evapotranspiration traveling from the coastal western portion of the watershed to the eastern portion.

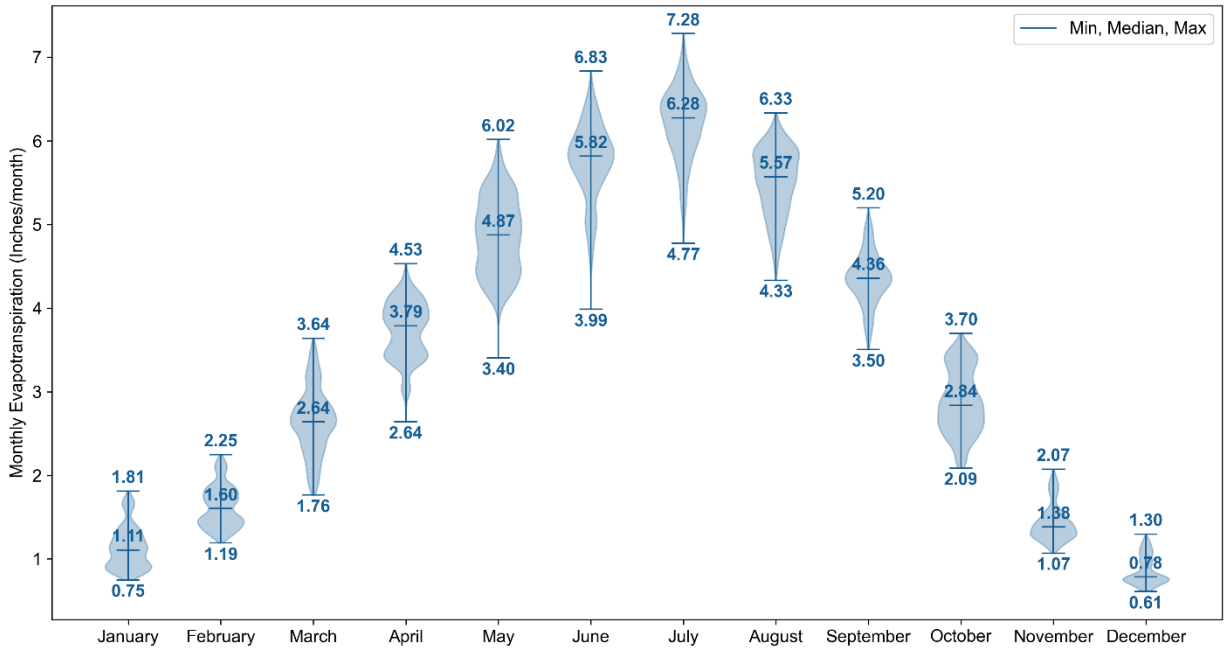

Figure 4-7. Distribution of monthly total ET_o across all CIMIS spatial grid points within the Gualala River watershed for Water Years 2004 to 2023.

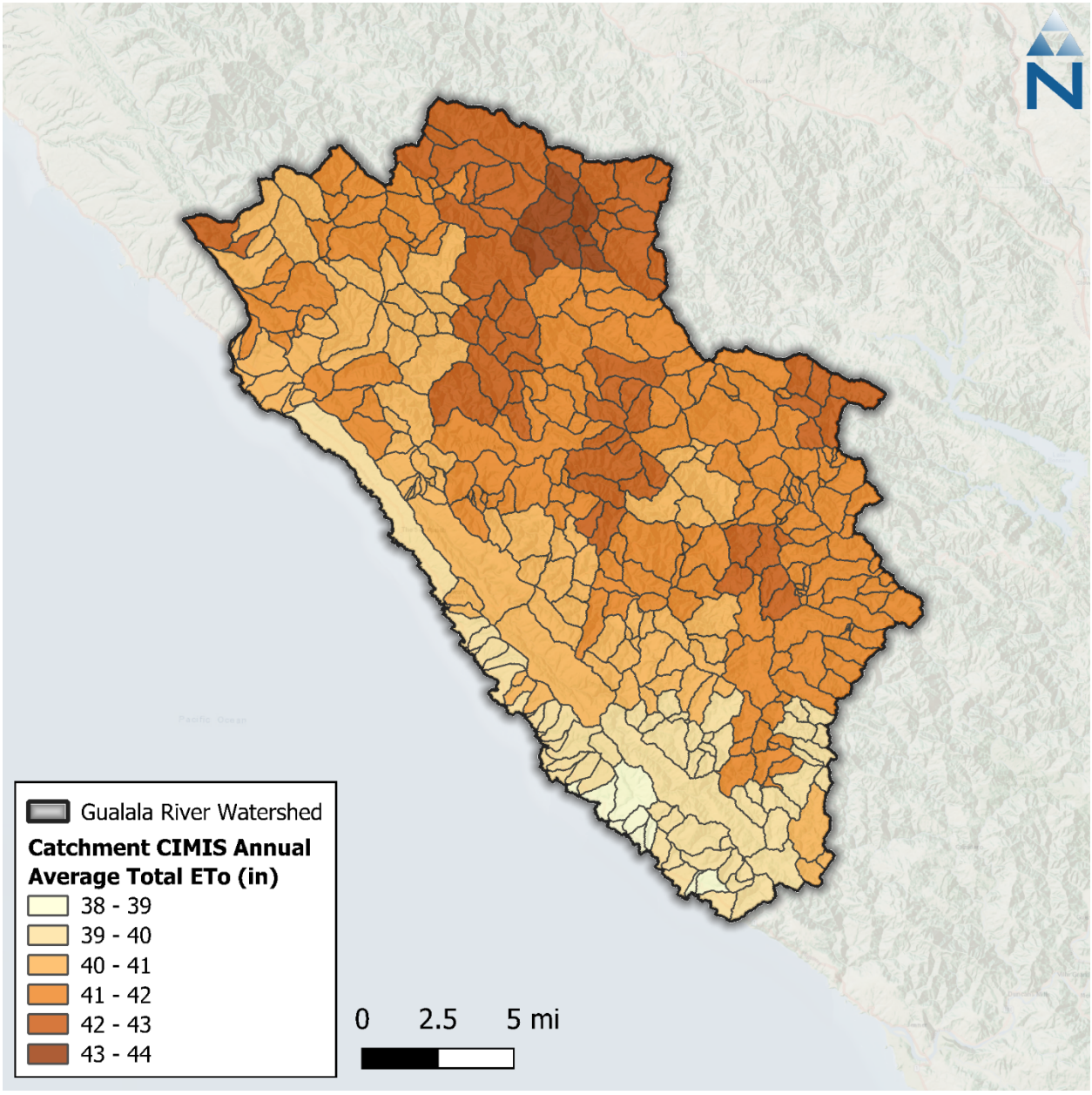

Figure 4-8. CIMIS annual average total ET_o by catchment within the Gualala River watershed.

5 SURFACE WATER WITHDRAWALS

Datasets related to water rights, points of diversion (PODs), and irrigation use were identified through the Water Board's eWRIMS database and a University of California Cooperative Extension (UCCE) study assessing agricultural water needs in the nearby Navarro River and Russian River watersheds (McGourty et al., 2020). These data were used to represent diversions and withdrawals in the watershed model. Monthly data from 84 water rights within the Gualala River watershed from 2017 to 2023 were received from the Board's Supply and Demand Unit staff. Of these, 24 are related to irrigation and 60 are related to non-irrigation uses, including domestic use, municipal use, dust control, recreational activities, stock watering, and fish and wildlife preservation and enhancement.

Figure 5-1 shows the primary usage and volume of these water rights. Here, the 'Other' category groups together the following primary usages: dust control, stock watering, and fish and wildlife preservation and enhancement. Together, the 'Other' category makes up approximately 45% of the points in the watershed and 22% of the volume.

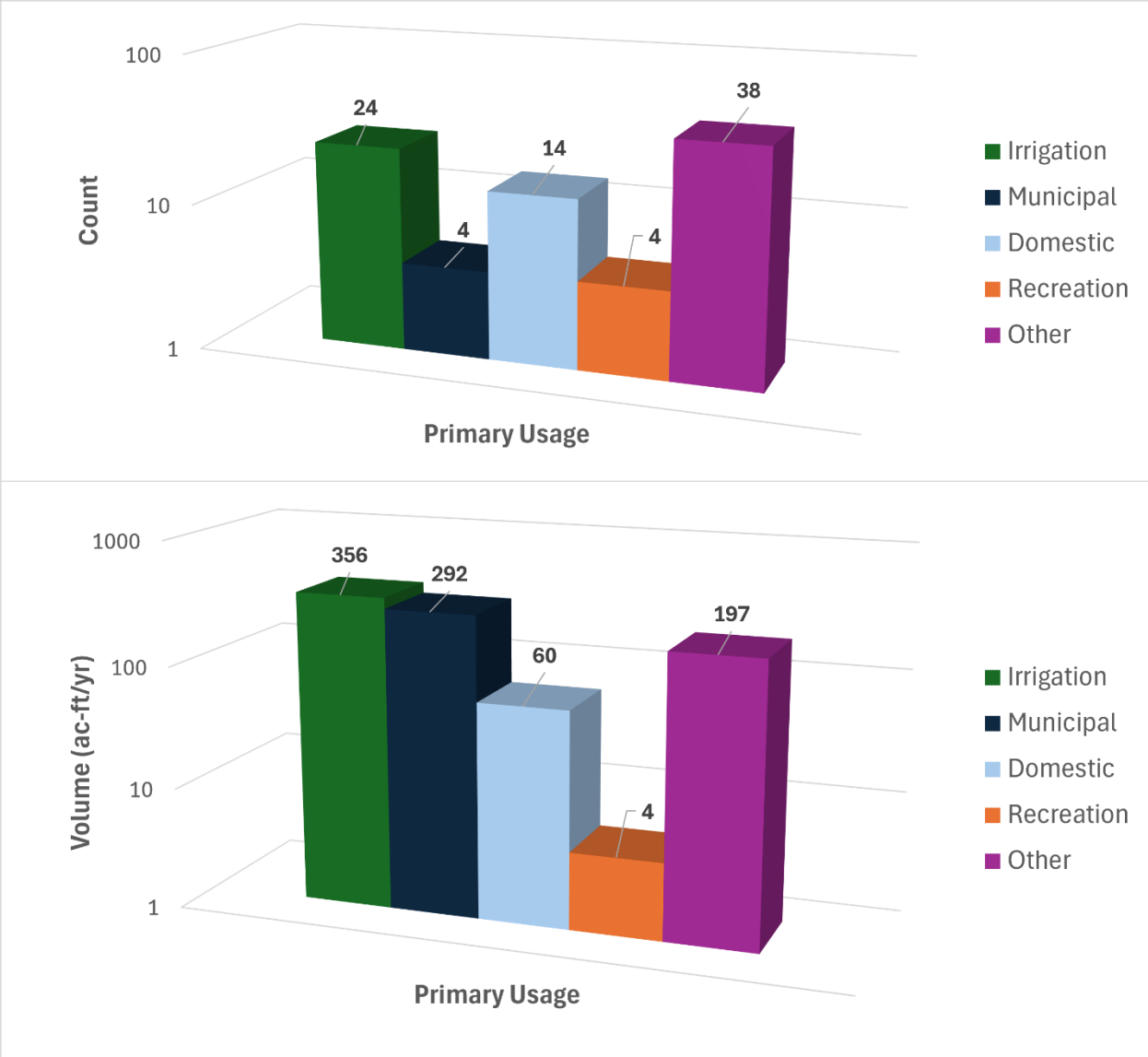

Figure 5-1. Primary usage of points of diversion within the Gualala River watershed. Note that these are presented on a log scale.

5.1 Points of Diversion

Figure 5-2 provides an overview of surface water diversion points in the watershed. PODs are primarily located along the Gualala River, which passes through the western length of the watershed. For the non-irrigated water demand, the received monthly data in acre-feet are summed by catchment and then converted to a flow rate for withdraw from the catchment's modeled reach segment. Irrigation demand is similarly converted from monthly volume into a withdraw rate by application number. Some of those withdrawals are moved to storage during the wet months and applied for irrigation during drier months; therefore, irrigation withdrawals and irrigation application were

indirectly coupled. In other words, the total volume of irrigated water demand from the POD data was assumed to be equal to the volume of applied irrigation water using LSPC's irrigation module, as described in Section 5.2, but application was assumed to occur in proportion to rainfall deficit. These water demand data are added to the LSPC model as surface water withdrawals from the appropriate reach segments based on the following considerations.

- Diversions were classified based on primary usage (irrigation, municipal, industrial, recreational, and others) as well as by allocation type (direct and storage).
- During simulations, diverted streamflow was routed out of the system to represent the different usages (i.e., irrigation).
- For instances where PODs in different catchments share the same application/permit number, water demand was proportionally distributed based on the magnitude of upstream drainage area.
- To approximate withdrawals over the entire modeled period, POD time series prior to 2017 were estimated as the monthly average volume based on the 2017-2023 data and extended to the latter of the beginning of the modeling period or to the start date of the water right associated with each POD.

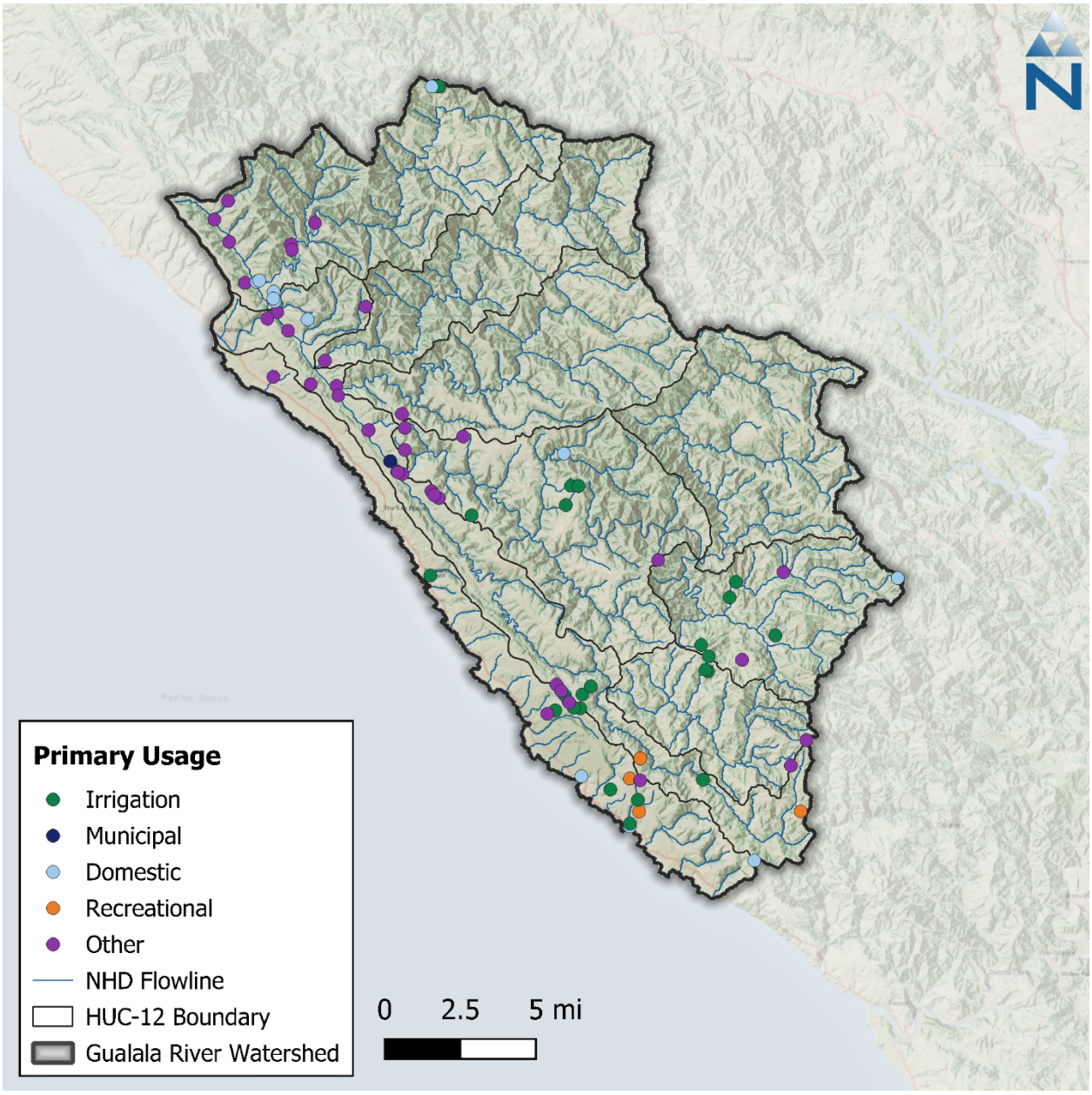

Figure 5-2. Points of diversion within the Gualala River watershed.

5.2 Irrigation

The LSPC irrigation module is designed to streamline the spatial and temporal representation of water demand, irrigation application, and associated return flows. In practice, irrigation demand is estimated as the deficit of precipitation from the product of a crop-specific evaporative coefficient (ETc) and reference evapotranspiration (PEVT). This LSPC configuration uses a similar approach but instead works backwards to estimate the monthly crop coefficients for agricultural HRUs by using observed irrigation demand and climate data. Those crop coefficients are then used with observed climate data to calculate irrigation application rates during LSPC simulations. The equation used to calculate monthly evaporative crop coefficients for agricultural HRUs is shown as Equation 2:

$$V_{irr} = (PEVT \times ET_c - PREC) \times A_{irr}$$

where (V_{irr}) is the volume of irrigation demand in acre-feet, (A_{irr}) is the cropland being irrigated in acres, (PEVT) is the reference evapotranspiration depth in feet, ET_c is the crop-specific evaporative coefficient, and (PREC) is the observed precipitation depth in feet. As mentioned in Section 5.1, irrigation demand was inferred from stream diversion records for each catchment. Because the exact location of irrigated vs. non-irrigated parcels was unknown, it was assumed that agricultural land located in catchments immediately draining to reach segments with irrigation PODs were irrigated.

The process for representing irrigation in the Gualala watershed is summarized by the following steps:

1. Estimate irrigation demand.
2. Define irrigated hydrologic response units.
3. Calculate crop evaporative coefficients.

5.2.1 Estimation of Irrigation Demand

Irrigation demand was inferred from eWRIMS stream diversion data for records between 2017 and 2023. For each LSPC catchment, the total monthly irrigation demand was estimated as the sum of all irrigation-associated stream diversions. As mentioned in Section 5.1, stream diversions were either directly used for the application or routed to a storage facility for later use. Due to data limitations, it was unknown exactly when and how stored streamflow was used for irrigation; however, because direct diversion is higher during the growing season and tends to follows PEVT, it was assumed that irrigation of stored water would also follow a similar pattern that scales in proportion to evaporative demand, which is higher during the warmer and drier growing season. Figure 5-3 shows average monthly diversion volumes vs. potential evapotranspiration.

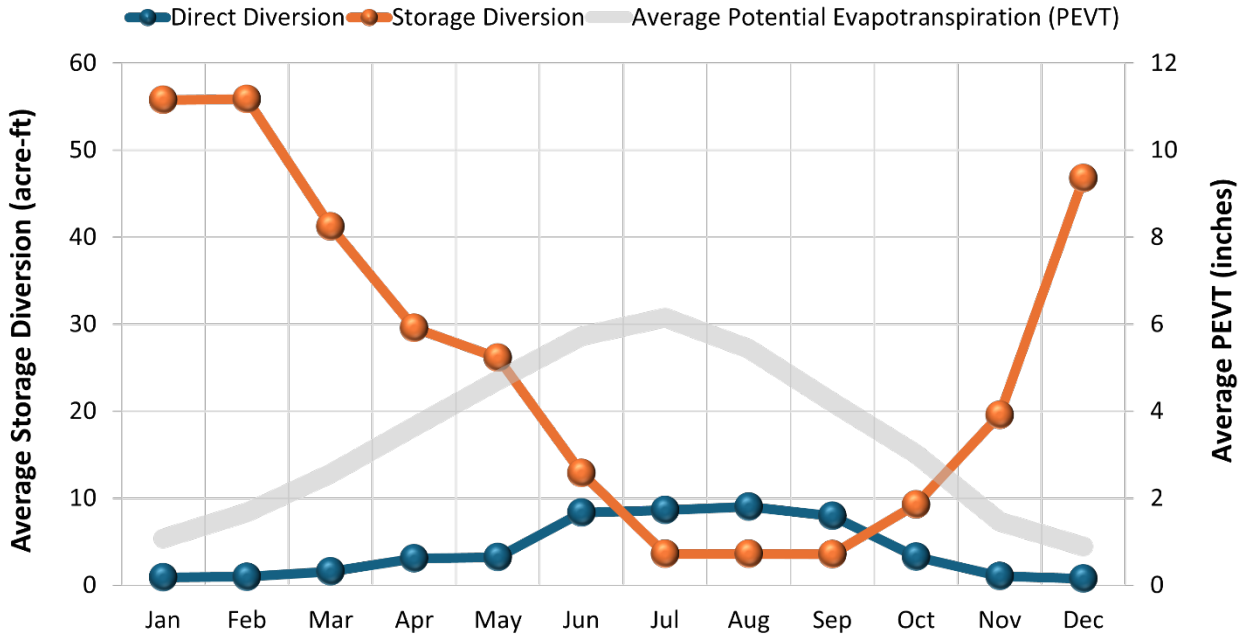

Figure 5-3. Total reported direct and storage diversions vs. average potential evapotranspiration.

5.2.2 Defining Irrigated Hydrologic Response Units

The LSPC model simulates irrigation on a unit-area basis. Agriculture and Pasture HRUs were partitioned into irrigated and non-irrigated HRU counterparts, as previously described in Section 3.6.2. Because the exact location of irrigated vs. non-irrigated parcels was unknown, it was assumed that agricultural and pasture land located in catchments immediately draining to reach segments with irrigation PODs were irrigated—15 out of the 397 catchments were irrigated. Only the agricultural and pastureland footprints, identified through the NLCD and CDL datasets within those catchments, were irrigated, totaling 504 acres, which is 2.5% of the total area of the 15 irrigated catchments.

As shown in Figure 5-4, the irrigated footprint area is a relatively small portion of the Gualala River model domain. The sum of all croplands, pasture, and grassland areas represents 4.6% of the watershed. Of that area, about one-tenth is within the 15 catchments with irrigation. Out of that tenth, "Agriculture" and "Pasture" HRUs make up 504 acres, all of which was modeled as "Irrigated" which is about 0.2% of the entire Gualala River watershed. Figure 5-5 shows the agriculture and pasture area that was classified as irrigated or non-irrigated within the Gualala River watershed. For the unit-area model representation, it was assumed that 50 percent of irrigation water was applied as sprinkler and 50 percent as flood irrigation. Sprinkler irrigation enters the model at the same layer as precipitation, making it subject to interception storage and associated evaporation. Flood irrigation enters the model below interception storage and is only subject to surface ponding and infiltration.

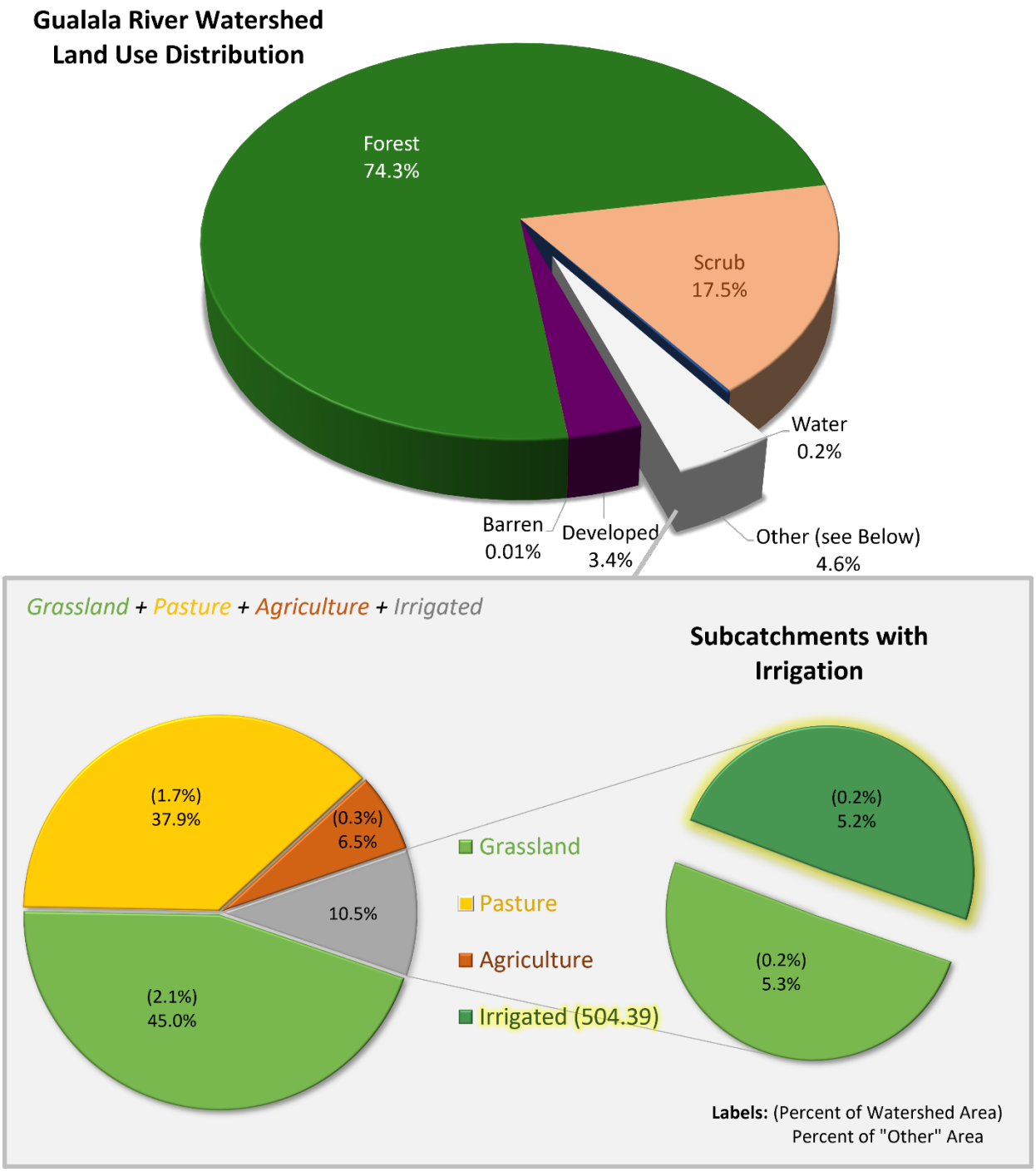

Figure 5-4. Irrigated area as a subset of the Gualala River watershed.

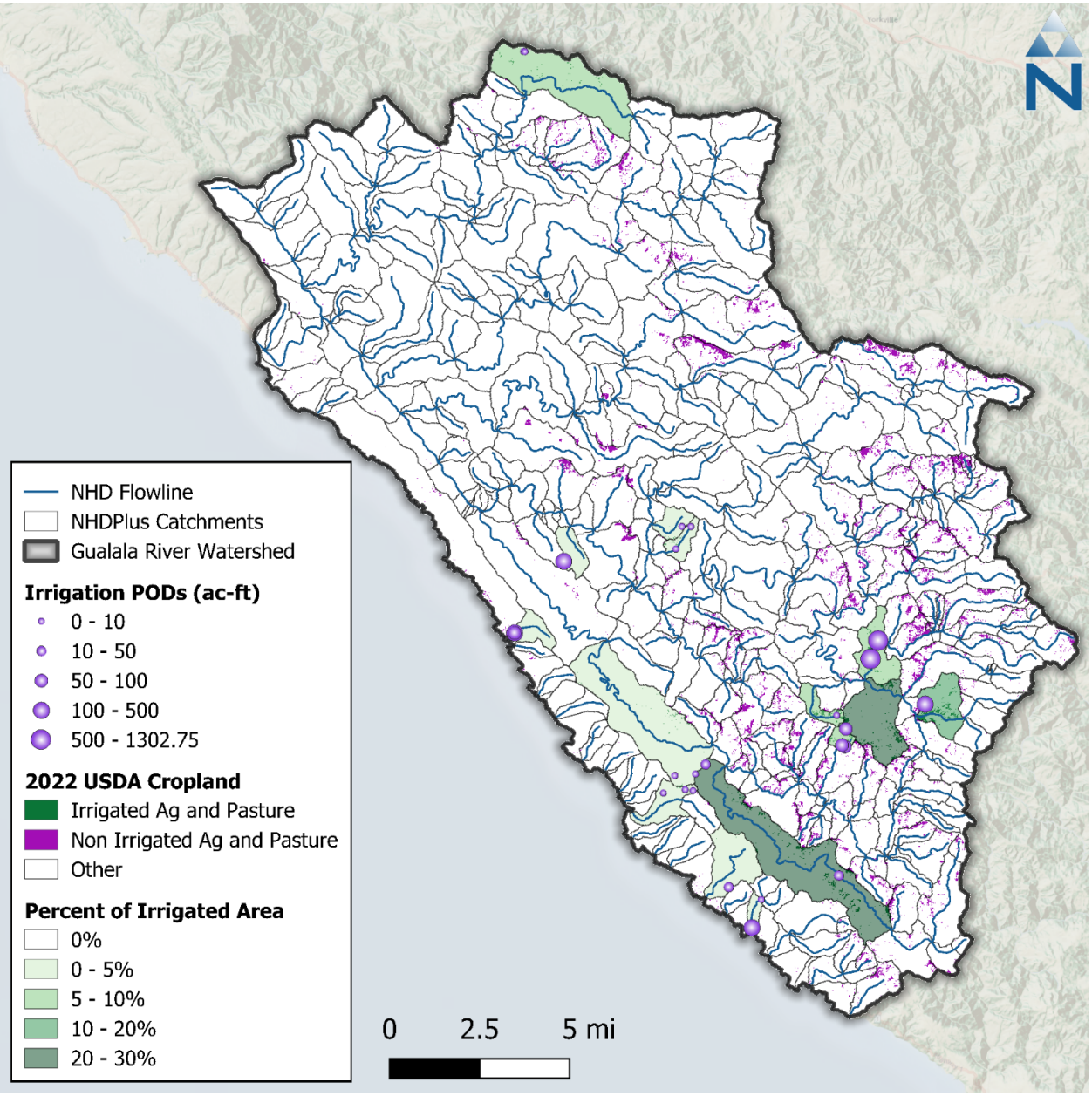

Figure 5-5. Irrigated and non-irrigated agriculture and pasture areas within the Gualala River watershed.

5.2.3 Calculation of Crop Evaporative Coefficients

Crop evaporative coefficient (ET_c) is used to adjust reference evapotranspiration rates to better represent an evaporative demand for a specific vegetation type. In the absence of high-resolution irrigation data, this crop-specific evaporative demand was used with observed precipitation data to predict irrigation demand. For this LSPC model instance, distinct crop types were not represented in hydrologic response units, therefore one value of crop evaporative coefficient was used to represent all irrigated areas. An initial estimate of 0.36 was obtained for this coefficient by optimizing ET_c in Equation 2 using Microsoft Excel solver to match total irrigation demand volume (V_{irr}) with the total withdrawal volume for irrigation use.

6 MODEL CALIBRATION

The goal of hydrology model calibration is to adjust model parameters to improve predictive performance based on comparisons to observed data. The desired outcome of the calibration process is a set of modeling parameters that characterize existing conditions for all processes in LSPC that vary by HRU (as described in Section 3), reach group, and process-based parameter groups. The model development approach prioritizes model configuration over calibration by investigating and expressing known physical characteristics of the watershed wherever possible and practical—only leaving responses that cannot be explained by physical characteristics to calibration of model parameters. The resulting model is parameterized in such a way that variability trends in the observed data are replicated relative to hydrological conditions (i.e., wet and dry streamflow conditions and rainfall magnitude). The resulting calibrated parameters are consistent by HRU, with responses varying as a function of HRU distribution and weather variability, which minimizes spatial biases and reduces the possibility of over-tuning during model calibration. A robustly calibrated model can then serve as the starting point for future watershed-specific applications, investigations, and management scenarios.

Figure 6-1 shows how the model configuration and calibration components are layered in the model. LSPC makes clear distinctions between inputs that are physical characteristics and process parameters. The term "parameters" refers to the rates and constants used to represent physical processes in the model. All other model inputs previously described, such as weather data, HRU distribution, and the length and slope of overland flow for individual HRUs, are generally considered physical characteristics of the watershed because they can be directly measured, assigned, or reasonably estimated from available spatial and temporal data sources. Those components are generally set during model configuration and are not varied during model calibration unless new information is received that justifies a systemwide change to those components.

Developing modeling parameters begins with specifying one set of parameters systemwide. The Gualala River model comprises 98 possible HRUs per catchment and 88 unique combinations of meteorological boundary conditions (i.e., unique combinations of precipitation time series and potential-evapotranspiration time series). Because the length (LSUR) and slope (SLSUR) of overland runoff are uniquely computed by HRU and catchment, the initial degrees of freedom are already quite broad. Consequently, using one parameter group, the model represents 8,624 unique non-zero area HRU × meteorological responses over the model domain of 397 catchments. Wherever model responses diverge from observed data in ways that the modeling parameters cannot explain, further investigation may warrant introducing a new parameter group or reach group to add more degrees of freedom to the range of model parameters. This methodical calibration sequence can also help to identify areas where additional data collection may be needed to characterize the physical system better.

Figure 6-5 shows the model calibration sequence, a top-down data approach that began with the extensive model configuration and quality control process previously described in Section 2 through Section 5. The sequence begins with climate-forcing data, followed by edge-of-stream land hydrology, water budget estimates, and representation of the stream routing network. This sequencing minimizes the propagation of uncertainty and error by distinguishing physical characteristics of the watershed that can be measured and configured from process-based parameters, which are rates and constants that can be estimated within a reasonable range of variability by HRU.

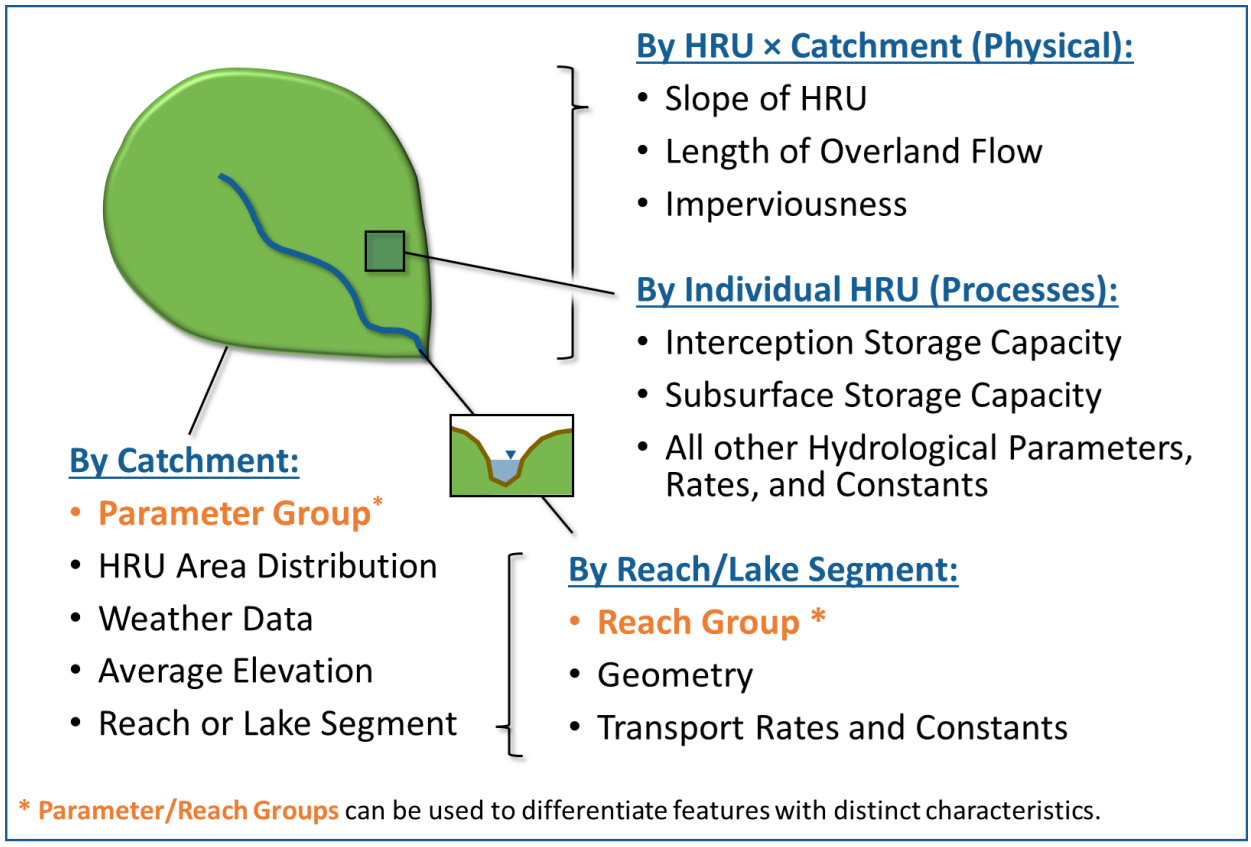

Figure 6-1. LSPC model configuration and calibration components.

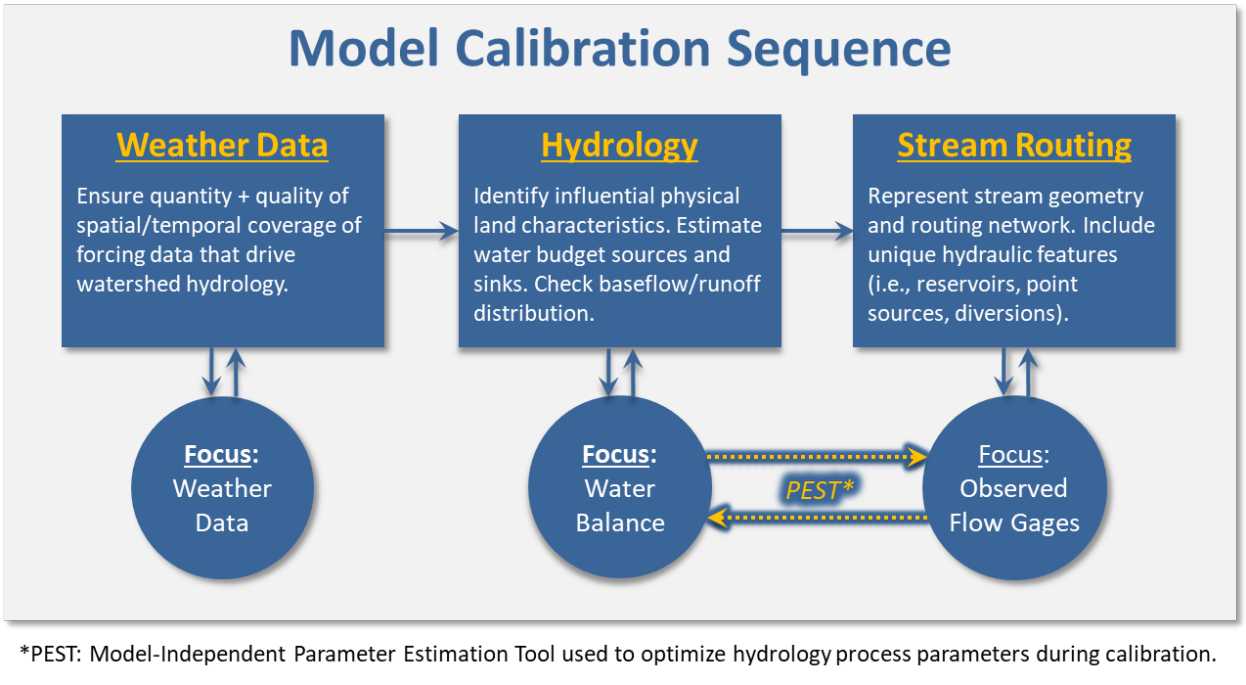

Figure 6-2. Top-down calibration sequence for hydrology model calibration.

As shown in Figure 6-3 and summarized in Table 6-1, streamflow data for the Gualala River watershed was available at four USGS flow stations. However, only one of these stations, Gualala River South Fork at Sea Ranch, had data of sufficient quality to be used for model calibration and validation. The other three stations were found to have inconsistent, possibly compromised data and were ultimately dropped from model calibration. Data from these stations were still incorporated into the validation procedure, which is discussed further in Section 7. Gualala River South Fork at Sea Ranch, which sits at a point on the stream draining about half the watershed's total area, was considered sufficiently characteristic, as the watershed is relatively homogenous in land cover, soil, and slope. Refer to Table 6-2 and Table 3-7 for a comparison of HRU characteristics between the drainage area of Gualala River South Fork at Sea Ranch and the entire watershed. The distribution of HRUs is quite similar, suggesting that this flow station effectively represents the entire watershed.

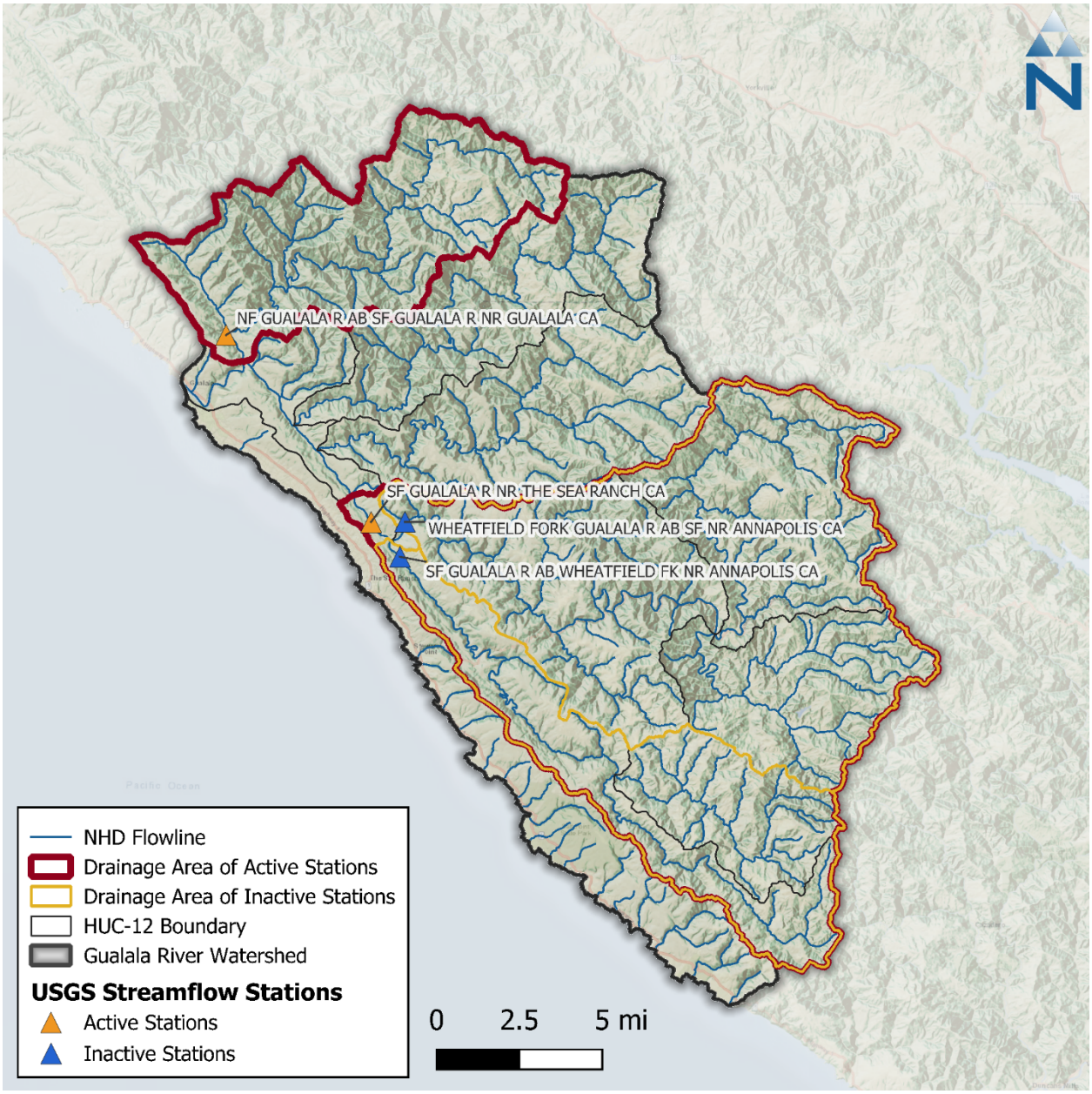

Figure 6-3. USGS streamflow stations in the Gualala River watershed.

Table 6-1. Summary of USGS daily streamflow data

Station Name	Station ID	Drainage Area (mi²)	Start Date	End Date	Status
NF GUALALA R AB SF GUALALA R NR GUALALA CA	11467553	47.1	10/01/2000	Present	Active
SF GUALALA R NR THE SEA RANCH CA	11467510	161	06/01/1991	Present	Active
SF GUALALA R AB WHEATFIELD FK NR ANNAPOLIS CA	11467295	48.2	11/18/2000	05/30/2006	Inactive
WHEATFIELD FORK GUALALA R AB SF NR ANNAPOLIS CA	11467485	111	10/01/2000	09/29/2007	Inactive

Table 6-2. Percent land cover distribution by mapped HRU category for the drainage area to Gualala River South Fork at Sea Ranch.

Land Use / Land Cover (LULC)	Total Area (%)	Soil Group (% LULC Area)				Slope (% LULC Area)		
		A	B	C	D	0-5	5-15	>15
Developed_Low_Intensity	0.1%	0.3%	35.2%	49.5%	15.1%	14.8%	24.5%	60.8%
Developed_Medium_Intensity	0.0%	1.0%	45.9%	45.9%	7.1%	33.7%	36.7%	29.6%
Developed_High_Intensity	0.0%	0.0%	25.0%	62.5%	12.5%	37.5%	43.8%	18.8%
Developed_Open_Space	2.5%	0.0%	51.7%	32.7%	15.5%	5.1%	22.3%	72.7%
Barren	0.0%	0.0%	100.0 %	0.0%	0.0%	0.0%	64.3%	35.7%
Forest	66.7%	0.0%	68.5%	23.5%	8.0%	1.1%	7.5%	91.4%
Scrub	24.5%	0.1%	27.7%	39.7%	32.5%	1.8%	11.1%	87.1%
Grassland	2.3%	0.1%	18.7%	45.3%	35.9%	3.1%	17.0%	80.0%
Pasture	3.1%	0.2%	12.0%	45.6%	42.2%	3.0%	18.4%	78.7%
Agriculture	0.6%	4.1%	22.8%	56.5%	16.7%	8.4%	40.1%	51.5%
Water	0.1%	0.0%	78.0%	13.0%	8.9%	25.4%	32.8%	41.9%
Total	**100.0%**	**0.1%**	**54.9%**	**29.1%**	**15.9%**	**1.6%**	**9.6%**	**88.9%**

Color gradients indicate more Watershed Area and an increasing percentage of Soil and Slope, respectively.

Twenty water years of meteorological forcing data between October 2003 and September 2023 were processed to drive the Gualala River watershed model. Because consumptive use data was only available between 2017 and 2023, these 6 water years were chosen as the calibration period, while the previous ten years of data recorded at this station, between 10/1/2007 and 9/30/2017, were leveraged for model validation. Furthermore, as shown in Figure 6-4, a 2-year subset of the calibration period, 2019 and 2020, were selected for Parameter Estimation. This process is further described in Section

6.2; the entire calibration period was not incorporated into that procedure because of the method's computational demand. Instead, a subset of two years with a diverse range of flow regimes and antecedent conditions was chosen.

The parameter values that PEST chose for this two-year period were then manually tuned to ensure the best possible performance over the entire calibration and validation periods.

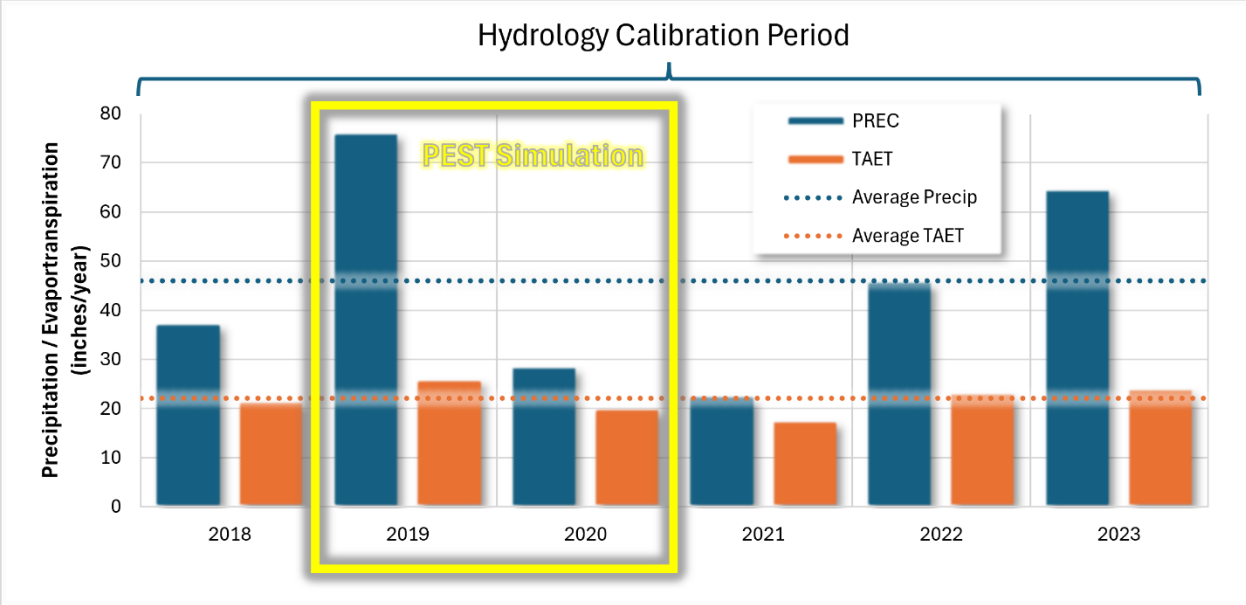

Figure 6-4. Annual average precipitation and evapotranspiration between water years 2018 – 2023, along with PEST simulation and hydrology calibration periods.

6.1 Calibration Assessment and Metrics

A combination of visual assessments and computed numerical evaluation metrics were used to assess model performance during calibration. Model performance was assessed using graphical comparisons of simulated vs. observed data (e.g., time-series plots, flow duration curves, etc.), quantitative metrics, and qualitative thresholds recommended by Moriasi et al. (2015) and Duda et al. (2012), which are considered highly conservative. Moriasi et al. (2007 and 2015) assign narrative grades for hydrology and water quality modeling to the percent bias (PBIAS), the ratio of the root-mean-square error to the standard deviation of measured data (RSR), and the Nash-Sutcliffe model efficiency (NSE). These metrics are defined as follows:

- The percent bias (PBIAS) quantifies systematic overprediction or underprediction of observations. Positive values of PBIAS reflect a bias towards underestimation, while negative values reflect a bias towards overestimation. Low magnitude values of PBIAS indicate better fit, with a value of 0 being optimal.
- The ratio of the root-mean-square error to the standard deviation of measured data (RSR) provides a measure of error based on the root-mean-square error (RMSE), which indicates error results in the same units as the simulated and observed data that is normalized based on the standard deviation of observed data. Values for RSR can be greater than or equal to 0, with a value of 0 indicating perfect fit. Moriasi et al. (2007) provides narrative grades for RSR.
- The Nash-Sutcliffe efficiency (NSE) is a normalized statistic that determines the relative magnitude of the residual variance compared to the measured data variance (Nash and Sutcliffe, 1970). NSE indicates how well the plot of observed versus simulated data fits the 1:1 line. Values for NSE can range between $-\infty$ and 1, with NSE = 1 indicating a perfect fit.

Other metrics were computed and used to assess calibrated model performance, including the Kling-Gupta Efficiency (KGE). This metric can provide additional or complementary information on model performance to the three metrics listed above:

- The Kling-Gupta Efficiency (KGE) metric is based on the Euclidean Distance between an idealized reference point and a sample's bias, standard deviation, and correlation within a three-dimensional space (Gupta et al. 2009). KGE attempts to address documented shortcomings of NSE, but the two metrics are not directly comparable. A KGE value of 1 indicates perfect fit, with agreement worsening for values less than 1. Knoben et al. (2019) have suggested a KGE value > -0.41 as a benchmark that indicates a model has more predictive skill than using the mean observed flow. Qualitative thresholds for KGE have been used by Kouchi et al. (2017).

Both simulated time series and observed data were binned into subsets of a year to highlight seasonal performance and different flow conditions. Hydrograph separation was also performed to assess stormwater runoff vs. baseflow periods to isolate model performance on storm flows and low flows. Table 6-3 is a summary of performance metrics that were used to evaluate the hydrology calibration. As shown in the table, "All Conditions" (i.e., annual interval) for R-squared and NSE is the primary condition typically evaluated during model calibration. For sub-annual intervals, the pattern established in the literature for PBIAS/RME when going from "All Conditions" to sub-annual intervals is to shift the qualitative assessment by one category (e.g., use the "good" range for "very good", "satisfactory" for "good", and so on). This pattern was followed for RSR and NSE qualitative assessments of sub-annual intervals.

Table 6-3. Summary of qualitative thresholds for performance metrics used to evaluate hydrology calibration

Performance Metric	Hydrological Condition	Performance Threshold for Hydrology Simulation			
		Very Good	Good	Fair	Poor
Percent Bias (PBIAS)	All Conditions [1]	<5%	5% - 10%	10% - 15%	>15%
	Seasonal Flows [2]	<10%	10% - 15%	15% - 25%	>25%
	Highest 10% of Daily Flow Rates [3]				
	Days Categorized as Storm Flow [4]				
	Days Categorized as Baseflow [4]				
RMSE – Std Dev Ratio (RSR)	All Conditions [1]	≤0.50	0.50 - 0.60	0.60 - 0.70	>0.70
	Seasonal Flows [2]	≤0.40	0.40 - 0.50	0.50 - 0.60	>0.60
Nash-Sutcliffe Efficiency (NSE)	All Conditions [1]	>0.80	0.70 - 0.80	0.50 - 0.70	≤0.50
	Seasonal Flows [2]	>0.70	0.50 - 0.70	0.40 - 0.50	≤0.40
Kling-Gupta Efficiency (KGE)	Monthly Aggregated [5]	≥0.90	0.90 - 0.75	0.75 - 0. 50	<0.50

1. All Flows considers all daily time steps in the model time series.
2. Seasonal Flows consider daily flows during a predefined, seasonal period (e.g., Wet Season and Dry Season). The Wet Season includes the months of October through April. The Dry Season includes the months of May through September.
3. Highest 10% of Flows considers the top 10% of daily flows by magnitude as determined from the observed flow duration curve.
4. Baseflows and Storm flows were determined from analyzing the daily model time series by applying the USGS hydrograph separation approach (Sloto and Crouse 1996).
5. KGE evaluated using thresholds for monthly aggregated time series (Kouchi et al. 2017).

6.2 Parameter Estimation

Parameter ESTimation (PEST) is a powerful, model-independent tool used for model parameter estimation, sensitivity analysis, and uncertainty analysis. It automates adjusting a specific set of model parameters within a reasonably constrained range of variability, with the objective of minimizing the differences between observed and simulated data. PEST minimizes the Sum of Squared Errors (SSE) across all specified observations and can be customized as needed to evaluate complete flow time series or other temporal categorizations, such as flow duration intervals, monthly volumes, wet and dry periods, etc. A supervised PEST simulation helps to ensure that recommended outcomes are realistic and representative of the natural system being modeled. PEST is versatile and can be integrated with a wide range of environmental and hydrological models, including LSPC.

Section 2 through Section 5 describe model configuration and quality control methods used to represent physical characteristics of the watershed that are either directly measurable or can be reasonably estimated from available spatial or temporal data. On the other hand, parameters associated with subsurface geology represent one of the areas of uncertainty in the model; this is where mathematical optimization of model parameters can improve performance. PEST was used in conjunction with model parameterization guidance documentation (BASINS Technical Note 6 [EPA 2000]) to vary six parameters associated with subsurface geology: the infiltration index parameter (INFILT), the lower zone nominal storage parameter (LZSN), the upper zone nominal storage parameter (UZSN), the non-linear groundwater recession flow parameter (KVARY), the active groundwater recession coefficient (AGWRC), and the interflow recession coefficient (IRC).

For optimizing the infiltration index parameter (INFILT), Technical Note 6 (TN6) suggests that, within a given hydrological soil group, INFILT typically varies between the minimum and maximum values shown in Table 6-4. Some model parameters are codependent. For example, TN6 recommends that, before calibration, the upper zone nominal storage parameter (UZSN) should first be estimated as a percentage of the lower zone nominal storage parameter (LZSN), taking into consideration other physical characteristics such as slope, vegetation cover, and depression storage. Table 6-5 shows recommended initial values for UZSN as a percentage of LZSN and other physical characteristics. The non-linear groundwater recession coefficient (KVARY) "is used when the observed groundwater recession demonstrates a seasonal variability with a faster recession (i.e., higher slope and lower AGWRC values) during wet periods, and the opposite during dry periods," according to TN6. The active groundwater recession coefficient (AGWRC), the ratio of current groundwater discharge to that of the previous day, was the fourth parameter optimized by PEST. TN6 notes that "the overall watershed recession rate is a complex function of watershed conditions, including climate, topography, soils, and land use" that can be estimated from observed time series—and then later adjusted during calibration (EPA 2000). The interflow recession coefficient (IRC), the ratio of the current daily interflow discharge to the interflow discharge on the previous day, affects the rate that interflow is discharged from storage and, therefore, the shape of the hydrograph receding limb after storm events. Model guidance and previous experience suggest that these parameters are both uncertain and very sensitive; therefore, using PEST to explore their impact and optimize performance is worthwhile and beneficial.

Table 6-4. Typical ranges by hydrological soil group for the infiltration index model parameter, INFILT

Hydrological Soil Group	INFILT Typical Ranges (in./hr)		Runoff Potential
	Low	High	
A	0.40	1.00	Low
B	0.10	0.40	Moderate
C	0.05	0.10	Moderate to High
D	0.01	0.05	High

Source: BASINS Technical Note 6 (EPA 2000)

Table 6-5. Recommended initial values for upper zone nominal storage (UZSN) as a percentage of lower zone nominal storage (LZSN) and other physical characteristics

Slope	Vegetation Cover	Depression Storage	UZSN (% of LZSN)
Very Mild	Heavy/Forest	High	14%
Moderate	Moderate	Moderate	8%
Steep	Moderate	Moderate	6%

Source: BASINS Technical Note 6 (EPA 2000)

PEST could optimize model parameters at the HRU level (up to 97 possible degrees of freedom per parameter for previous HRUs); however, to better manage the search space, those degrees of freedom were constrained to 12 combinations of hydrological soil group (4 types) × slope (3 categories). Figure 6-5 is a schematic of HRU-level LSPC hydrology parameters with the six PEST-optimized parameters and process pathways highlighted. Table 6-6 shows the minimum and maximum parameter value ranges used to constrain PEST optimization by hydrological soil group and slope. Table 6-7 shows the initial and final PEST-optimized estimates for subsurface process parameters, summarized by hydrological soil group and slope—the data bars show the relative magnitude of the initial and estimated parameter value within the PEST min/max range (a full cell indicates the maximum value, while an empty cell indicates the minimum value).

After PEST was run and calibration performance was quantified, the model was further tuned to improve performance during the calibration and validation periods. While PEST parameters performed well during the calibration period, they underestimated baseflows during the validation period, likely due to PEST attempting to match the sharp peaks characteristic of the observed hydrograph at Gualala River South Fork at Sea Ranch. To improve calibration while maintaining validation performance, baseflows were raised using INFILT, though INTFW was kept as low as possible to capture peak flows. In addition, LZSN was lowered for all HRUs to address the slight model underestimation observed for both the calibration and validation periods. The baseflow recession rate (AGWRC) and seasonal recession (KVARY) estimated by PEST performed well across all periods and were not changed.

Finally, UZSN and CEPSC were varied monthly to reflect seasonality in soil moisture and interception storage. Current CEPSC values were maintained during dry periods but raised during the wet season to account for seasonal drying and greening and to suppress model overestimation for small storm events. For UZSN, PEST was run again focusing on monthly UZSN over the same two-year period as the initial run. As UZSN was found to be more sensitive to slope, the results of this run were averaged by land cover and soil and then area-weighted to determine ideal UZSN values by slope category. The UZSN values applied to the final model are shown in Figure 6-7. High-sloped UZSN values were kept constant at 0.75 inches because PEST variation was negligible.

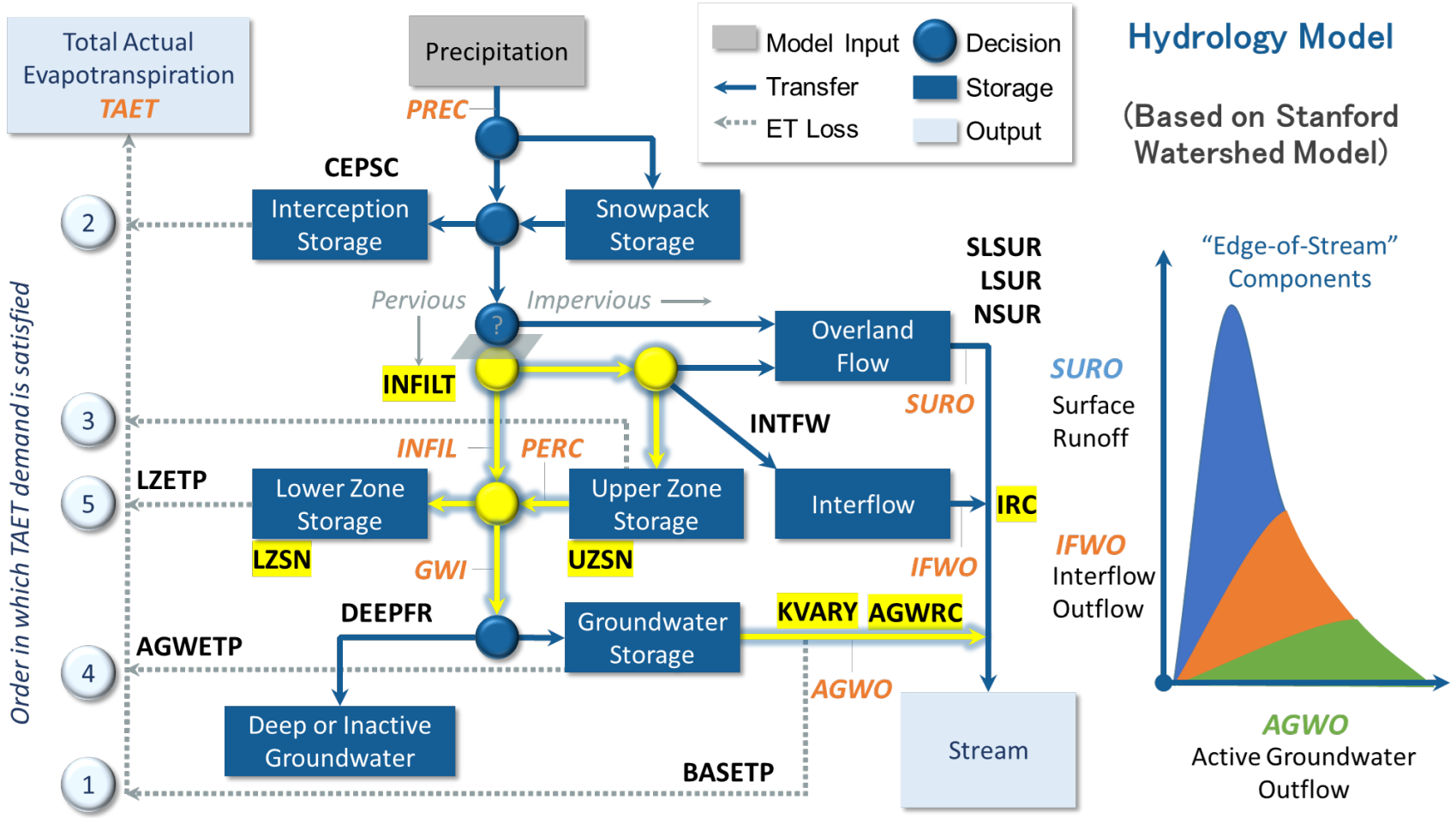

PEST: LSPC parameters and process optimized by Parameter Estimation (PEST) during hydrology calibration.

Figure 6-5. HRU-level LSPC hydrology parameters with PEST-optimized parameters and process pathways highlighted.

Table 6-6. Minimum and maximum parameter value ranges used to constrain PEST optimization, by hydrological soil group and slope

Hydrological Soil Group	Slope	Area (ac)	Area (%)	LZSN		INFILT		KVARY		AGWRC		UZSN (% LZSN)		IRC	
				Min	Max	Min	Max	Min	Max	Min	Max	Min	Max	Min	Max
A	Low	956	0.5%	2	15	0.4	1	0.0001	3	0.84	0.999	1	20	0.3	0.85
A	Med	875	0.4%	2	15	0.4	1	0.0001	3	0.84	0.999	1	20	0.3	0.85
A	High	776	0.4%	2	15	0.4	1	0.0001	3	0.84	0.999	1	20	0.3	0.85
B	Low	1,708	0.8%	2	15	0.1	0.4	0.0001	3	0.85	0.999	1	20	0.3	0.85
B	Med	9,939	4.7%	2	15	0.1	0.4	0.0001	3	0.85	0.999	1	20	0.3	0.85
B	High	111,092	52.5%	2	15	0.1	0.4	0.0001	3	0.85	0.999	1	20	0.3	0.85
C	Low	2,593	1.2%	2	15	0.5	1	0.0001	3	0.85	0.999	1	20	0.3	0.85
C	Med	11,372	5.4%	2	15	0.5	1	0.0001	3	0.85	0.999	1	20	0.3	0.85
C	High	53,590	25.3%	2	15	0.5	1	0.0001	3	0.85	0.999	1	20	0.3	0.85
D	Low	396	0.2%	2	15	0.001	0.05	0.0001	3	0.84	0.999	1	20	0.3	0.85
D	Med	1,946	0.9%	2	15	0.001	0.05	0.0001	3	0.84	0.999	1	20	0.3	0.85
D	High	16,544	7.8%	2	15	0.001	0.05	0.0001	3	0.84	0.999	1	20	0.3	0.85

Table 6-7. Initial and final PEST optimized estimates for subsurface process parameters, summarized by hydrological soil group and slope

HSG	Slope	Area (ac)	Area (%)	LZSN			INFILT		KVARY		AGWRC		UZSN[2]		IRC	
				Initial[1]	Estimated		Initial[1]	Est.	Initial[1]	Est.	Initial[1]	Est.	Initial[1]	Est.	Initial[1]	Est.
					Forest	Others										
A	Low	956	0.5%	10.18	6.13	10.22	0.5	0.4	0.21	1.31	0.85	0.84	14.26	14.31	0.65	0.30
A	Med	875	0.4%	10.18	6.13	10.22	0.5	0.4	2.50	1.31	0.85	0.84	8.15	8.18	0.70	0.30
A	High	776	0.4%	10.18	6.13	10.22	0.5	0.4	0.00	1.31	0.85	0.84	6.11	6.13	0.70	0.30
B	Low	1,708	0.8%	12.50	6.99	11.65	0.2	0.1	2.85	2.71	0.95	0.96	17.50	16.16	0.70	0.51
B	Med	9,939	4.7%	12.50	6.99	11.65	0.2	0.1	0.21	2.71	0.95	0.96	10.00	9.23	0.65	0.51
B	High	111,092	52.5%	12.50	6.99	11.65	0.2	0.1	2.50	2.71	0.95	0.96	7.50	6.92	0.70	0.51
C	Low	2,593	1.2%	13.00	8.20	13.67	0.06	0.05	0.00	0.00	0.97	0.97	18.00	19.58	0.70	0.85
C	Med	11,372	5.4%	13.00	8.20	13.67	0.06	0.05	2.85	0.00	0.97	0.97	12.00	13.05	0.70	0.85
C	High	53,590	25.3%	13.00	8.20	13.67	0.06	0.05	0.21	0.00	0.97	0.97	9.00	9.79	0.65	0.85
D	Low	396	0.2%	13.00	9.00	15.00	0.0068	0.01	2.50	0.00	0.85	0.84	18.00	16.05	0.70	0.85
D	Med	1,946	0.9%	13.00	9.00	15.00	0.0068	0.01	0.00	0.00	0.85	0.84	12.00	10.70	0.70	0.85
D	High	16,544	7.8%	13.00	9.00	15.00	0.0068	0.01	2.85	0.00	0.85	0.84	9.00	8.02	0.70	0.85

1: Initial parameters from calibrated Navarro model, unless manually adjusted away from max and min in PEST

2: UZSN is estimated as a percent of LZSN based on guidance from BASINS Technical Note 6 (EPA 2000)

Data Bars Show the relative magnitude of the parameter values within the PEST min/max ranges (See Table 6-6).

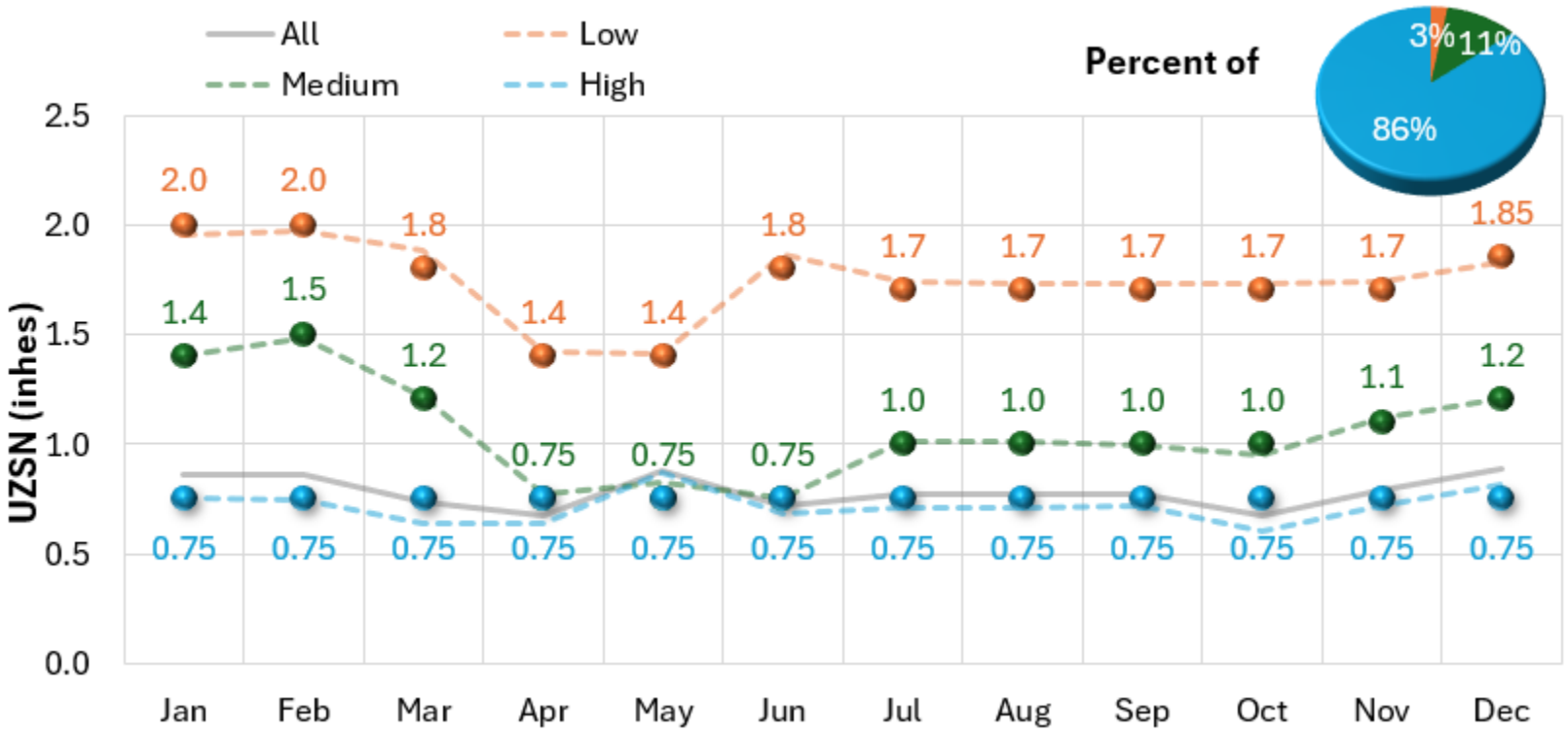

Figure 6-6. Area-weighted UZSN by slope category, average over soil type and land cover.

6.3 Calibration Results

Using the PEST estimated parameters, the model was run for water years 2018 through 2023, and calibration performance was evaluated. As shown in Table 6-8, performance across the calibration period was "Very Good" for PBIAS, with simulated flow volumes slightly overpredicted by 2.9%. Wet season and dry season PBIAS were "Very Good", with 3.0% and 0.5% overprediction, respectively. RSR and NSE were "Very Good" across the entire calibration period and seasons. KGE (calculated with daily flow values) had similar results. These metric values indicate the model is performing well at capturing the observed volume (PBIAS) and trends in wet and dry season flow (RSR, NSE, KGE).

Examination of daily and normalized monthly streamflow (Figure 6-7 and Figure 6-8, respectively) shows that, as indicated by the metrics, the most extreme peaks are slightly underestimated, but general rising/falling patterns in the hydrographs are well-captured. Figure 6-9 and Figure 6-10 present the interquartile ranges and averages, respectively, of monthly normalized flow—both show a high degree of correspondence between observed and simulated values. The flow duration curve (FDC) shown in Figure 6-11 indicates that the observed flow regime trends are generally well-matched by the model. Below the 45th percentile (~10 cfs), modeled flows are higher than observed; it should be noted that modeled and observed FDCs are calculated independently, and flows of the same percentile do not necessarily occur at the same time.

Table 6-8. Summary of daily calibration performance metrics for Gualala River South Fork at Sea Ranch

Hydrology Monitoring Locations	Performance Metrics (10/01/2017 - 09/30/2023)														
	PBIAS						RSR			NSE			KGE		
	All	Wet Season	Dry Season	>10th%ile Flows	Storm Flows	Baseflow	All	Wet Season	Dry Season	All	Wet Season	Dry Season	All	Wet Season	Dry Season
GUALALA R NR THE SEA RANCH CA	-2.9%	-3.0%	-0.5%	4.8%	1.5%	-10.4%	0.31	0.31	0.18	0.91	0.9	0.97	0.92	0.9	0.91

Table 6-9. Summary of performance metrics using monthly average for Gualala River South Fork at Sea Ranch

Calibration Metrics for Monthly Flow	Calibration: 10/01/2017 - 09/30/2023			Validation: 10/01/2007 - 09/30/2017		
	All	Wet Season	Dry Season	All	Wet Season	Dry Season
Count:	72	42	30	124	74	50
PBIAS	-2.8%	-2.9%	-0.4%	2.5%	2.4%	6.2%
RSR	0.15	0.16	0.15	0.19	0.21	0.42
NSE	0.98	0.98	0.99	0.96	0.96	0.83
KGE	0.92	0.9	0.91	0.96	0.96	0.86

1. RSR is the ratio of the root-mean-square error to the standard deviation of observations

Very Good Good Fair Poor

\- Overpredicts + Underpredicts

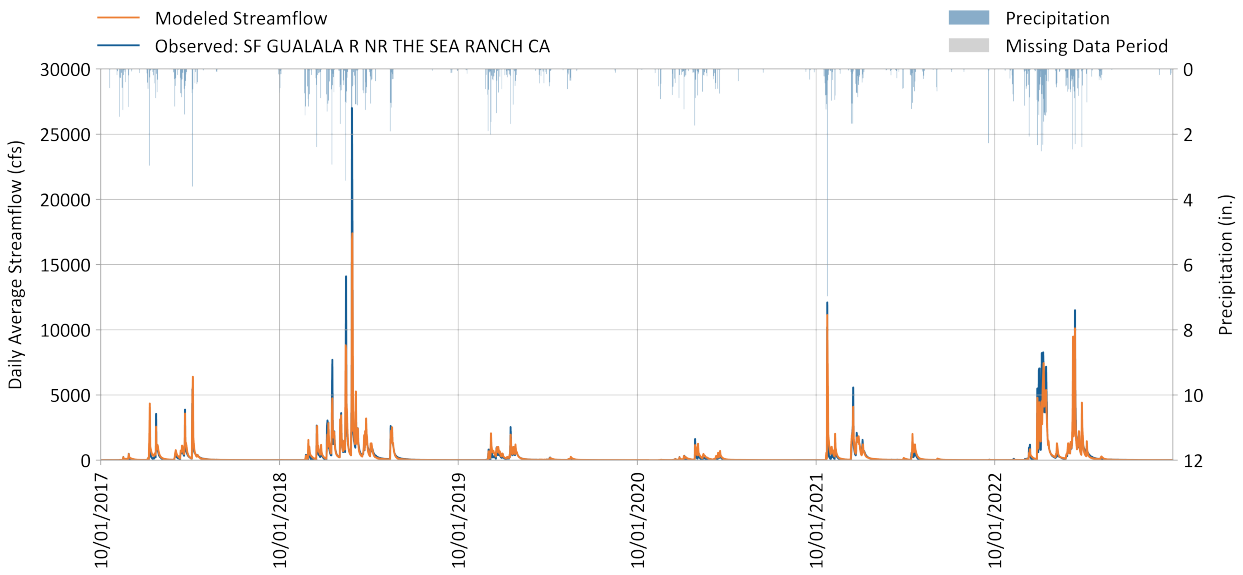

Figure 6-7. Daily Simulated vs. observed streamflow for Gualala River South Fork at Sea Ranch.

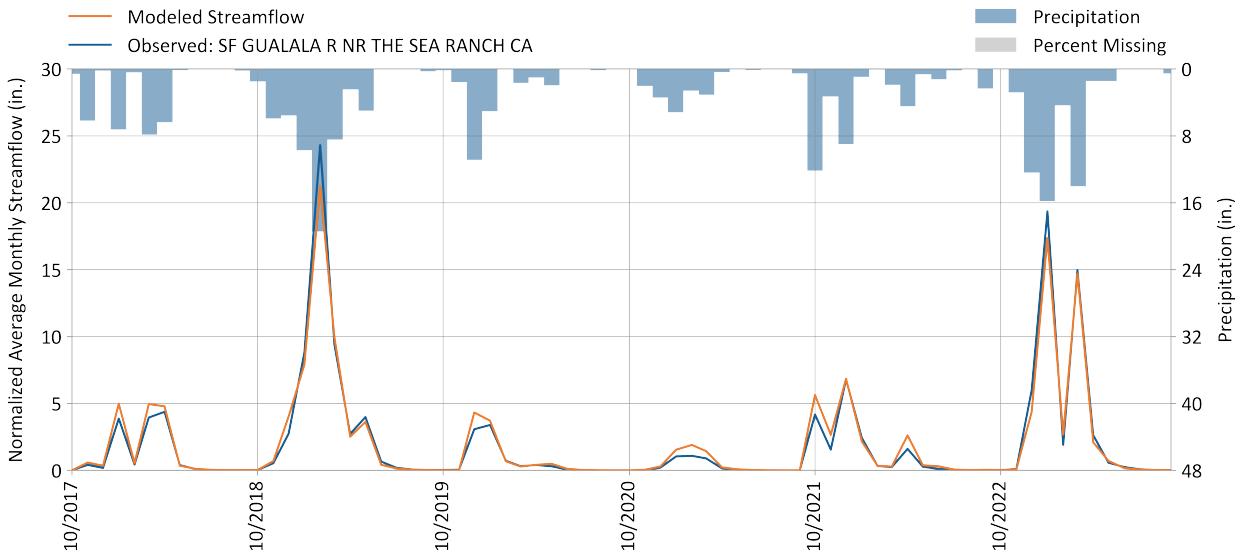

Figure 6-8. Monthly simulated vs. observed streamflow for Gualala River South Fork at Sea Ranch.

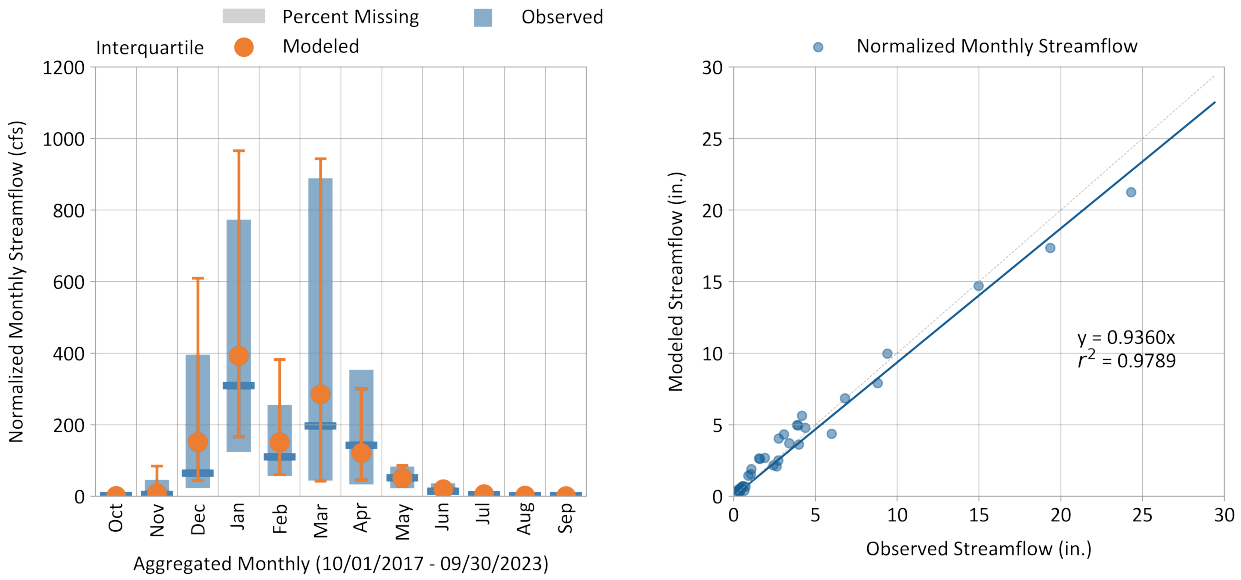

Figure 6-9. Monthly simulated vs. observed streamflow for Gualala River South Fork at Sea Ranch.

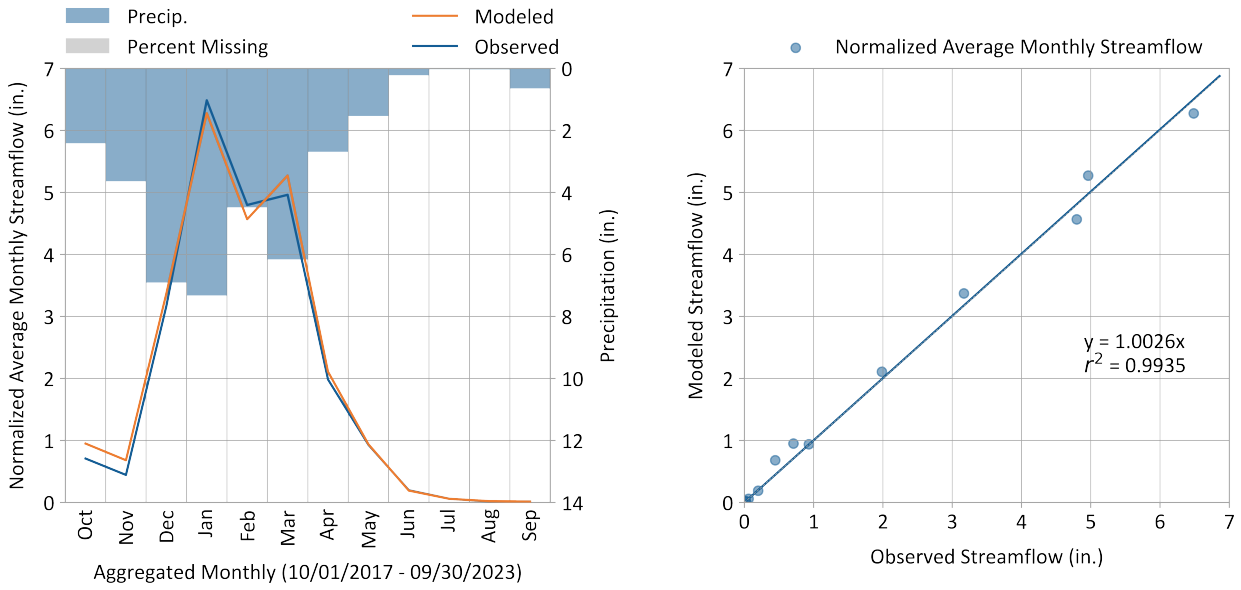

Figure 6-10. Average Monthly simulated vs. observed streamflow for Gualala River South Fork at Sea Ranch.

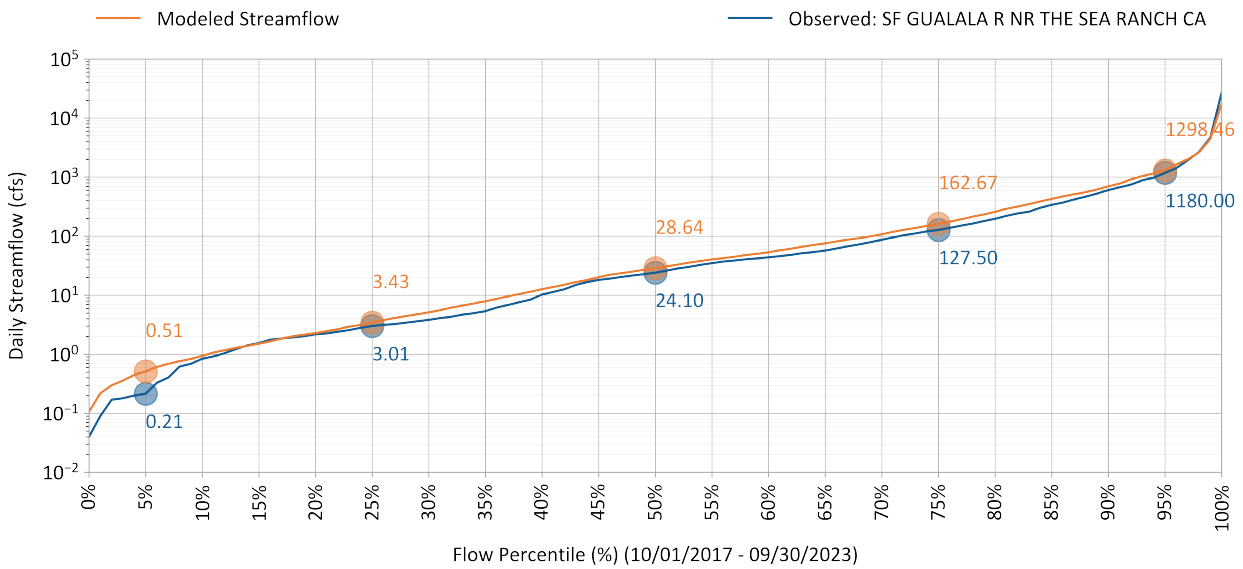

Figure 6-11. Simulated vs. observed flow duration curve for Gualala River South Fork at Sea Ranch.

PBIAS, NSE, and RSR performance values by season and flow regime are shown in Table 6-10, Table 6-11 and Table 6-12, respectively. The "Days Categorized as Baseflow" metric, which is derived from hydrograph separation, consistently shows "Very Good" or "Good" model performance across all conditions and all metrics. Using hydrograph separation to classify baseflow and stormflow provides a more reliable method for assessing low-flow model performance than using the lowest 50% of flows, a metric widely used in hydrology model calibration as a convenient indicator of low-flow model performance. There are several key reasons for this:

- **Improved Representation of Low-Flow Conditions:** The lowest 50% of flows include not only baseflow but also portions of stormflow as the hydrograph rises and falls. This can mask the true low-flow or baseflow behavior of the system, as the transitions from baseflow to stormflow can have very different physical and hydrological drivers. By using hydrograph separation, baseflow, which is primarily driven by groundwater contributions, can be isolated from storm flows, which are influenced by rainfall (Smakhtin 2001). This provides a clearer, more consistent metric for assessing low-flow conditions during model calibration and performance evaluation.
- **Reduction in Variability of Metrics:** Because the rising and falling limbs of the hydrograph are affected by factors such as precipitation intensity, antecedent moisture conditions, and catchment characteristics, including portions of these limbs in the low-flow metric can lead to high variability in model performance metrics. This variability can obscure the modeler's ability to assess low-flow performance accurately. Hydrograph separation, on the other hand, offers a cleaner classification, resulting in lower variability and a more stable and reliable assessment of baseflow model performance.
- **Better Calibration for Baseflow-Driven Processes:** In many hydrological studies, low flows are important for understanding groundwater-surface water interactions, sustaining streamflow during dry periods and supporting aquatic habitats. Hydrograph separation allows for the explicit calibration of baseflow processes, providing a better assessment of groundwater dynamics and groundwater-fed contributions to the stream network. Without separating baseflow and stormflow, calibration based on the lowest 50% of flows may inadvertently skew model performance statistics by over-emphasizing short-term stormflow events and recession behavior, rather than the sustained low flow processes crucial to many hydrological applications.

- **Alignment with Process-Based Hydrology:** Hydrograph separation aligns with a process-based understanding of hydrology, where distinct processes govern baseflow and stormflow. This approach respects the inherent differences in generation mechanisms: baseflow is usually a slower, more consistent groundwater-driven process, while stormflow is a quicker response to precipitation events. This distinction is essential for accurately simulating hydrological systems and ensuring that model results are realistic and representative of different flow conditions. Models that capture these distinct flow components are better suited for making predictions about changes in land use, climate, or other factors that affect baseflow and stormflow differently.
- **Widely Accepted in Hydrological Modeling:** Hydrograph separation techniques are well-established and widely used in hydrological research and practice, offering a consistent framework for distinguishing between baseflow and stormflow (Arnold et al. 1995; Nathan and McMahon 1990). Techniques like those used in the United States Geological Survey (USGS) Hydrograph SEParation (HySEP) methodology provide different options for empirically parsing baseflow time series from storm flows (Sloto and Crouse 1996). The sliding interval method was used to separate both observed and simulated hydrographs at a daily timestep. For a wet water year (2019), Figure 6-12 and Figure 6-13 compare simulated and observed hydrograph separation for the wet and dry seasons, respectively. Similarly, for a dry water year (2020), Figure 6-14 and Figure 6-15 contain simulated and observed hydrograph separation for the wet and dry seasons, respectively. The HySEP methodology's sliding interval method provides a consistent approach for the rollup and comparison of hydrograph components. This approach is robust because it can be directly applicable to time series data as a function of the upstream drainage area. It also performs well on natural hydrological watersheds like the Gualala River.

Upstream of Gualala River South Fork at Sea Ranch, 90% of rainfall occurs during days with the highest 50% of flow, and only 35% of days within the lowest 50% of flows are in the wet season. Because most rainfall and runoff occur during the highest 50% of flows, the lowest 50% of flows metric was not used to evaluate model calibration in the Gualala River watershed. The current calibrated model slightly overpredicts streamflow during low flow conditions, as indicated by the FDC (Figure 6-11), which is conservative for management scenarios focused on maintaining minimal flows.

Table 6-10. Simulated vs. observed daily streamflow PBIAS at Gualala River South Fork at Sea Ranch

Calibration Metrics *(10/01/2017 - 09/30/2023)*	Percent Bias (PBIAS)		
	All Seasons	Wet Season	Dry Season
All Conditions	-2.9%	-3.0%	-0.5%
Highest 10% of Daily Flow Rates	4.8%	4.8%	4.0%
Days Categorized as Storm Flow	1.5%	1.6%	-0.8%
Days Categorized as Baseflow	-10.4%	-11.5%	-0.3%

Table 6-11. Simulated vs. observed daily streamflow Gualala River South Fork at Sea Ranch

Calibration Metrics *(10/01/2017 - 09/30/2023)*	Nash-Sutcliffe Efficiency (NSE)		
	All Seasons	Wet Season	Dry Season
All Conditions	0.91	0.9	0.97
Highest 10% of Daily Flow Rates	0.87	0.87	0.87
Days Categorized as Storm Flow	0.9	0.98	0.96
Days Categorized as Baseflow	0.93	0.93	0.98

Table 6-12. Simulated vs. observed daily streamflow RSR at Gualala River South Fork at Sea Ranch

Calibration Metrics *(10/01/2017 - 09/30/2023)*	RMSE-Std-Dev. Ratio (RSR)		
	All Seasons	Wet Season	Dry Season
All Conditions	0.31	0.31	0.18
Highest 10% of Daily Flow Rates	0.36	0.36	0.35
Days Categorized as Storm Flow	0.32	0.32	0.2
Days Categorized as Baseflow	0.26	0.27	0.14

Very Good Good Fair Poor
\- Overpredicts + Underpredicts

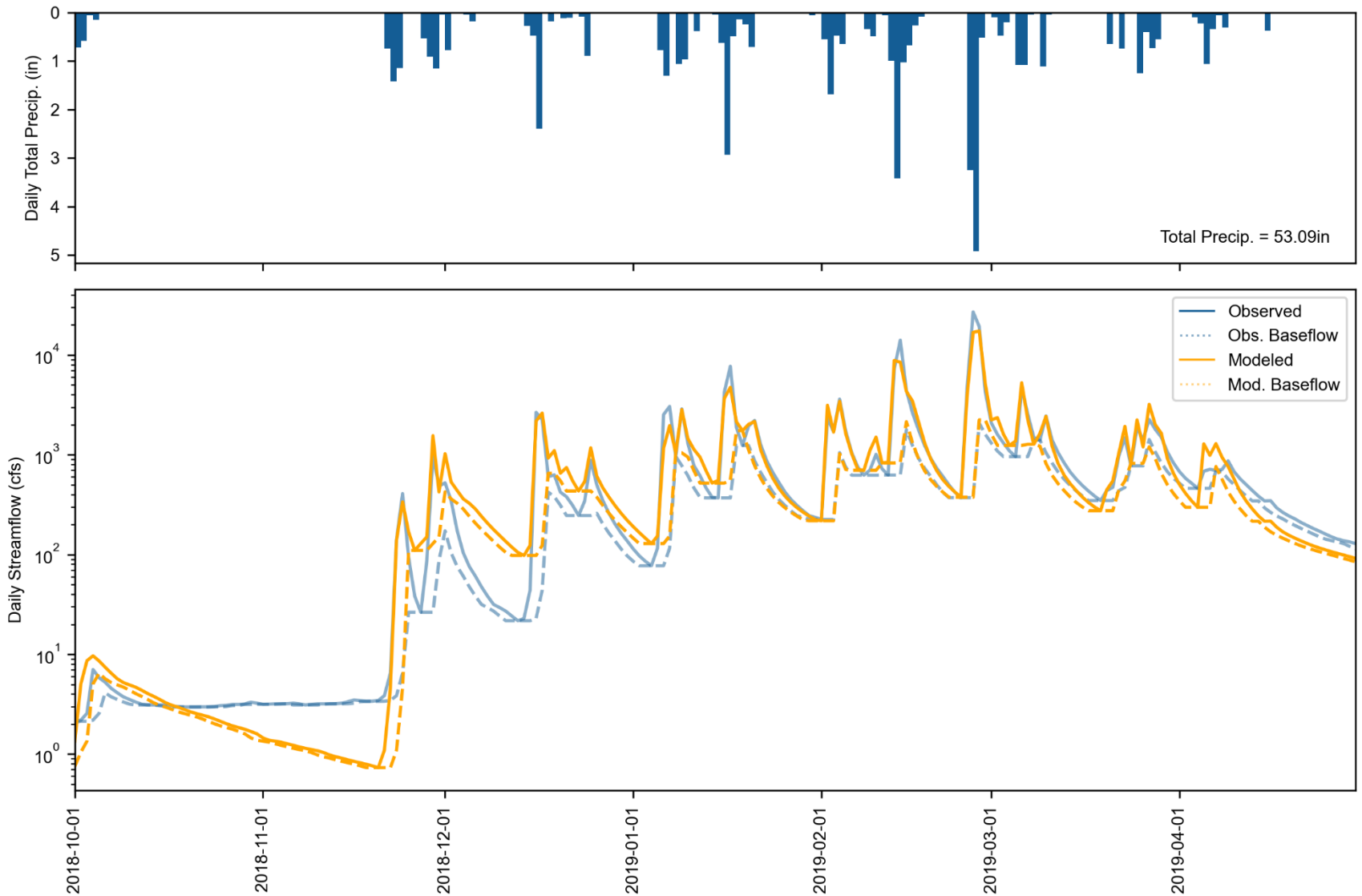

Figure 6-12. Water Year 2019 Wet season daily total precipitation (top) and streamflow (bottom) at Gualala River South Fork at Sea Ranch. Observed and simulated baseflow are calculated with HYSEP; grey shading indicates observed flow is less than the 50th percentile.

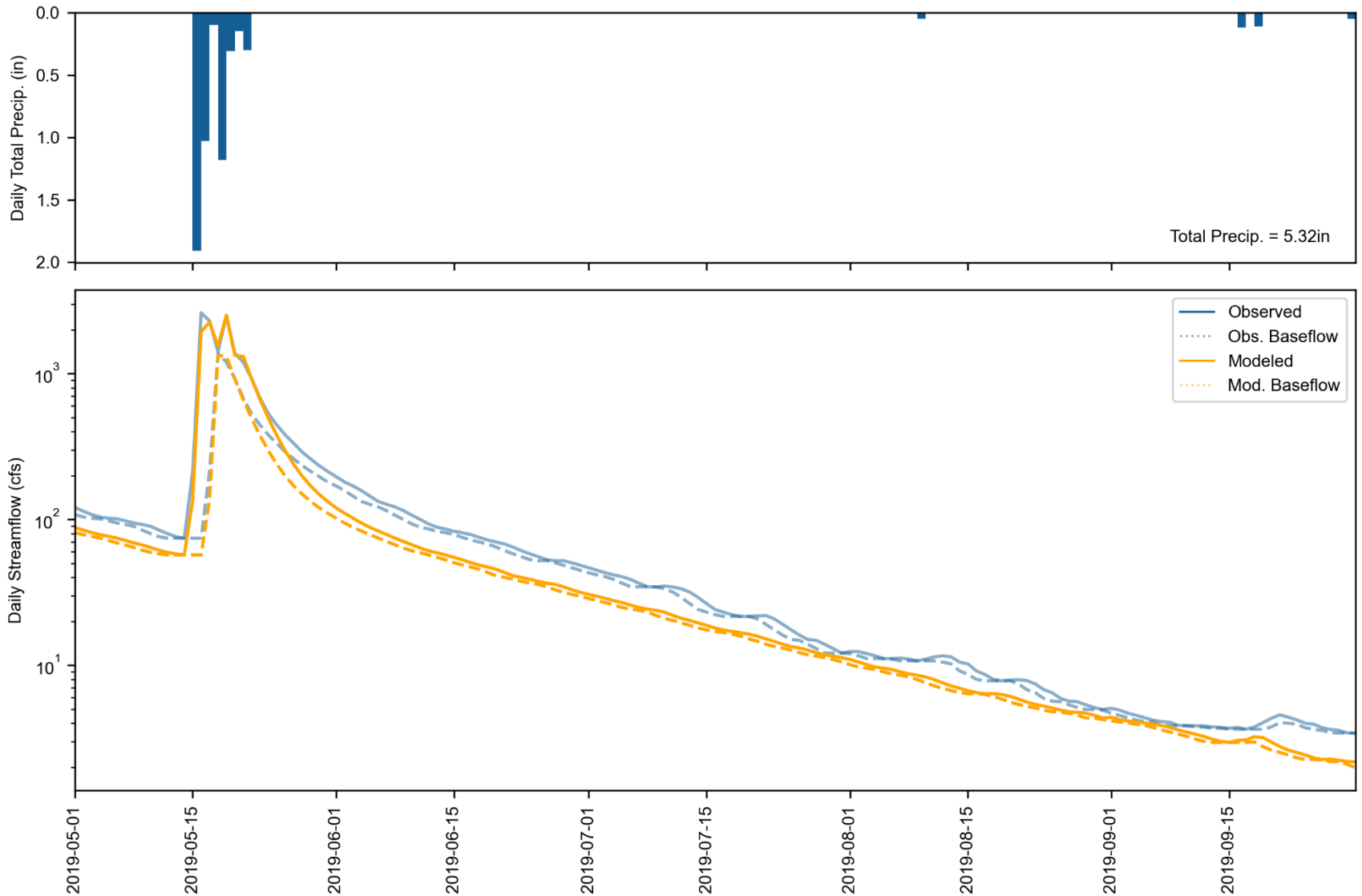

Figure 6-13. Water Year 2019 Dry season daily total precipitation (top) and streamflow (bottom) at Gualala River South Fork at Sea Ranch. Observed and simulated baseflow are calculated with HYSEP; grey shading indicates observed flow is less than the 50th percentile.

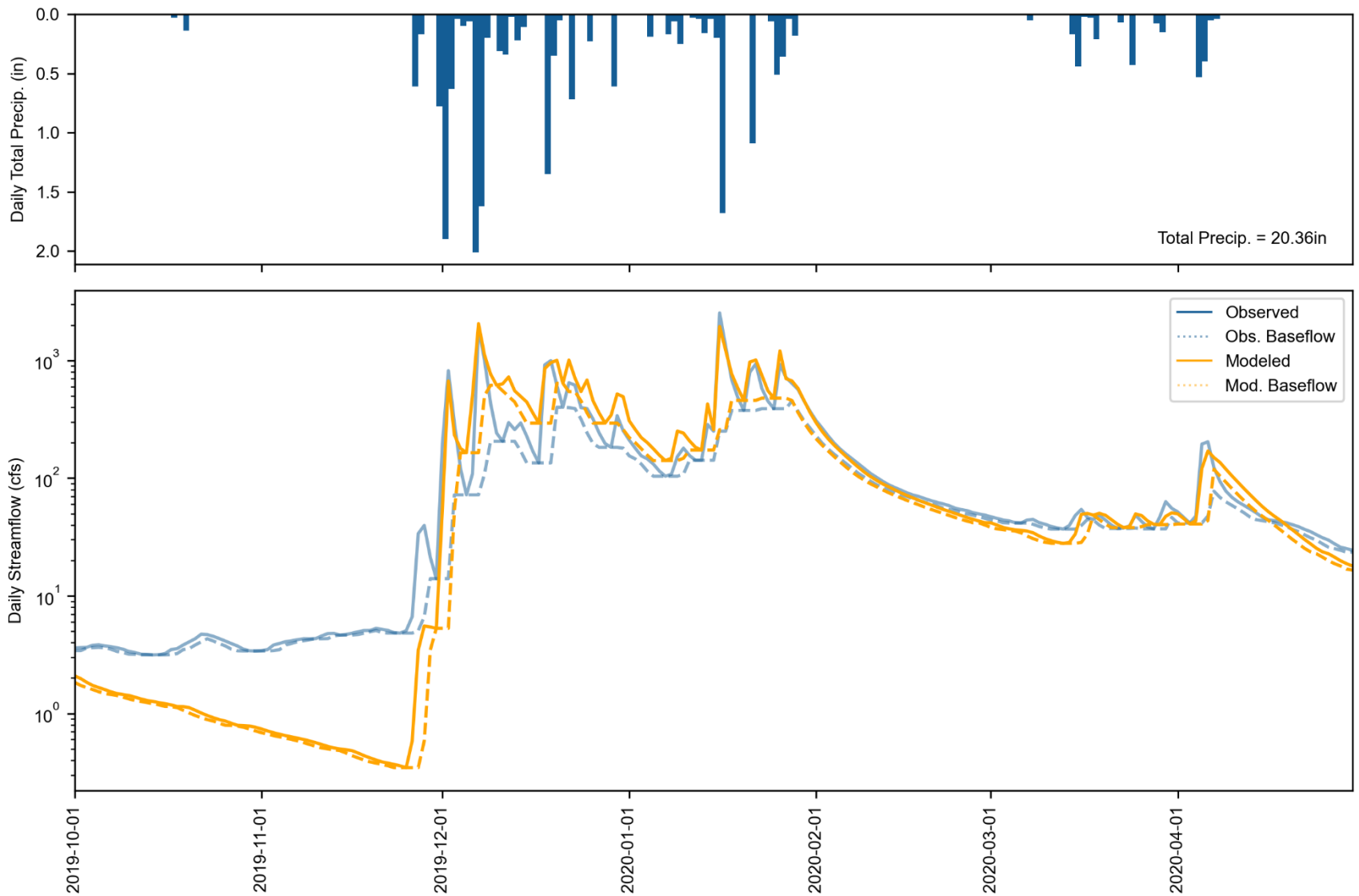

Figure 6-14. Water Year 2020 Wet season daily total precipitation (top) and streamflow (bottom) at Gualala River South Fork at Sea Ranch. Observed and simulated baseflow are calculated with HYSEP; grey shading indicates observed flow is less than the 50th percentile.

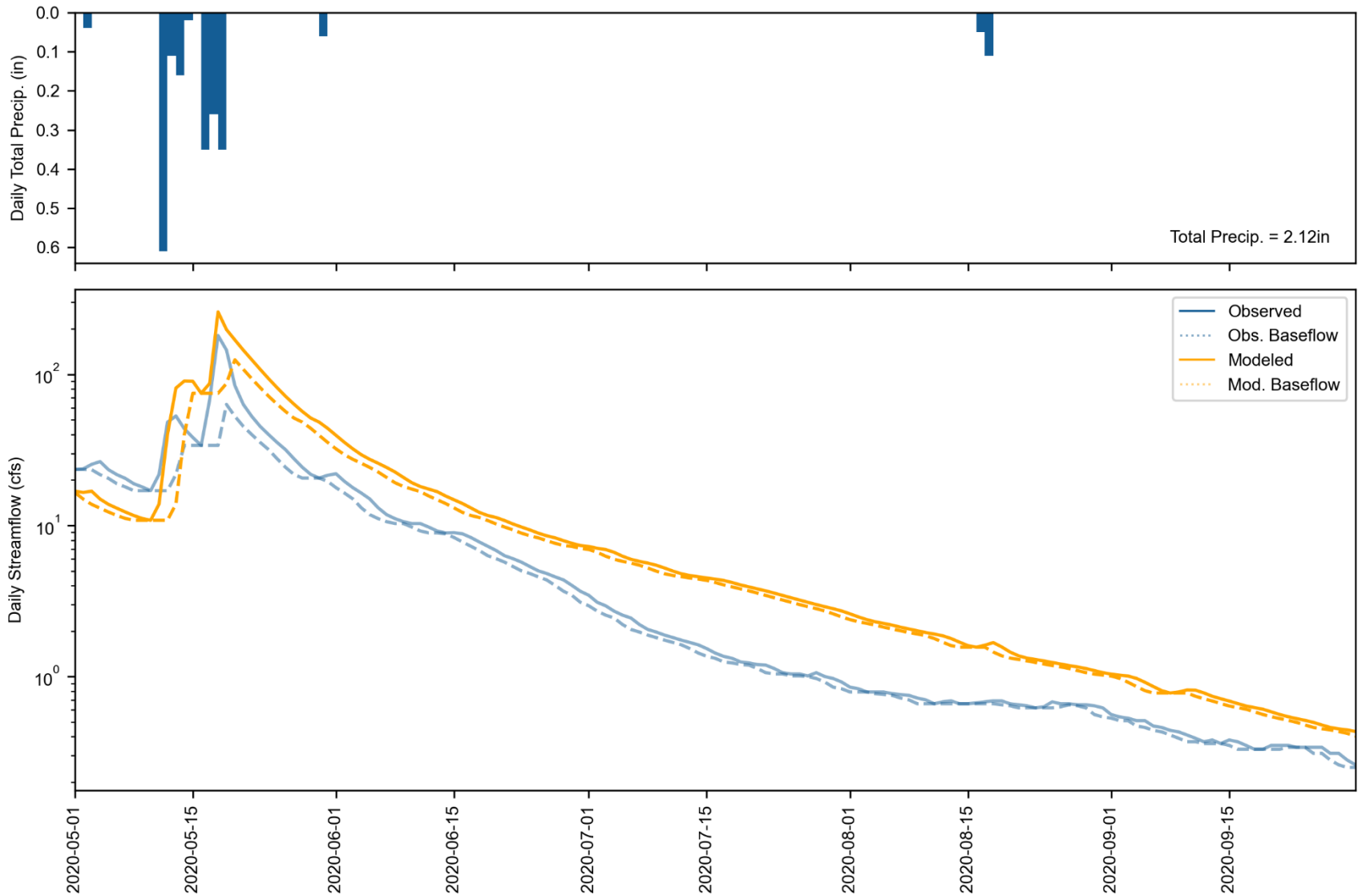

Figure 6-15. Water Year 2020 Dry season daily total precipitation (top) and streamflow (bottom) at Gualala River South Fork at Sea Ranch. Observed and simulated baseflow are calculated with HYSEP; grey shading indicates observed flow is less than the 50th percentile.

7 MODEL VALIDATION

The model was calibrated for water years 2018-2023 (6 years) and validated for water years 2008-2017 (prior 10 years), using flow data from Gualala River South Fork at Sea Ranch. First, a water budget analysis was conducted for the period 2018-2023 because reported diversion estimates were only available for that period. Next, the irrigation water budget was confirmed by normalizing associated inputs and outputs by total irrigated area. This validation check was to confirm that applied irrigation water and withdrawals—as represented using the coefficients, rates, and methods described in Section 5—produced a reasonable and representative average monthly distribution relative to the precipitation and evapotranspiration meteorological forcing data. Irrigation was simulated for the full period from 2008-2023. No withdrawal data were available prior to water year 2018; therefore, average monthly withdrawals reported between 2018-2023 were applied for water years 2008-2017. This section presents results for the water budget analysis (Section 7.1) and the validation period performance at the USGS flow station (Section 7.2). Data from the other three flow stations in the watershed, including the two inactive flow stations (Gualala River Wheatfield Fork and Gualala River South Fork at Annapolis, CA), were considered for validation and discussed in detail in Section 7.3.

7.1 Water Budget

A water budget analysis was conducted to validate a match between the sum of model inputs and outputs. Water inputs include precipitation (both to land segments and water body surfaces) and applied irrigation water. Water outputs include terminal outflow at our assessment for Gualala River, total actual evapotranspiration (from land segments + direct evaporation from water bodies), and total withdrawals (i.e., irrigation and non-irrigation diversion). The water budget was calculated from October 2017 through September 2023, the period where withdrawal information was available. The water budget validation showed a close match between all model inputs and outputs—there is a 0.05% difference between inflow and outflow, which represents net volume to the system storage over the 6-year simulation period. Figure 7-1 shows the simulated water balance expressed as total volumes and area-normalized annual average depths for water years 2018-2023 at the Gualala River South Fork station. For the same period, Figure 7-2 shows the monthly average area-normalized components of the simulated water balance. In both figures, intermediate values for edge-of-stream outflows prior to stream routing (i.e., surface runoff + interflow outflow + active groundwater outflow) and inflow to active groundwater storage are presented to illustrate the relative scale of those components. The monthly summary also illustrates the expected system lag of approximately 6 months between peak rainfall (Dec-Jan) and peak evapotranspiration (Jun-Jul).

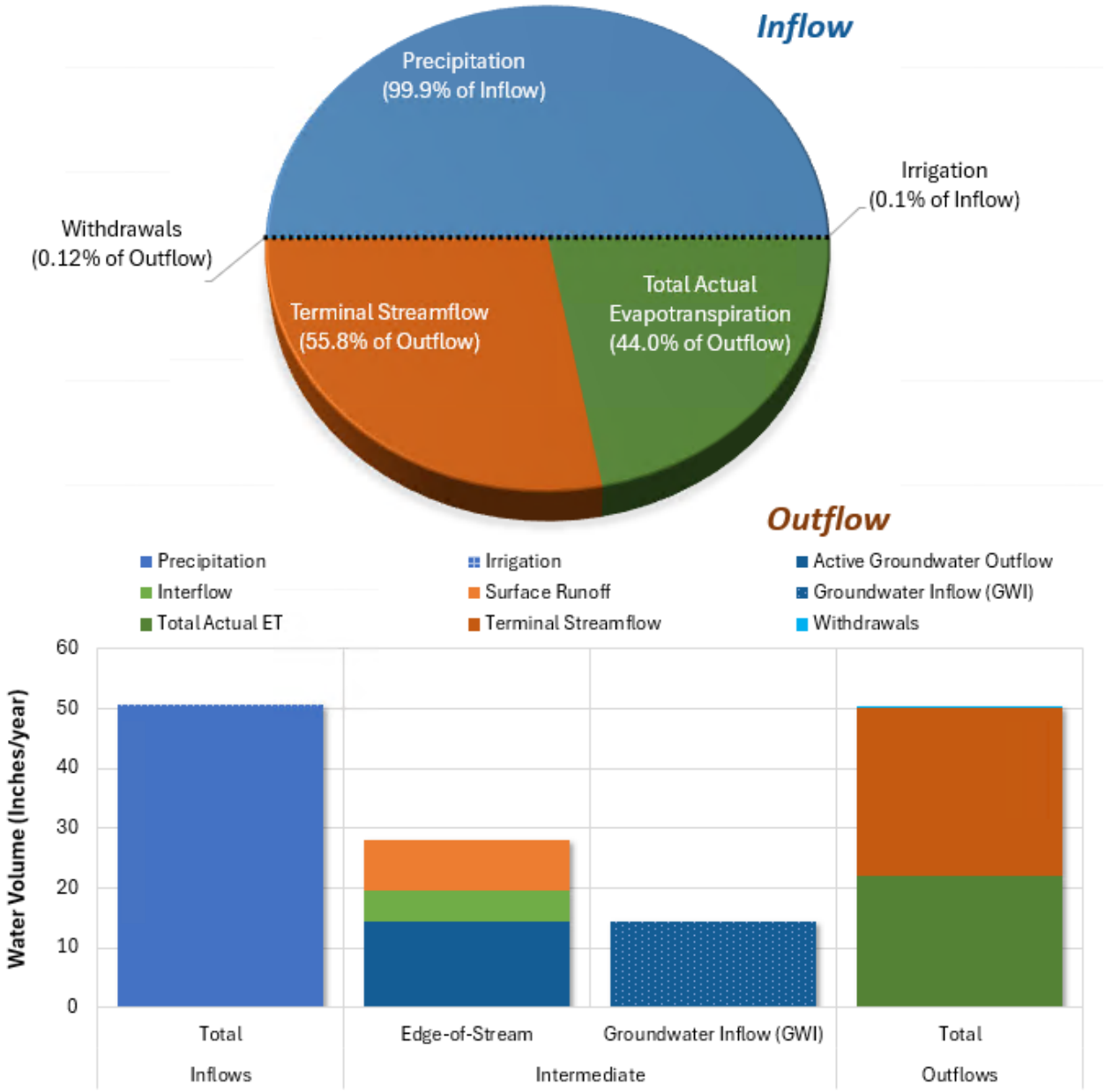

Figure 7-1. Simulated water balance expressed as total volumes and area-normalized annual average depths for the calibration period (water years 2018-2023) at the Gualala River South Fork at Sea Ranch station.

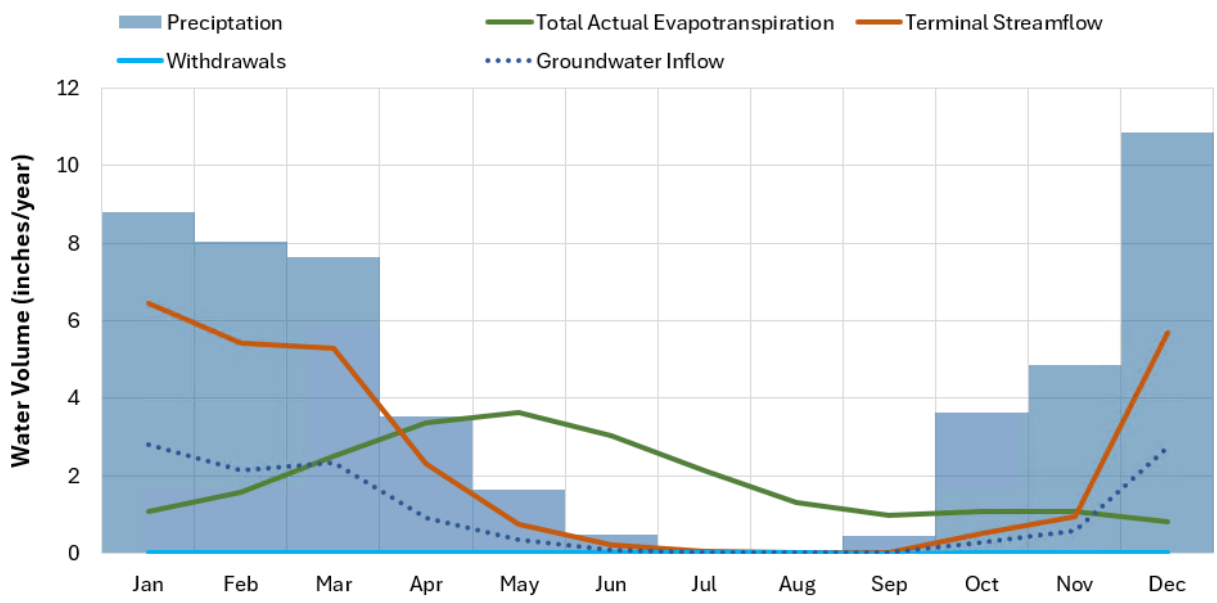

Figure 7-2. Monthly average area-normalized simulated water balance components for water years 2018-2023 at the Gualala River South Fork at Sea Ranch station.

The water budget for applied irrigation volume was also summarized from calibrated model outputs. On average, a total of 34 acre-feet of irrigation water per year was applied on 504 acres of land in the Gualala model. Irrigation volume was temporally distributed as 37% of potential evapotranspiration so that more irrigation occurred during the drier months, as shown in Figure 7-3. The total reported volume of surface water withdrawn either for direct irrigation or storage represents about 103% of the total volume of irrigation water applied.

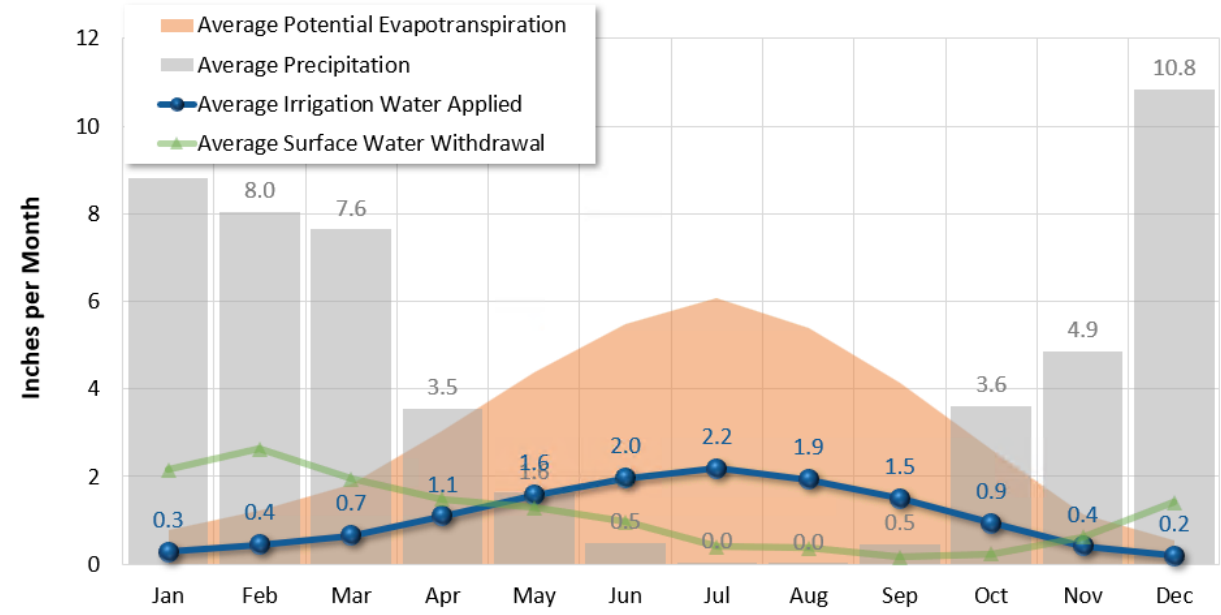

Figure 7-3. Monthly average area-normalized irrigation water balance for irrigated HRUs in the Gualala River watershed upstream of South Fork at Sea Ranch.

7.1.1 ET Comparison

Because the Gualala River watershed only has one active streamflow station with continuous flow data for estimating water balance components, limited data were available to validate evapotranspiration, a major component of the estimated water balance. Evapotranspiration is a key predicted model component of the water budget upstream of the streamflow station, so OpenET was treated as an alternate source of "observed" data for confirming the simulated magnitude, spatial distribution, and temporal variability of evapotranspiration.

The OpenET project is an operational system for generating and distributing ET data at a field scale using an ensemble of six well-established satellite-based approaches for mapping ET (Melton et al. 2022). Within California, OpenET has data beginning in 2018 and uses CIMIS meteorological datasets to compute reference ET and actual ET. OpenET has undergone extensive intercomparison and accuracy assessment conducted using ground measurements of ET; for agricultural areas, results of these assessments demonstrate strong agreement between the satellite-driven ET models and observed flux tower ET data. However, for natural land covers like forests, scrub, and grasslands, which are the dominate land cover types in the Gualala River watershed (Table 7-1**),** the OpenET ensemble is known to be biased towards overprediction (OpenET 2021). OpenET data were used in an exploratory comparison with simulated total actual ET (TAET) and the CIMIS reference ET at the HUC-12 scale and were not used for calibration because of the known biases. In highly agricultural watersheds, OpenET could prove to be a valuable data point for model calibration and validation; however, in the Gualala River watershed, OpenET closely resembles CIMIS reference ET.

For the Gualala River watershed, at both HUC-12 and watershed-wide scales, monthly total OpenET, CIMIS reference ET, and LSPC TAET were compared for the period with available OpenET and meteorological data (October 2003 – September 2023). As seen in Figure 7-4, OpenET is similar in magnitude and timing to the CIMIS reference ET, and both datasets are high, as expected for reference ET. When estimated as annual average observed precipitation minus annual average observed streamflow, actual ET (and a storage component) is approximately 61% of the outflow portion of the water budget. This is close to the simulated value of 64% from the calibration period (see Section 7.1) and 65% for the OpenET period.

At the HUC-12 scale, ET datasets were mapped as the ratio of annual average totals for: (1) TAET:OpenET, (2) OpenET:PEVT (CIMIS reference ET), (3) PREC:OpenET. These comparisons are shown in Figure 7-5, Figure 7-6, and Figure 7-7, respectively. A fixed legend scale of ratios (i.e., between 0.5 and 1.9) was used across all three maps to highlight differences in magnitude and spatial variation of the ratios. These maps show that TAET is between 52% to 70% of OpenET (Figure 7-5), OpenET is between 93% and 102% of CIMIS reference ET (Figure 7-6), and OpenET ranges from 103% to 183% of total annual precipitation (Figure 7-7)—note the inverted phase shift between the two (Figure 7-4).

Table 7-1 Comparison Summary of HRU area grouped by land cover for HUC-12s within the Gualala River watershed

HUC-12		HRU Land Cover Area (%)								
Name	Area (ac)	Developed Pervious	Barren	Forest	Scrub	Grassland	Pasture	Agriculture	Irrigation	Water
Marshall Creek	12,662.50	3.01%	0.00%	55.53%	31.81%	3.82%	4.30%	1.41%	0.11%	0.01%
House Creek	18,236.60	0.82%	0.00%	55.37%	35.82%	3.03%	4.13%	0.26%	0.34%	0.23%
Upper Wheatfield Fork Gualala River	24,464.99	2.41%	0.01%	59.89%	30.69%	2.42%	4.37%	0.17%	0.00%	0.03%
Lower Wheatfield Fork Gualala River	28,724.08	3.35%	0.00%	81.68%	11.35%	1.12%	1.73%	0.54%	0.00%	0.23%
Buckeye Creek	25,727.75	2.42%	0.00%	80.27%	13.96%	1.40%	1.59%	0.32%	0.00%	0.04%
Russian Gulch-Frontal Pacific Ocean	21,429.08	11.67%	0.03%	64.77%	15.45%	6.75%	0.71%	0.11%	0.00%	0.50%
Rockpile Creek	22,412.06	0.87%	0.00%	83.67%	13.65%	1.14%	0.64%	0.00%	0.00%	0.01%
North Fork Gualala River	30,623.10	2.76%	0.00%	86.17%	8.81%	1.50%	0.61%	0.12%	0.02%	0.01%
South Fork Gualala River-Gualala River	28,188.77	3.45%	0.01%	81.61%	11.60%	1.42%	0.94%	0.24%	0.25%	0.47%
Total	**212,468.93**	**3.40%**	**0.01%**	**74.33%**	**17.54%**	**2.29%**	**1.89%**	**0.30%**	**0.07%**	**0.18%**

Color Gradient: Lowest | Low | Med | High | Highest

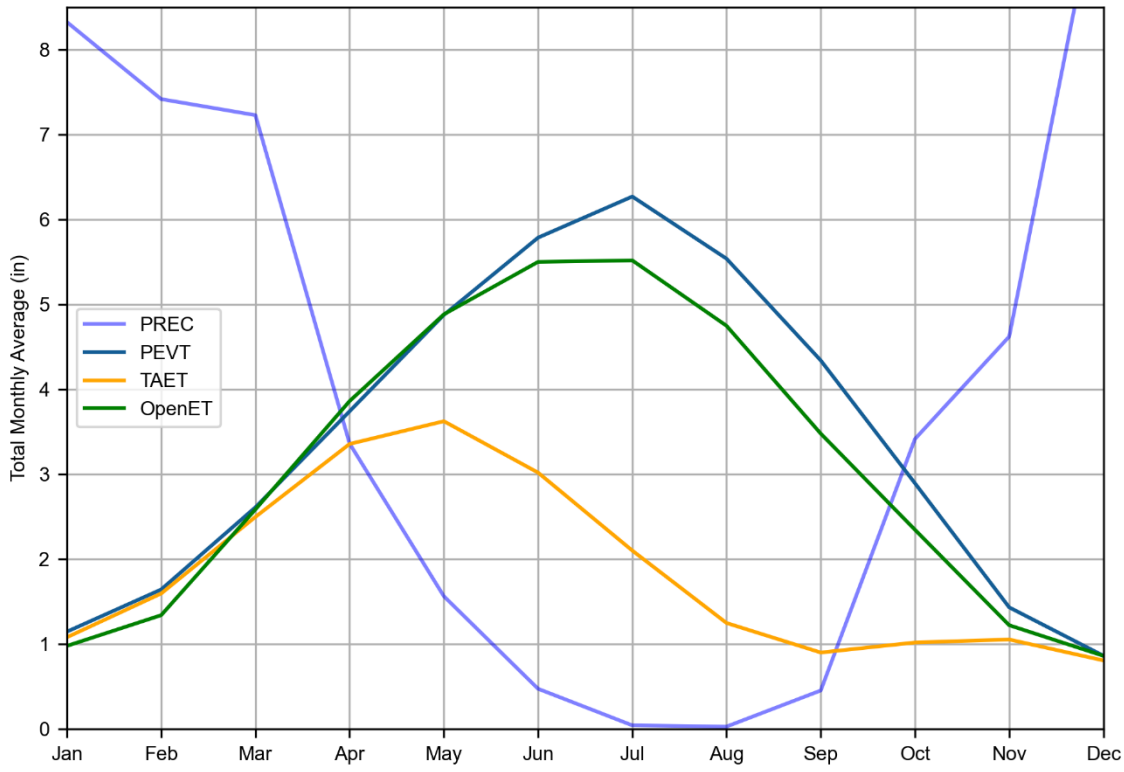

Figure 7-4. Comparison of average monthly totals from October 2003 – September 2023 for rainfall (PREC), potential ET (PEVT), and simulated total actual ET (TAET) for the Gualala River watershed.

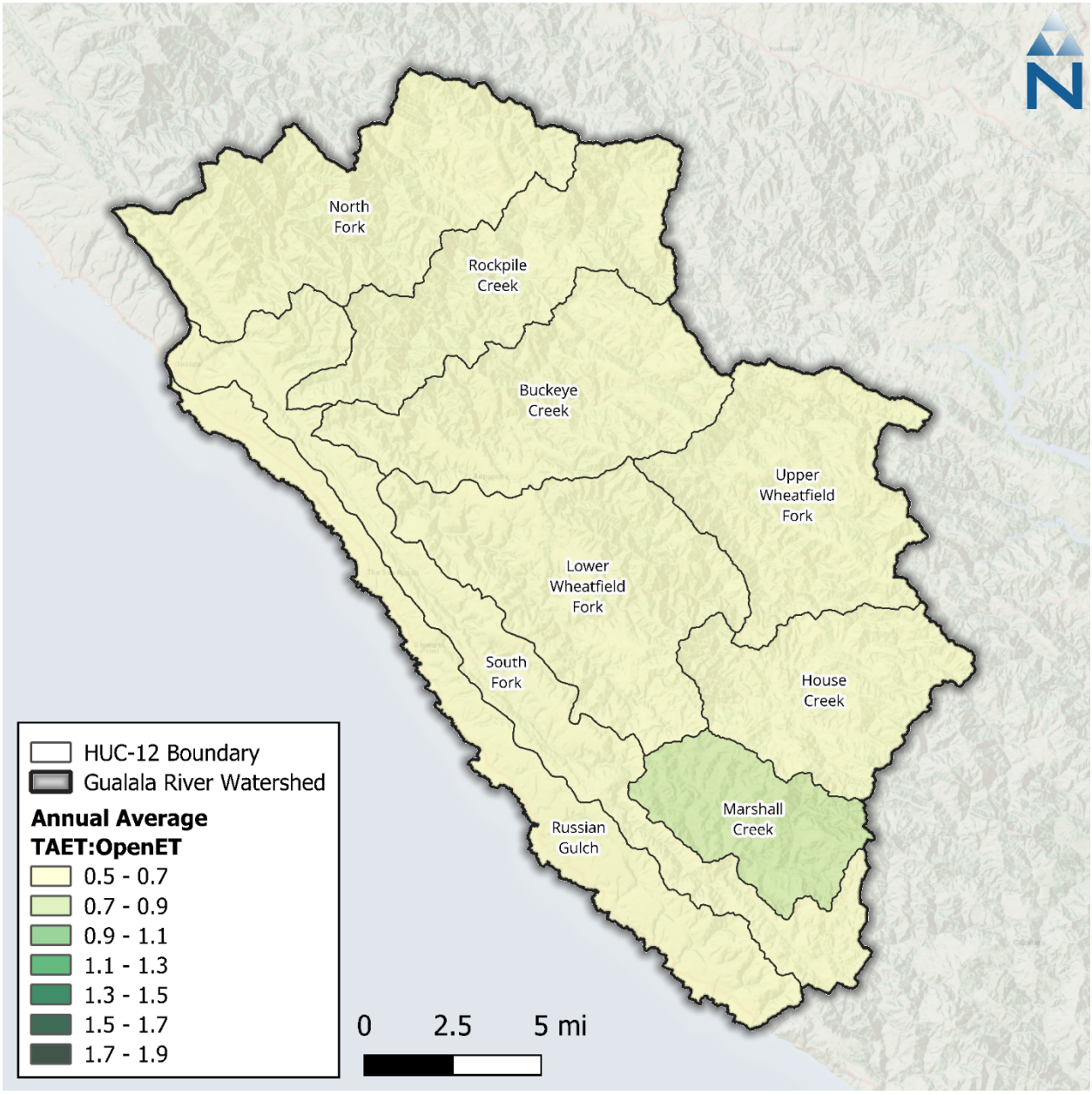

Figure 7-5. Ratio of annual average simulated total actual ET (TAET) to OpenET by HUC-12 within the Gualala River watershed.

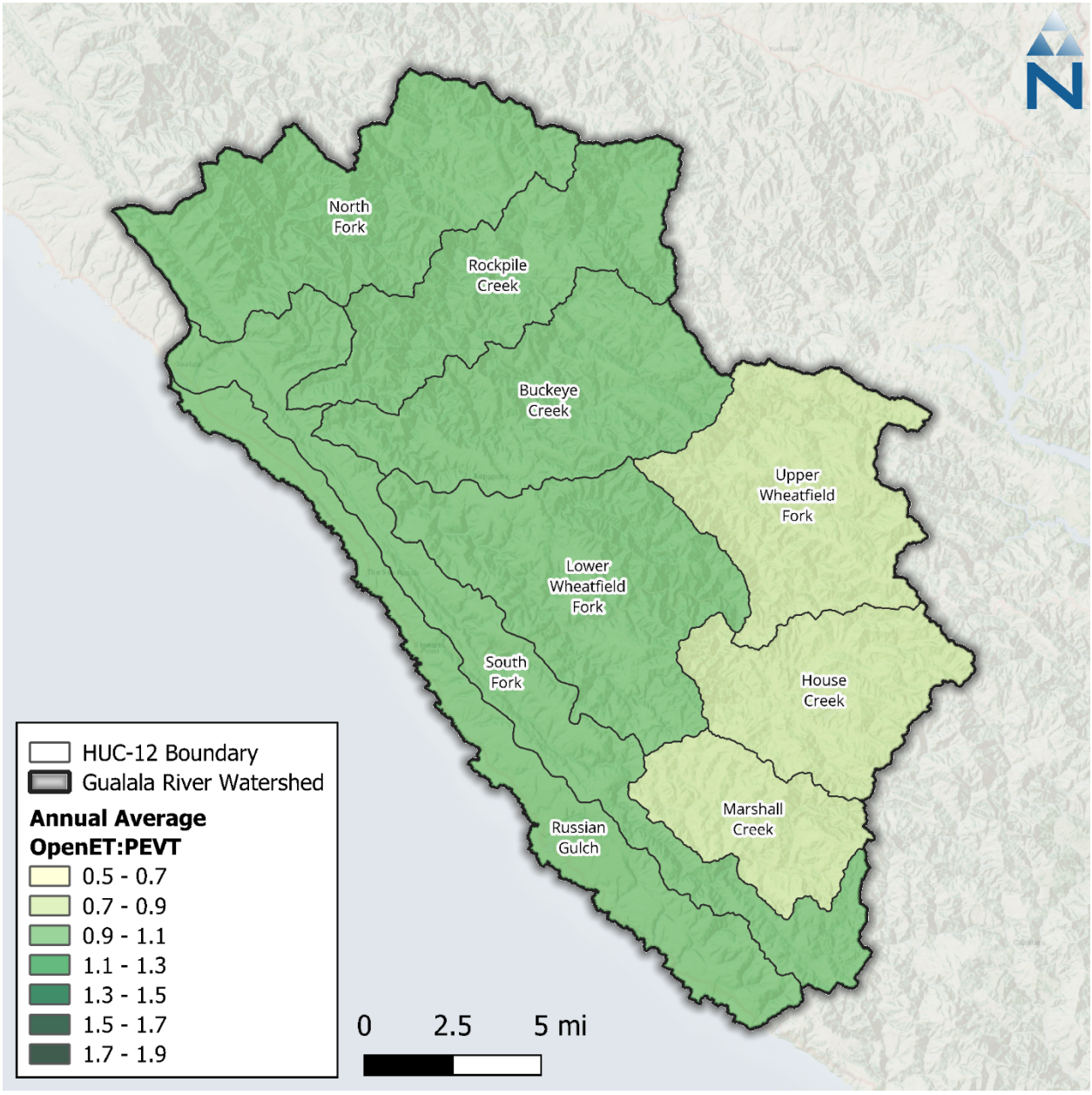

Figure 7-6. Ratio of annual average OpenET to CIMIS reference ET (PEVT) by HUC-12 within the Gualala River watershed.

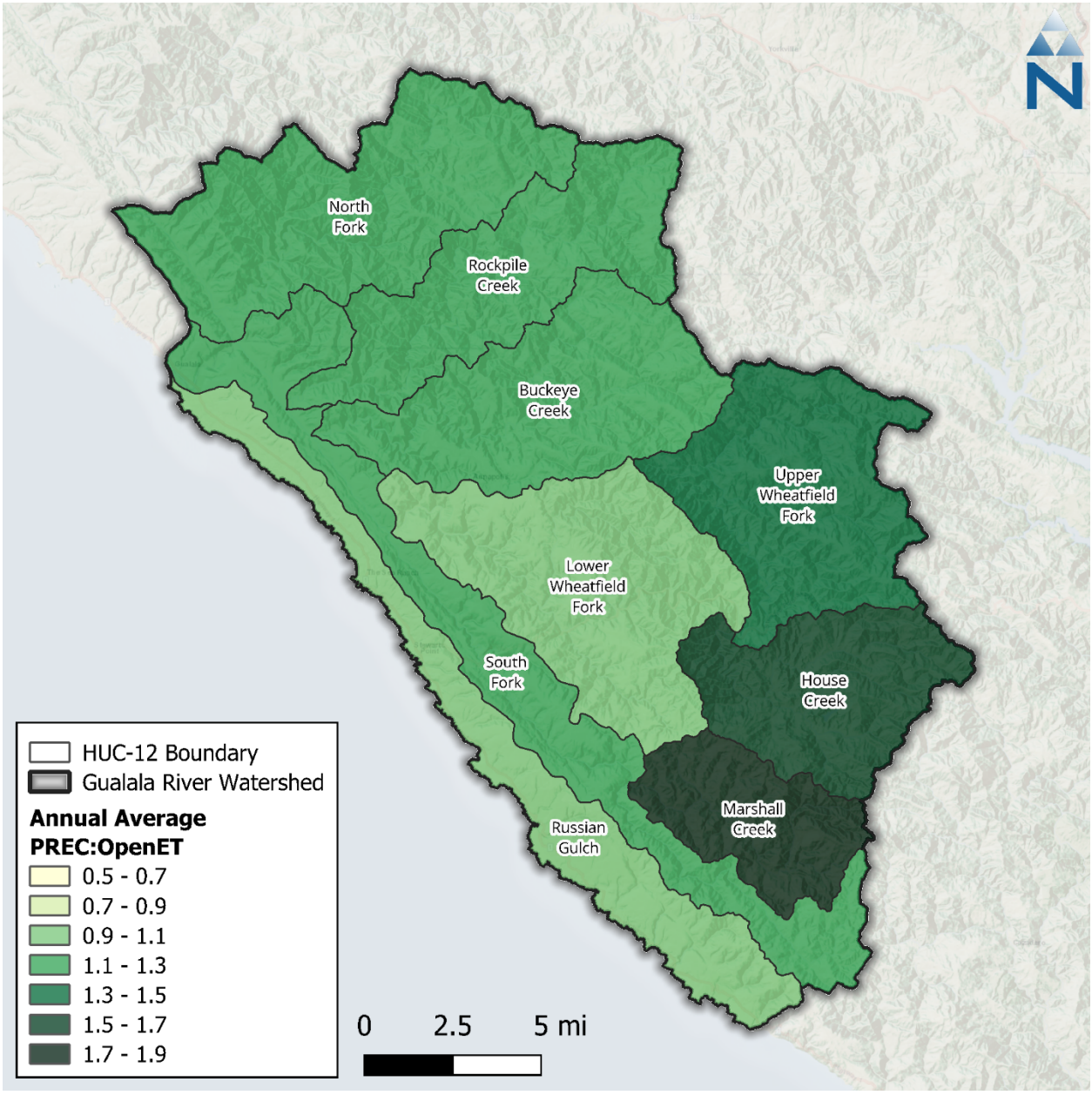

Figure 7-7. Ratio of annual average precipitation (PREC) to OpenET by HUC-12 within the Gualala River watershed.

7.2 Hydrology

Across the validation period (water years 2008 to 2017), hydrologic performance was similar to the calibration period. To avoid skewing volume-sensitive error statistics, an outlier storm event starting at the very beginning of the dry season on 5/5/2009 and 5/6/2009 was removed from the observed data record for Gualala River South Fork at Sea Ranch. The combined volume from those two days is almost 12% of the total overall volume across the fifty months of dry period data in the validation period. Figure 7-8 shows the average monthly hydrograph for only dry season days for water years 2008-2017; the chart highlights the impact of the outlier days in the observed flow. After removing those days in 2009, the modeled vs. observed dry-season PBIAS improves from 13.9% to 6.3%.

In addition, POD data was extended back to the beginning of the water right to properly capture the impact on low flows during the validation period.

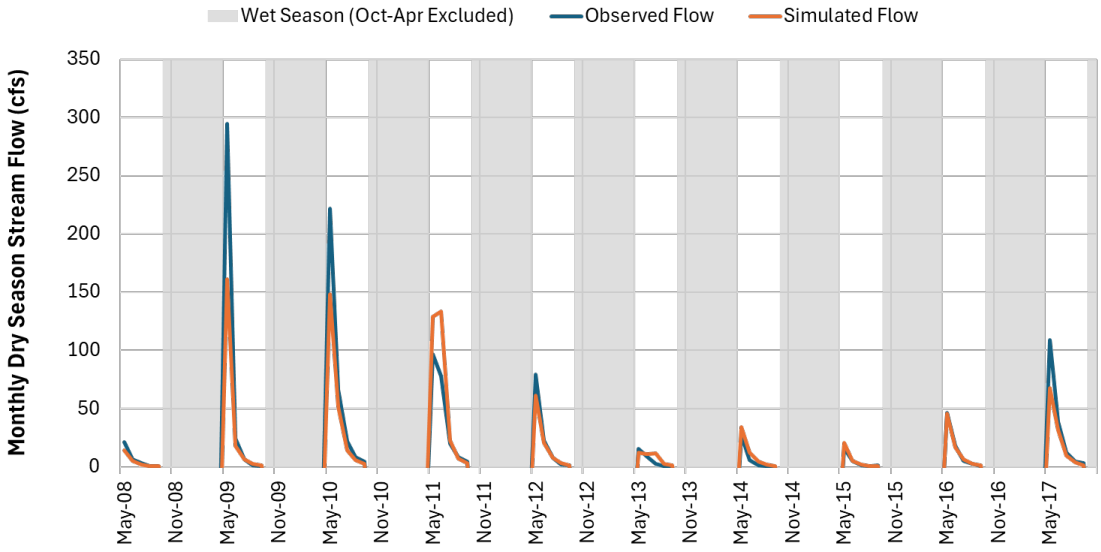

Figure 7-8. Hydrograph of dry season flow during validation period at Gualala River South Fork at Sea Ranch.

Over the entire simulation period, including both calibration and validation periods, PBIAS is "Very Good" and slightly underpredicted (Table 7-2); similarly, seasonal PBIAS values were "Very Good", also slightly underpredicting. All calibration statistics discussed so far, including those in Table 7-2, were computed using daily average time series and include higher resolution flow-regime metrics, like the highest 10% of flows, storm flows, and baseflow. As expected, PBIAS is not impacted by the time step change; however, RSR and NSE both show notable improvement in performance compared to using the daily average time series.

Examination of daily and normalized monthly streamflow (Figure 7-9 and Figure 7-10, respectively) shows that the most extreme peaks are slightly underestimated, similar to the calibration period results, but general rising/falling patterns in the hydrographs are well-captured. Figure 7-11 and Figure 7-12 present the interquartile ranges and averages, respectively, of monthly normalized flow—both show a high degree of correspondence between observed and simulated values. The flow duration curve (FDC) shown in Figure 7-13 indicates that observed flow regime trends are generally well-matched by the model. Below the 17th percentile (~2 cfs), modeled flows are higher than observed; it should be

noted that modeled and observed FDCs are calculated independently, and flows of the same percentile do not necessarily occur at the same time.

Table 7-2. Summary of daily validation performance metrics for entire period

Hydrology Monitoring Locations	Performance Metrics (10/01/2007- 09/30/2023)														
	PBIAS						RSR			NSE			KGE[1]		
	All	Wet Season	Dry Season	>10th %ile Flows	Storm Flows	Baseflow	All	Wet Season	Dry Season	All	Wet Season	Dry Season	All	Wet Season	Dry Season
Gualala River South Fork at Sea Ranch	0.9%	0.6%	7.6%	6.9%	3.6%	-3.2%	0.35	0.38	0.49	0.88	0.87	0.78	0.95	0.94	0.84

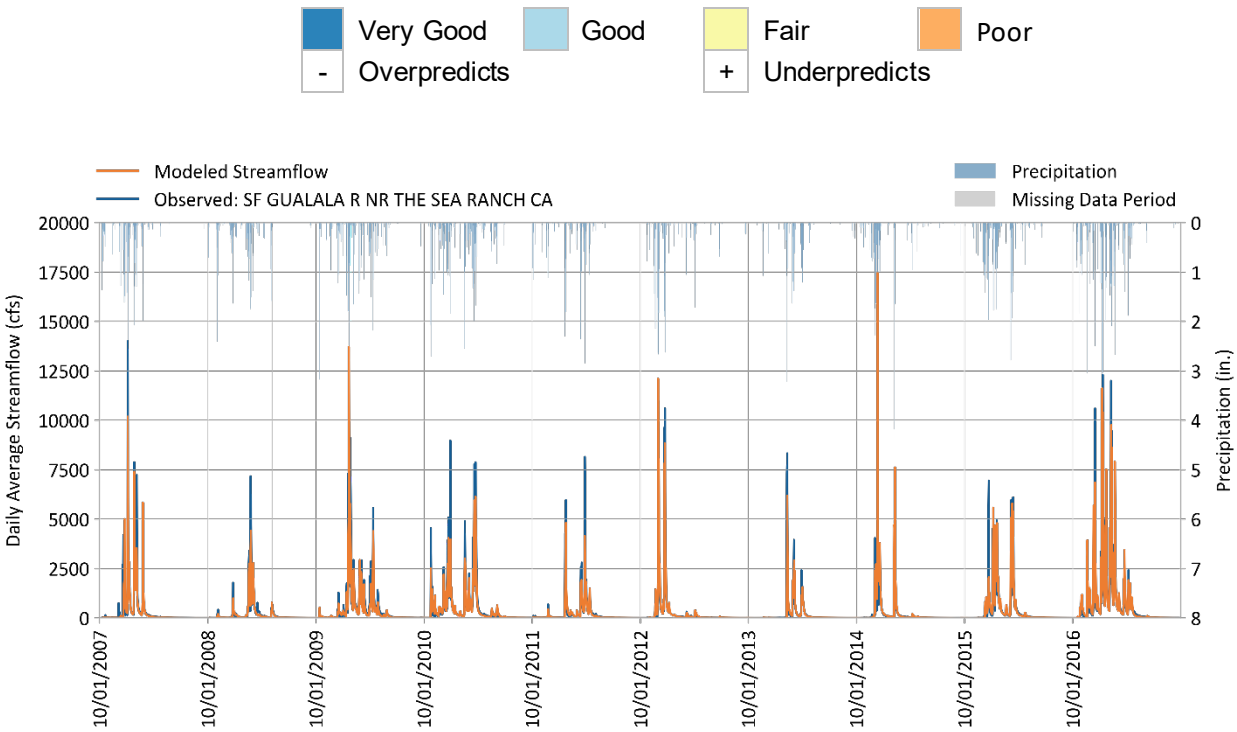

Figure 7-9. Daily simulated vs. observed streamflow for Gualala River South Fork at Sea Ranch.

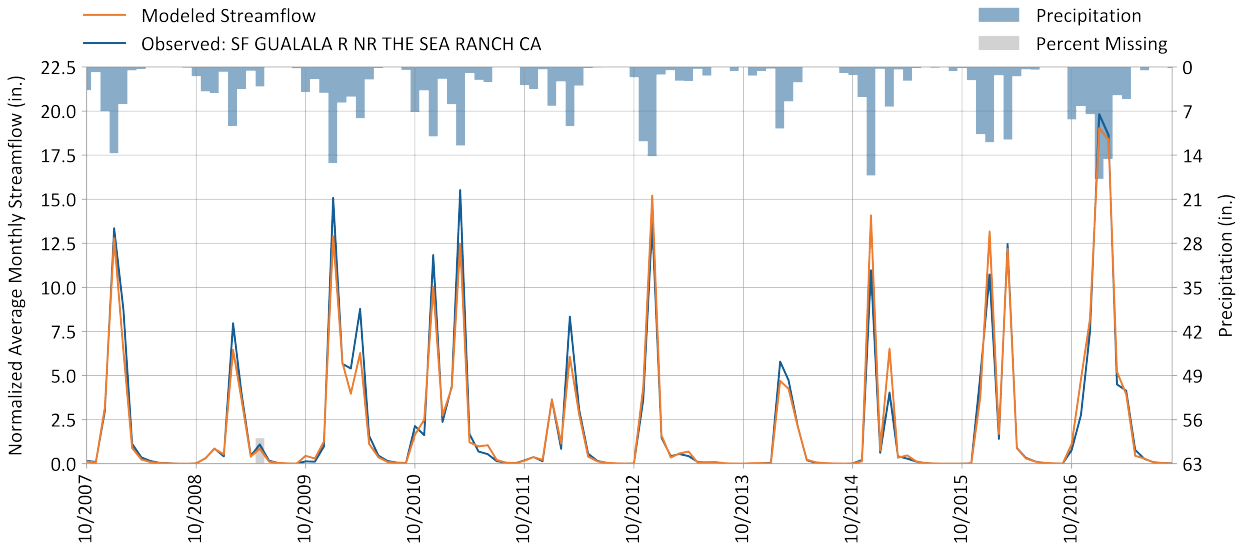

Figure 7-10. Monthly simulated vs. observed streamflow for Gualala River South Fork at Sea Ranch.

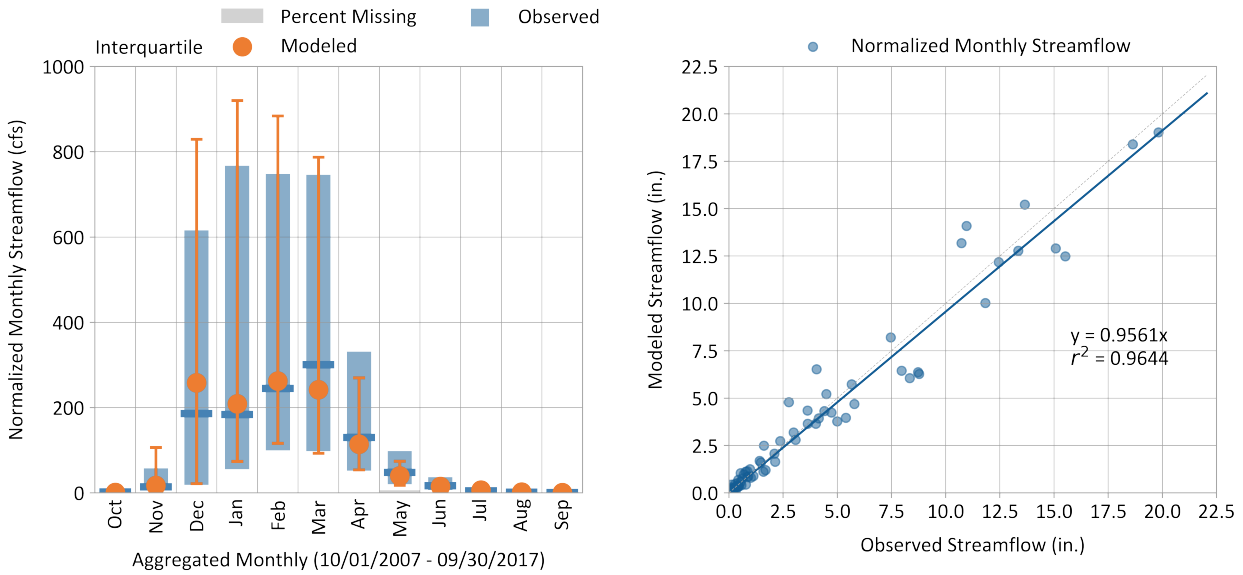

Figure 7-11. Monthly simulated vs. observed streamflow for Gualala River South Fork at Sea Ranch.

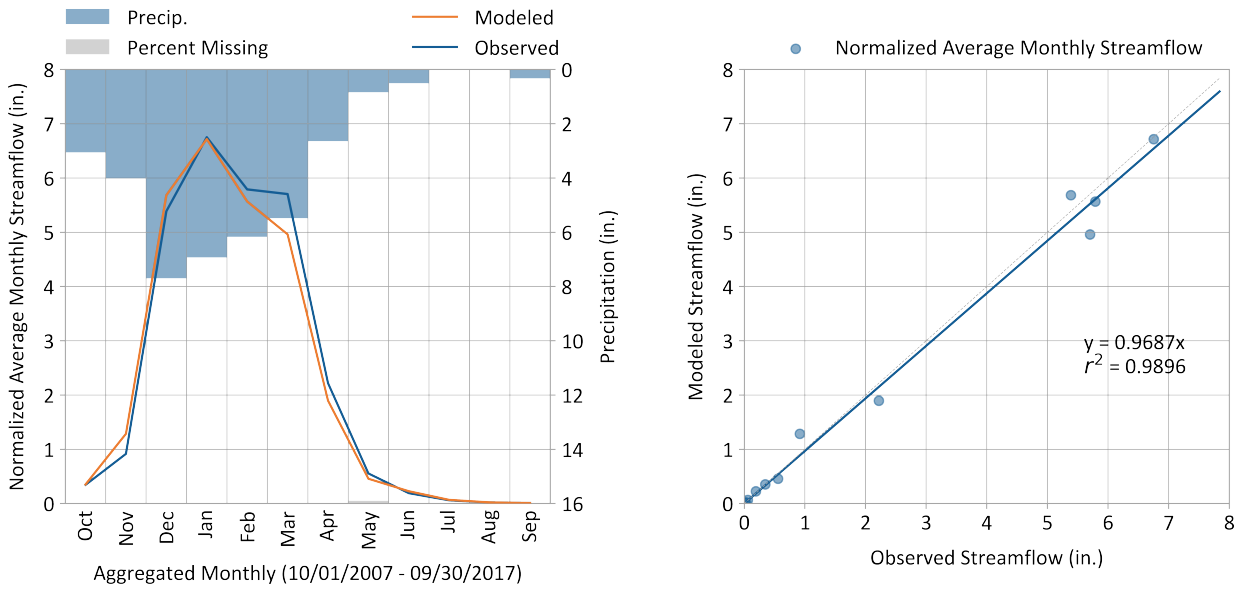

Figure 7-12. Average monthly simulated vs. observed streamflow for Gualala River South Fork at Sea Ranch.

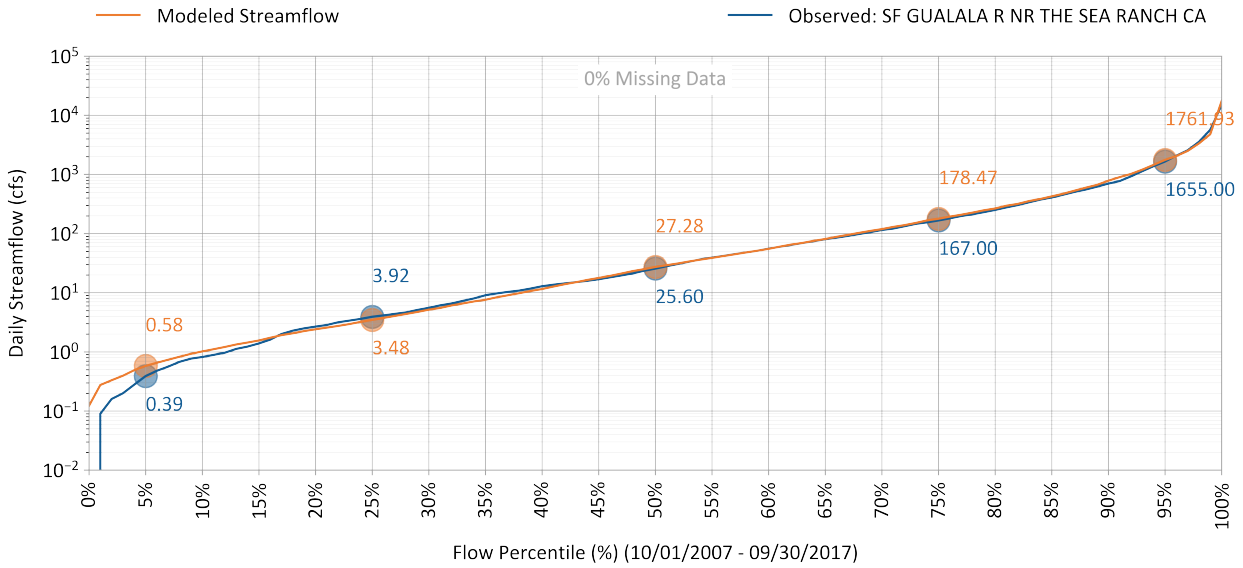

Figure 7-13. Simulated vs. observed flow duration curve for Gualala River South Fork at Sea Ranch.

PBIAS, NSE, and RSR performance values by season and flow regime are shown in Table 7-3, Table 7-4, and Table 7-5, respectively. The "Days Categorized as Baseflow" metric, which is derived from hydrograph separation, consistently shows "Very Good" or "Good" model performance across all conditions and metrics, except for RSR in the dry season, which is "Fair". Figure 7-14 and Figure 7-15 show the simulated and observed sliding-interval hydrograph separation for the wet and dry seasons of a wet water year (2009).

Table 7-3. Simulated vs. observed daily streamflow PBIAS at Gualala River South Fork at Sea Ranch

Validation Metrics *(10/01/2004 - 09/30/2017)*	Percent Bias (PBIAS)		
	All Seasons	Wet Season	Dry Season
All Conditions	2.5%	2.4%	6.3%
Highest 10% of Daily Flow Rates	7.7%	7.7%	N/A
Days Categorized as Storm Flow	4.3%	4.5%	-13.1%
Days Categorized as Baseflow	0.0%	-0.7%	11.9%

Table 7-4. Simulated vs. observed daily streamflow NSE at Gualala River South Fork at Sea Ranch

Validation Metrics *(10/01/2004 - 09/30/2017)*	Nash-Sutcliffe Efficiency (NSE)		
	All Seasons	Wet Season	Dry Season
All Conditions	0.86	0.85	0.68
Highest 10% of Daily Flow Rates	0.75	0.75	N/A
Days Categorized as Storm Flow	0.86	0.85	0.56
Days Categorized as Baseflow	0.86	0.85	0.72

Table 7-5. Simulated vs. observed daily streamflow RSR at Gualala River South Fork at Sea Ranch

Validation Metrics *(10/01/2004 - 09/30/2017)*	RMSE-Std-Dev. Ratio (RSR)		
	All Seasons	Wet Season	Dry Season
All Conditions	0.37	0.38	0.57
Highest 10% of Daily Flow Rates	0.5	0.5	N/A
Days Categorized as Storm Flow	0.38	0.39	0.68
Days Categorized as Baseflow	0.38	0.39	0.53

Very Good Good Fair Poor
\- Overpredicts + Underpredicts

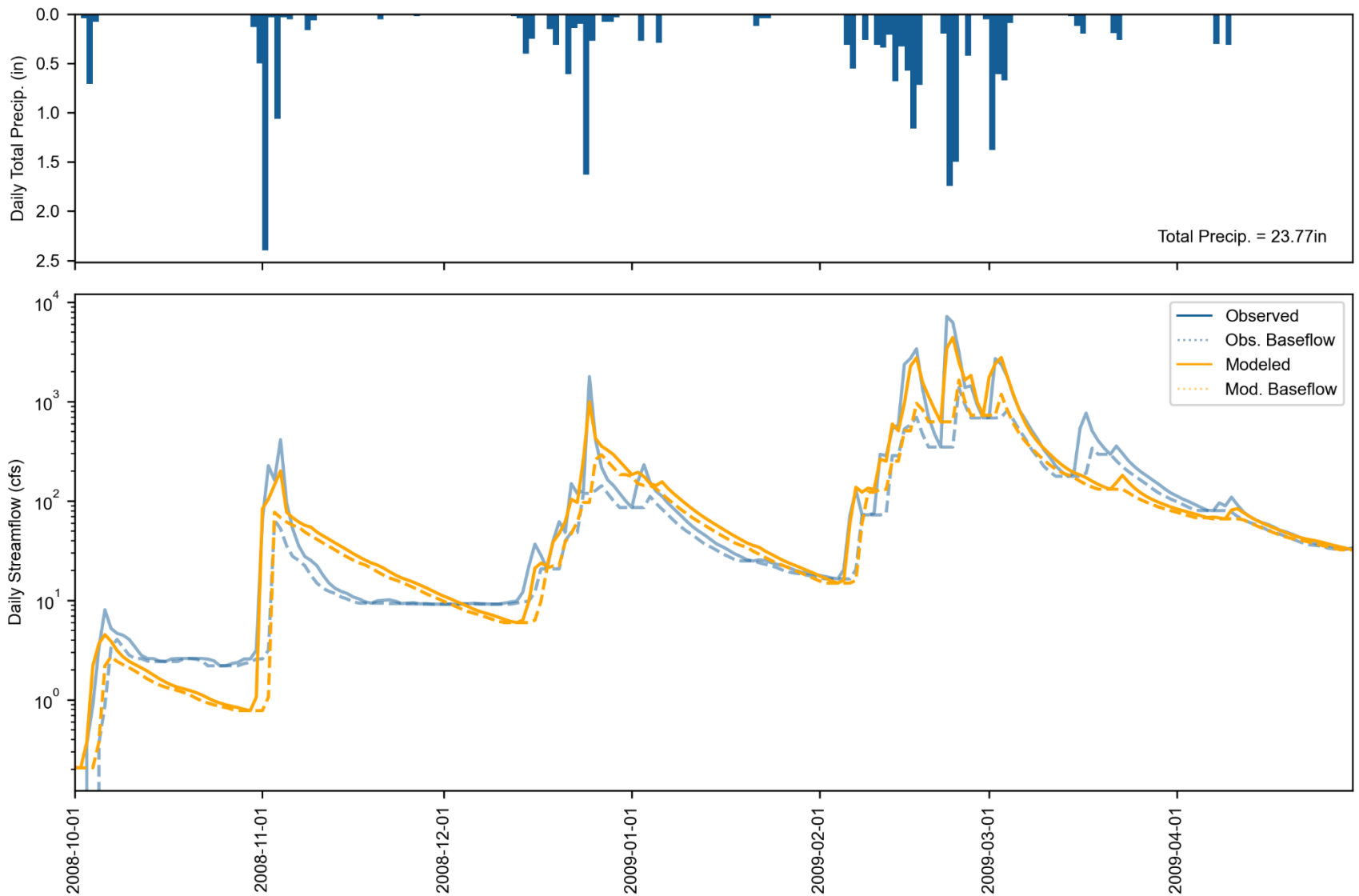

Figure 7-14. Water Year 2009 Wet season daily total precipitation (top) and streamflow (bottom) at Gualala River South Fork at Sea Ranch. Observed and simulated baseflow are calculated with HYSEP; grey shading indicates observed flow is less than the 50th percentile.

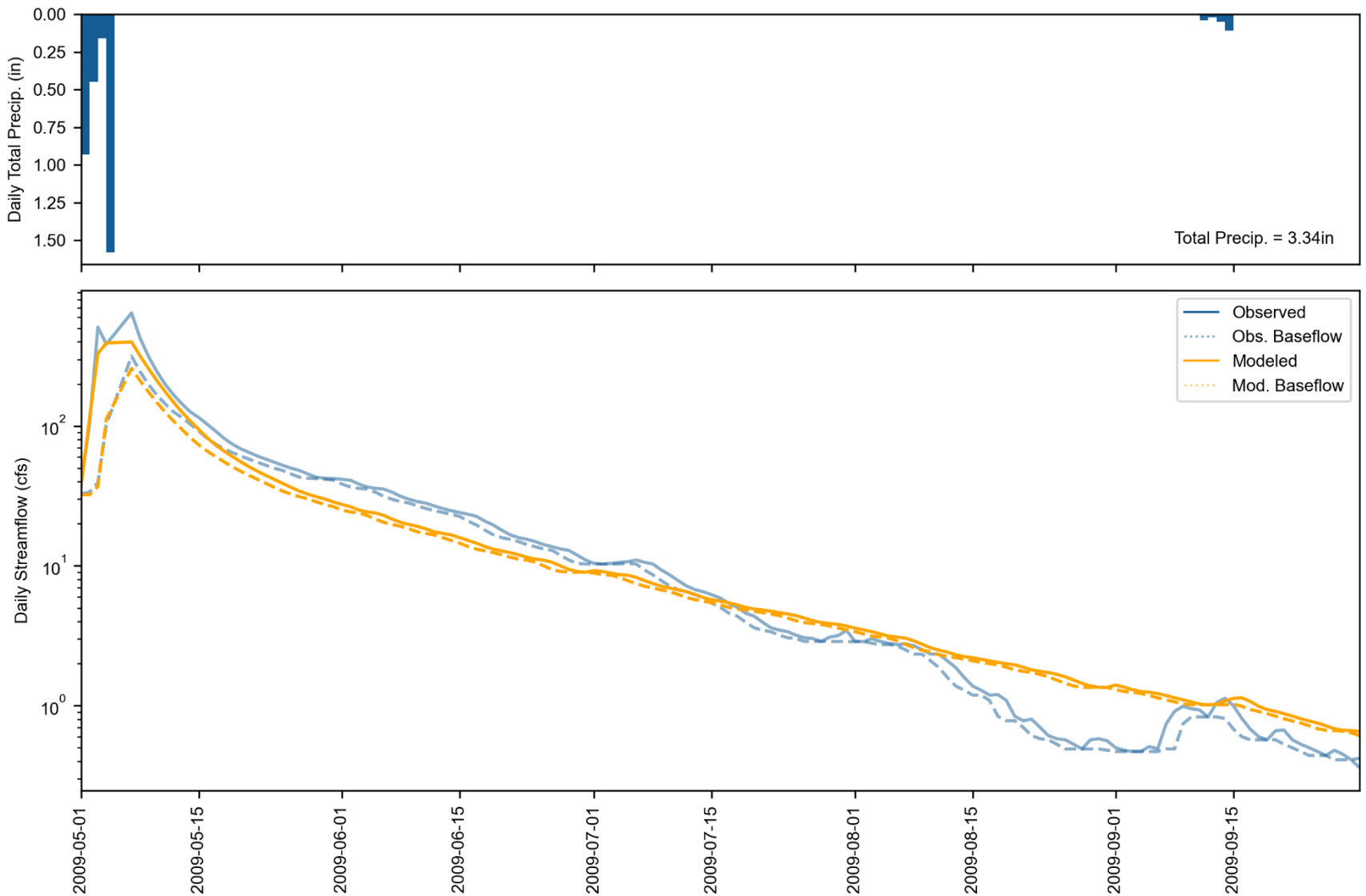

Figure 7-15. Water Year 2009 Dry season daily total precipitation (top) and streamflow (bottom) at Gualala River South Fork at Sea Ranch. Observed and simulated baseflow are calculated with HYSEP; grey shading indicates observed flow is less than the 50th percentile.

7.3 Other USGS Flow Stations

The streamflow data at Gualala River North Fork, Gualala River South Fork at Annapolis, and Wheatfield Fork at Annapolis were processed and considered for independent model validation. Gualala River North Fork had full data coverage before 5/30/2006, but it was only rated for 400 cfs after this date. The two inactive flow stations, Gualala River South Fork at Annapolis and Wheatfield Fork, had only two years and three years of data, respectively, coinciding with meteorological forcing inputs (limited to this period by availability of historical ET data and a one-year model warmup period).

However, the performance at these stations was not considered when calibrating the model. The runoff ratios were found to differ significantly between stations, with lower runoff ratios at Gualala River South Fork at Sea Ranch and Wheatfield Fork and much higher runoff ratios at North Fork and Gualala River South Fork at Annapolis, CA. This disagreement between stations was difficult to account for in a watershed as homogenous as the Gualala River in weather, land cover, hydrologic soil group, channel characteristics, and slope. To improve validation performance at a station with a high runoff ratio such as North Fork, calibration performance at South Fork at Sea Ranch would be impaired, which had a much lower runoff ratio despite an almost identical average yearly area-weighted rainfall. The probability of groundwater intrusion from another watershed is extremely low, and there is no snowfall in the watershed to account for the mismatch in water balance between stations.

In addition, flow volumes were directly compared between the South Fork at Sea Ranch and the two inactive flow stations, both directly upstream of the former. Though the three flow stations had no concurrent data, average yearly rainfall and runoff were compared, as shown in Table 7-6. Though the 2-3 years on record at the inactive stations were wetter on average than the 20 years recorded at South Fork at Sea Ranch, the difference is not large enough to account for the unusually large flow volume at the upstream stations, which combine for a volume over twice that recorded directly downstream.

Table 7-6. Summary of USGS daily streamflow data

Station*	Average Yearly Rainfall (inches)	Average Yearly Flow Volume (cubic feet)	Runoff Ratio
Gualala River South Fork at Sea Ranch CA	16.60	17,024.56	24%
Gualala River South Fork at Annapolis, CA	22.27	18,515.08	63%
Wheatfield Fork	19.22	17,016.59	30%

*Note that there are no data gaps in the record for the data given in this table

Monthly average streamflow was used to evaluate the low flow conditions for the other three stations. Table 7-7 summarizes metrics for the average monthly flow in the dry, wet, and overall seasons, including PBIAS, RSR, NSE, and KGE for additional validation checks. The model consistently underpredicts flow for all conditions, including the dry and wet seasons at the South Fork at Annapolis and North Fork stations (see Table 7-7, Figure 7-16, Figure 7-18, Figure 7-19, and Figure 7-21). The model's overall performance is "Very Good" to "Fair" for Wheatfield Fork at Annapolis (see Table 7-7, Figure 7-17, and Figure 7-20).

Table 7-7. Summary of performance metrics using monthly average for other three Gualala River stations

Calibration Metrics for Monthly Flow	Wheatfield Fork at Annapolis, CA: 10/01/2004 - 09/27/2007			South Fork at Annapolis, CA: 10/01/2004 - 05/30/2006			North Fork: 10/01/2004 - 09/30/2023		
	All	Wet Season	Dry Season	All	Wet Season	Dry Season	All	Wet Season	Dry Season
Count:	32	21	11	20	14	8	166	96	70
PBIAS	-4.10%	-5.50%	17.00%	18.10%	17.70%	23.80%	22.60%	17.90%	58.60%
RSR	0.14	0.16	0.23	0.26	0.29	0.33	0.43	0.48	0.77
NSE	0.98	0.98	0.95	0.93	0.91	0.89	0.82	0.77	0.41
KGE	0.95	0.93	0.71	0.74	0.74	0.59	0.72	0.74	0.24

Very Good Good Fair Poor
\- Overpredicts + Underpredicts

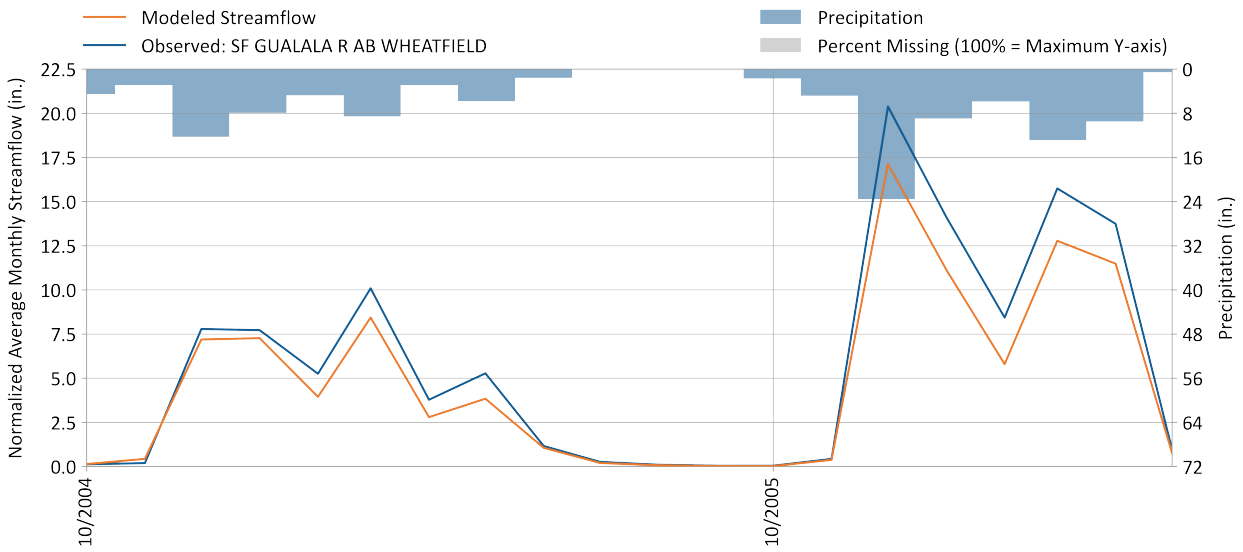

Figure 7-16. Monthly average flow for Gualala River South Fork at Annapolis, CA.

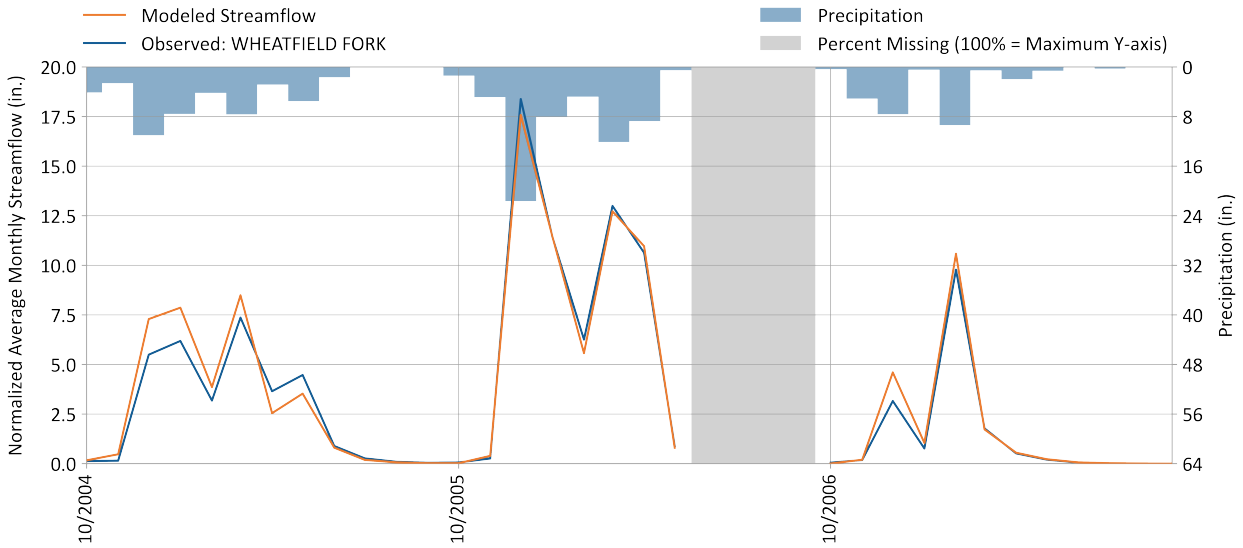

Figure 7-17. Monthly average flow for Wheatfield Fork.

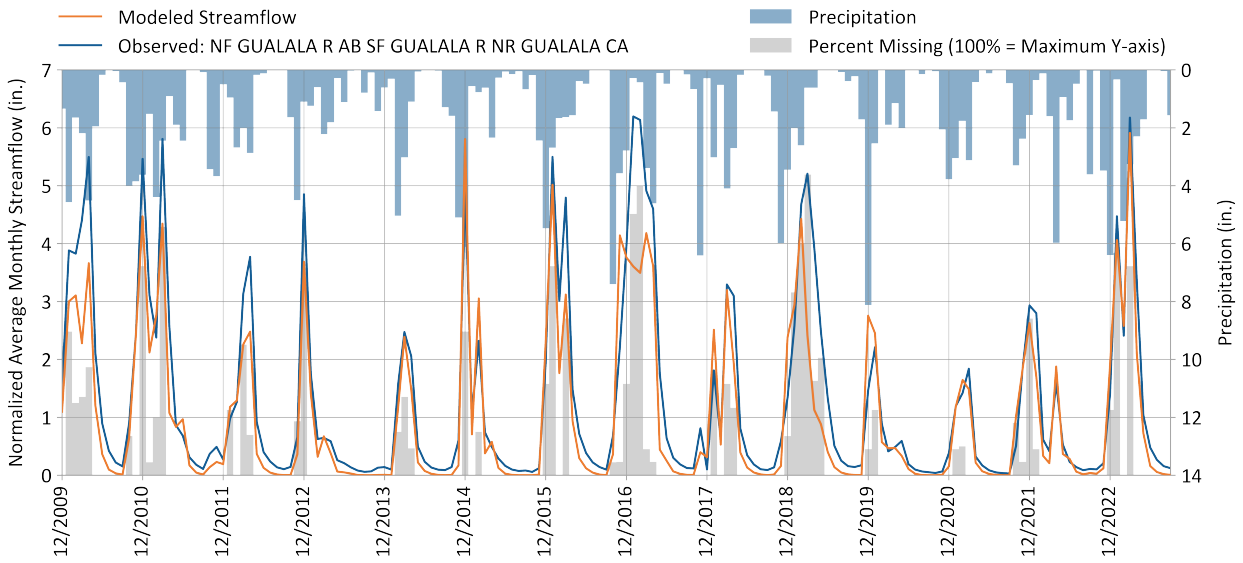

Figure 7-18. Monthly average flow for Gualala River North Fork.

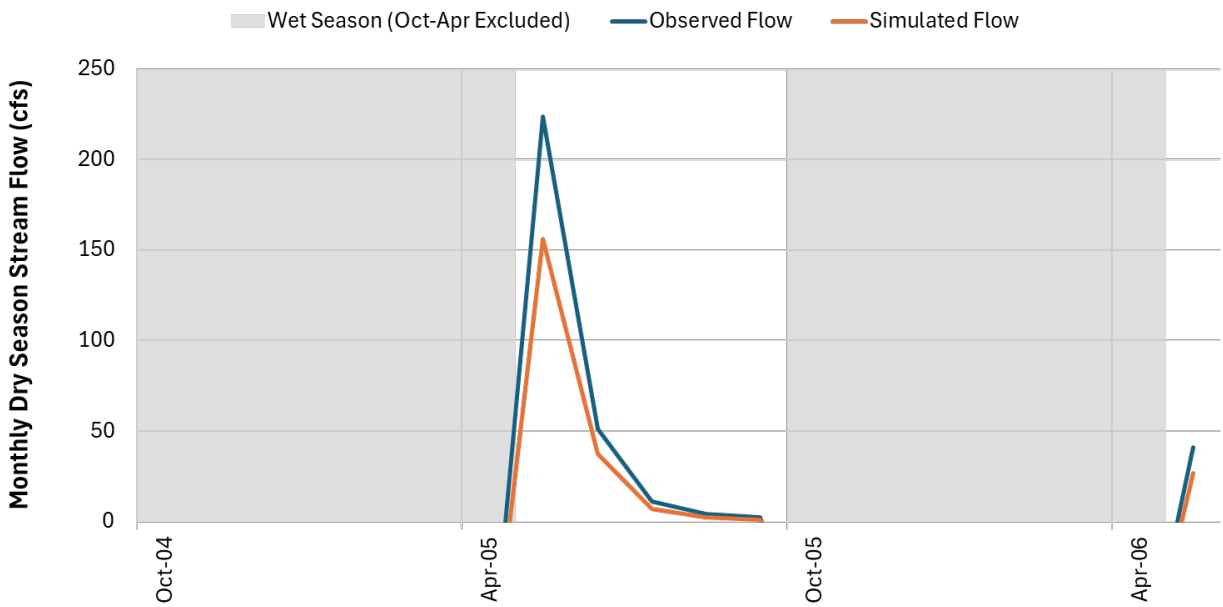

Figure 7-19. Monthly average dry season flow for Gualala River South Fork at Annapolis, CA.

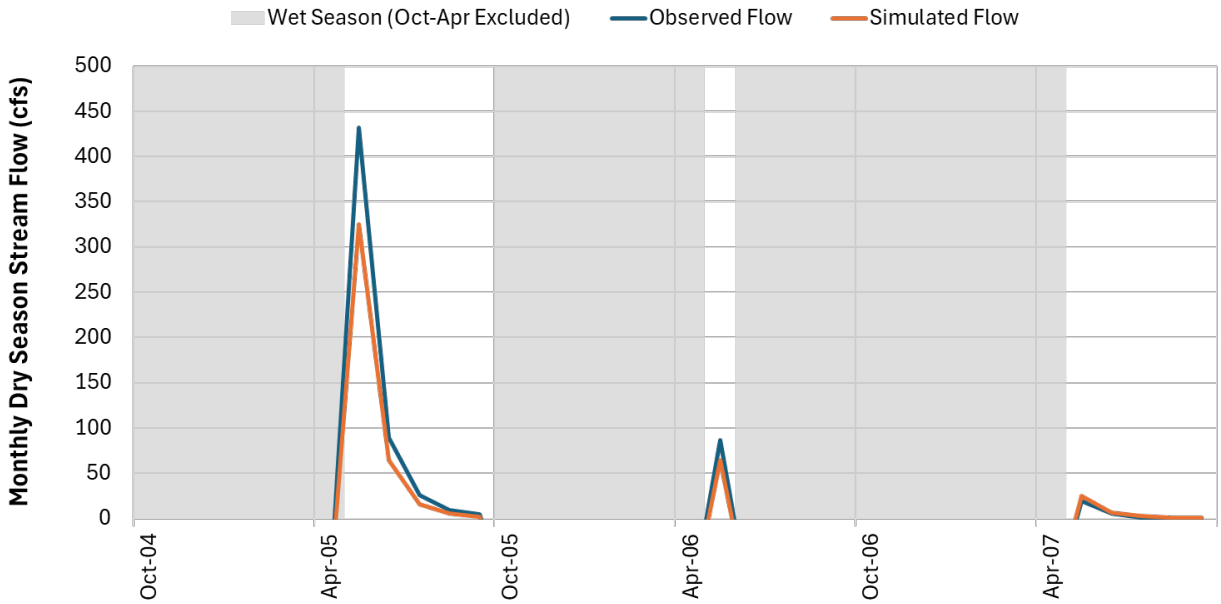

Figure 7-20. Monthly average dry season flow for Wheatfield Fork.

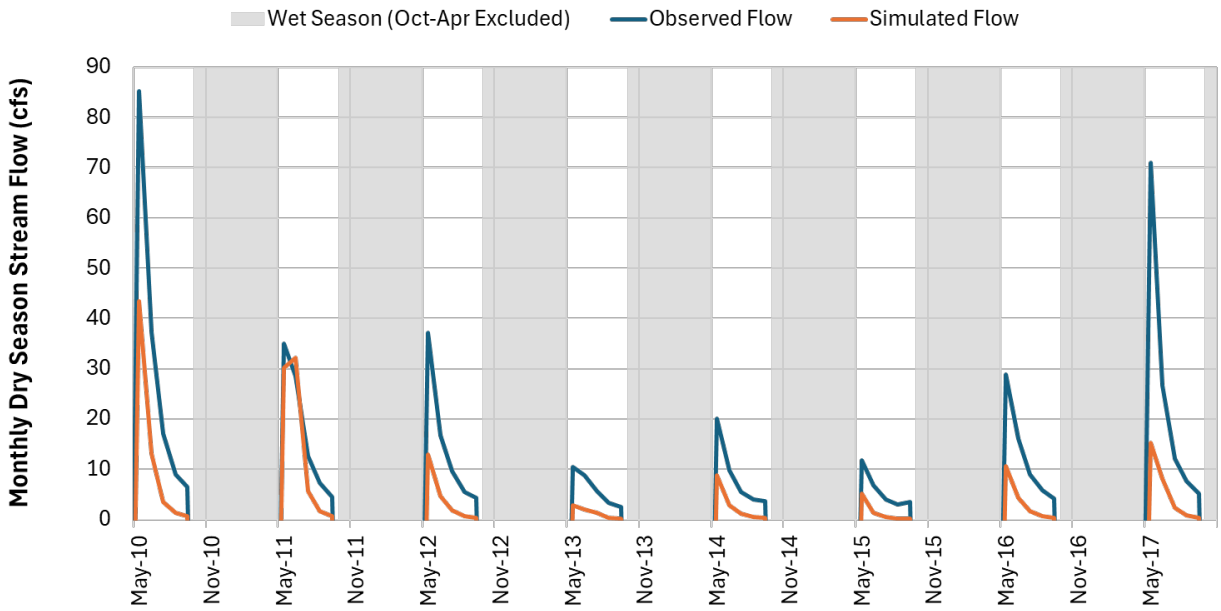

Figure 7-21. Monthly average dry season flow for Gualala River North Fork.

8 SUMMARY

This report documented the configuration, calibration, and validation of an LSPC hydrology model for the Gualala River watershed. The Water Board will use this model to help facilitate water use planning to ensure adequate, minimal water supplies for critical purposes. The Gualala River watershed model provides a comprehensive planning and decision-making tool by serving as an evaluation platform for (1) simulating existing instream flows that integrate current water management activities and consumptive uses and (2) evaluating the range of impacts of alternative management scenarios, including water allocation, changes in demand, and the impact of extreme events (e.g., droughts, atmospheric rivers, etc.).

The Gualala River watershed model was configured based on authoritative and comprehensive datasets suitable for characterizing hydrology within the region. The model uses HRUs that capture physical attributes controlling the rainfall-runoff response and are driven by long-term meteorological forcing time series representing the spatial and temporal range of precipitation and evapotranspiration conditions in the watershed. The model was calibrated and validated with the USGS streamflow station located at Gualala River's South Fork—at a point draining almost half of the total watershed area. This is the only long-term streamflow dataset with good-quality data for the modeled period (Water Years 2008-2023). The other station with data during this time period, Gualala River North Fork, was found to have substandard data quality and was excluded from the analysis.

Overall, model performance during the calibration period from 2017-2023 across the evaluated performance metrics was "Very Good" to "Good." Metrics during the validation period at the same station from 2007-2017 were also generally in the "Very Good" to "Good" range, with some exceptions during the dry season. The validation effort highlights possible areas for future improvement in dry-season predictions. The daily hydrographs provided for both the validation and calibration periods show the model's tendency to overpredict dry season baseflow following particularly dry wet seasons, while underpredicting baseflow after especially rainy wet seasons. However, while the percent difference between modeled and observed flow may be large, the flows during the periods in which significant under/overprediction occurs are quite rare. As a result, the absolute difference rarely rises above a single cfs for any given day. Finally, efforts could be made to salvage North Fork data for dry-weather validation and calibration purposes, as it was discovered that the station operates at an upper limit of 400 cfs.

In conclusion, the Gualala River watershed model is a robust platform for representing existing conditions and setting up future management scenarios. An important benefit of the model development approach described in this report is that it is modular. Key components can be refined and improved over time as new and better information becomes available.

9 REFERENCES

Arcement, G.J., Schneider, V.R. 1989. Guide for selecting Manning's roughness coefficients for natural channels and flood plains. USGS Water-Supply Paper 2339.

Arnold, J.G., Allen, P.M., Muttiah, R., and Bernhardt, G. 1995. Automated Base Flow Separation and Recession Analysis Techniques. Groundwater 33:1010–1018.

Bent, G.C., Waite, A.M. 2013. Equations for Estimating Bankfull Channel Geometry and Discharge for Streams in Massachusetts. U.S. Geological Survey Scientific Investigations Report 2013–5155 62. https://doi.org/https://doi.org/10.3133/sir20135155

Cosgrove, B.A., Lohmann, D., Mitchell, K.E., Houser, P.R., Wood, E.F., Schaake, J.C., Robock, A., Marshall, C., Sheffield, J., Duan, Q., Luo, L., Higgins, R.W., Pinker, R.T., Tarpley, J.D., Meng, J. 2003. Real-time and retrospective forcing in the North American Land Data Assimilation System (NLDAS) project. Journal of Geophysical Research: Atmospheres 108, 8842. https://doi.org/10.1029/2002jd003118

Daly, C., Taylor, G. H., Gibson, W. P., Parzybok, T. W., Johnson, G. L., Pasteris, P. A. 2000. High-Quality Spatial Climate Data Sets for the United States and Beyond. Transactions of the ASAE 43, 1957–1962. https://doi.org/10.13031/2013.3101

Daly, C., Neilson, R.P., Phillips, D.C. 1994. A Statistical-Topographic Model for Mapping Climatological Precipitation over Mountainous Terrain. J Appl Meteorol Climatol 33, 140–158.

Daly, C., Taylor, G., Gibson, W. 1997. The Prism Approach to Mapping Precipitation and Temperature, in: 10th AMS Conf. on Applied Climatology. Reno, NV, pp. 10–12.

Doherty, J. 2015. Calibration and Uncertainty Analysis for Complex Environmental Models - PEST: complete theory and what it means for modelling the real world. ISBN: 978-0-9943786-0-6

Duda, P.B., Hummel, P.R., Donigian, A.S., and Imhoff, J.C. 2012. BASINS/HSPF: Model Use, Calibration, and Validation. Transactions of the ASABE 55:1523–1547.

EPA (U.S. Environmental Protection Agency). 2000. BASINS Technical Note 6 Estimating Hydrology and Hydraulic Parameters for HSPF.

Gibson, W.P., Daly, C., Kittel, T., Nychka, D., Johns, C., Rosenbloom, N., McNab, A., Taylor, G.H. 2002. Development of a 103-Year High-Resolution Climate Data Set for the Conterminous United States, in: Proceedings of the 13th AMS Conference on Applied Climatology. Portland, OR, pp. 181–183.

Gupta, H. V., Kling, H., Yilmaz, K. K., and Maritinez, G.F. 2009. Decomposition of the Mean Squared Error and NSE Performance Criteria: Implications for Improving Hydrological Modelling. Journal of Hydrology 377:80–91.

Henn, B., Newman, A.J., Livneh, B., Daly, C., Lundquist, J.D. 2018. An assessment of differences in gridded precipitation datasets in complex terrain. J Hydrol (Amst) 556, 1205–1219. https://doi.org/10.1016/j.jhydrol.2017.03.008

Kim, S., Paik, K., Johnson, F.M., Sharma, A. 2018. Building a Flood-Warning Framework for Ungauged Locations Using Low Resolution, Open-Access Remotely Sensed Surface Soil Moisture, Precipitation, Soil, and Topographic Information. IEEE J Sel Top Appl Earth Obs Remote Sens 11, 375–387. https://doi.org/10.1109/JSTARS.2018.2790409

Knoben, W.J.M., Freer, J.E., and Wood, R.A. 2019. Technical Note: Inherent Benchmark or Not? Comparing Nash–Sutcliffe and Kling–Gupta Efficiency Scores. Hydrology and Earth System Sciences 23:4323–4331

Kouchi, D.H., Esmaili, K., Faridhosseini, A., Sanaeinjejad, S.H., Khalili, D., and Abbaspour, K.C. 2017. Sensitivity of Calibrated Parameters and Water Resource Estimates on Different Objective Functions and Optimization Algorithms. Water 9. doi:10.3390/w9060384.

LACFCD (Los Angeles County Flood Control District), 2020. WMMS Phase I Report: Baseline Hydrology and Water Quality Model. Prepared for the Los Angeles County Flood Control District by Paradigm Environmental. Alhambra, CA.

Looper, J.P., Vieux, B.E. 2012. An assessment of distributed flash flood forecasting accuracy using radar and rain gauge input for a physics-based distributed hydrologic model. J Hydrol (Amst) 412–413, 114–132. https://doi.org/10.1016/j.jhydrol.2011.05.046

McCandless, T.L. 2003a. Maryland stream survey: Bankfull discharge and channel characteristics in the Allegheny Plateau and the Valley and Ridge hydrologic region. Annapolis, MD.

McCandless, T.L. 2003b. Maryland Stream Survey: Bankfull Discharge and Channel Characteristics in the Coastal Plain Hydrologic Region. Annapolis, MD.

McCandless, T.L., Everett, R.A. 2002. Maryland stream survey: Bankfull discharge and channel characteristics in the Piedmont hydrologic region. Annapolis, MD.

McGourty, G., et al. 2020. Agricultural water use accounting provides path for surface water use solutions. California Agriculture, 74(1), 46–57. https://doi.org/10.3733/CA.2020A0003

Melton, F.S., Huntington, J., Grimm, R., Herring, J., Hall, M., Rollison, D., Erickson, T., Allen, R., Anderson, M., Fisher, J.B., Kilic, A., Senay, G.B., Volk, J., Hain, C., Johnson, L., Ruhoff, A., Blankenau, P., Bromley, M...R.G. Anderson. 2022. OpenET: Filling a Critical Data Gap in Water Management for the Western United States. JAWRA Journal of the American Water Resources Association 58:971–994.

Mitchell, K.E., Lohmann, D., Houser, P.R., Wood, E.F., Schaake, J.C., Robock, A., Cosgrove, B.A., Sheffield, J., Duan, Q., Luo, L., Higgins, R.W., Pinker, R.T., Tarpley, J.D., Lettenmaier, D.P., Marshall, C.H., Entin, J.K., Pan, M., Shi, W., Koren, V…Bailey, A.A. 2004. The multi-institution North American Land Data Assimilation System (NLDAS): Utilizing multiple GCIP products and partners in a continental distributed hydrological modeling system. Journal of Geophysical Research: Atmospheres 109. https://doi.org/10.1029/2003jd003823

Moriasi, D. N., Arnold, J. G., Van Liew, M. W., Binger, R. L., Harmel, R. D., and Veith, T. L. 2007. Model Evaluation Guidelines for Systematic Quantification of Accuracy in Watershed Simulations. Transactions of the ASABE 50:885–900.

Moriasi, D.N., M.W. Gitau, N. Pai, and P. Daggupati, 2015. Hydrologic and Water Quality Models: Performance Measures and Evaluation Criteria. Transactions of the ASABE 58:1763–1785.

Nash, J.E. and Sutcliffe, J. V. 1970. River Flow Forecasting through Conceptual Models Part I - A Discussion of Principles. Journal of Hydrology 10:282–290.

Nathan, R.J. and McMahon, T.A. 1990. Evaluation of Automated Techniques for Base Flow and Recession Analyses. Water Resources Research 26:1465–1473.

Quirmbach, M., Schultz, G.A. 2002. Comparison of rain gauge and radar data as input to an urban rainfall-runoff model. Water Science and Technology 45, 27–33. https://doi.org/10.2166/wst.2002.0023

Sloto, R.A. and Crouse, M.Y. 1996. HYSEP: A Computer Program for Streamflow Hydrograph Separation and Analysis: U.S. Geological Survey Water-Resources Investigations Report 1996–4040. doi:10.3133/wri964040.

Smakhtin, V.U. 2001. Low Flow Hydrology: A Review. Journal of Hydrology 240:147–186.

SWRCB (State Water Resource Control Board). 2024. Watershed Supply and Demand Allocations: Gualala River Work Plan.

SWRCB (State Water Resource Control Board). 2025. Supply and Demand Assessment (SDA) – Navarro River. Watershed Supply and Demand Allocations. https://www.waterboards.ca.gov/waterrights/water_issues/programs/supply-and-demand/navarro-river.html

Sutherland, R.C. 2000. Methods for Estimating the Effective Impervious Area of Urban Watersheds, Technical Note 58, in: Scueler, T.R., Holland, H.K. (Eds.), The Practice of Watershed Protection. Center for Watershed Protection, Ellicot City, MD, pp. 193–195.

USDA (United States Department of Agriculture). 2024. Cropland Data Layer. https://croplandcros.scinet.usda.gov/ (accessed 4.25.24).

Xia, Y., Mitchell, K., E.K., M., Cosgrove, B., Sheffield, J., Luo, L., Alonge, C., Wei, H., Meng, J., Livneh, B., Duan, Q., Lohmann, D. 2012a. Continental-scale water and energy flux analysis and validation for North American Land Data Assimilation System project phase 2 (NLDAS-2): 2. Validation of model-simulated streamflow. Journal of Geophysical Research Atmospheres 117. https://doi.org/10.1029/2011JD016051

Xia, Y., Mitchell, K., Ek, M., Sheffield, J., Cosgrove, B., Wood, E., Luo, L., Alonge, C., Wei, H., Meng, J., Livneh, B., Lettenmaier, D., Koren, V., Duan, Q., Mo, K., Fan, Y., Mocko, D. 2012b. Continental-scale water and energy flux analysis and validation for the North American Land Data Assimilation System project phase 2 (NLDAS-2): 1. Intercomparison and application of model products. Journal of Geophysical Research Atmospheres 117, 3109. https://doi.org/10.1029/2011JD016048